Towards a Function for a Novel Pollen-Specific *Arabidopsis thaliana* Protein Family DUF1216

Dissertation

zur

Erlangung der naturwissenschaftlichen Doktorwürde

(Dr. sc. nat.)

vorgelegt der

Mathematisch-naturwissenschaftlichen Fakultät

der

Universität Zürich

von

Anna Nestorova

aus

Bulgarien

Promotionskomitee

Prof. Dr. Ueli Grossniklaus (Leitung der Dissertation)

Prof. Dr. Enrico Martinoia

Prof. Dr. Niko Geldner

Zürich, 2015

Abbreviations

amiRNA – artificial microRNA

BCP – bicellular pollen

cDNA – complementary DNA

Col-0 – Columbia

DAPI – 4',6-diamidino-2-phenylindole

DNA – deoxyribonucleic acid

DUF – domain of unknown function

EDTA – ethylenediaminetetraacetic acid

GFP – green fluorescent protein

HeZ – heterozygous

HoZ – homozygous

KO – knock out

LB – lysogeny broth / Luria-Bertani medium

Ler – Landsberg erecta

MGU – male germ unit

MP – mature pollen

MS – Murashige and Skoog medium

ORF – open reading frame

PCR – polymerase chain reaction

PCR-RFLP / CAPS – polymerase chain reaction-restriction fragment length polymorphism/ cleaved amplified polymorphic sequence

PMI, PMII – pollen mitosis I, pollen mitosis II

PMC – pollen mother cell

RFP – red fluorescent protein

RNA – ribonucleic acid

RSE-PCR – restriction site extension polymerase chain reaction

RT-PCR – reverse transcription polymerase chain reaction

TAIL-PCR – thermal asymmetric interlaced polymerase chain reaction

TCP – tricellular pollen

TE – transmission efficiency

TGN – trans-Golgi network

UCM – unicellular pollen

WT – wild type

Table of contents

I. List of figures

II. List of Tables

1 Abstract

In plants, during sexual reproduction the growing pollen tube delivers the male gametes (sperm cells) to the female gametophyte (ovule) enabling the double fertilization process.
Therefore, studying the male gametophyte is of major importance for understanding the process of plant sexual reproduction. In the recent years several large-scale transcriptome and proteome studies provided novel insights into pollen biology, highlighting whole gene- and protein regulatory networks, and also revealing novel players involved in pollen development, pollen germination, and fertilization.
These studies revealed the existence of a novel pollen-specific protein family DUF1216, named after the domain of unknown function, shared by all members. Ten of the twelve family members have been detected at the protein level in the mature pollen grain and as mRNA during earlier developmental stages, but no functional homologs of DUF1216 have been identified. Nevertheless, theoretical predictions have proposed a role in the subcellular trafficking machinery for the DUF1216 proteins. Preliminary analysis provided evidence for functional redundancy within the family. In addition, the chromosomal location of the DUF1216 genes forming a compact cluster on chromosome 3, represents a technical challenge for applying standard reverse-genetics approaches, such as generating multiple knock out insertional mutants to study the function of the DUF1216 proteins.
Therefore, in order to establish a genetic system allowing the functional characterization of the DUF1216 members, an artificial microRNA-based reverse-genetics approach was chosen. *Arabidopsis thaliana* lines stably expressing amiRNA constructs against multiple DUF1216 members showed downregulation of six of the genes at the mRNA level. The mutant lines displayed pollen degeneration starting during the first mitotic division of microgametogenesis, as well as reduced male fertility. However, both the downregulation of the target genes and the observed phenotypic effects were highly variable, and a direct link between the DUF1216 gene expression and phenotypic effects could not be established. Statistical analysis of a large dataset containing gene expression and phenotype quantification measurements from single individuals indicated that the difference in the expression of multiple members of the DUF1216 correlates with the reproductive phenotype, but the contribution of the different genes remains unknown. Potentially, complex interactions characterize the mode of action of the DUF1216 family members and introducing an amiRNA targeting several of them interferes with the complex biological system resulting in a variable phenotypic outcome. Although the results presented in this work provide evidence that the members of the

DUF1216 protein family are playing a role during pollen development and have an impact on the male reproductive function, the exact molecular role of this novel group of proteins is a subject of further research.

Zusammenfassung

In Pflanzen findet während der sexuellen Reproduktion eine doppelte Befruchtung statt. Die männlichen Gameten (Spermazellen) werden durch den wachsenden Pollenschlauch zu dem weiblichen Gametophyten (Embryosack) transportiert.

Um den Prozess der pflanzlichen sexuellen Reproduktion zu verstehen, ist es von grosser Bedeutung den männlichen Gameten zu studieren. Aus diesem Grund wurden in den letzten Jahren verschiedene grossformatige Transkriptom- und Proteomstudien durchgeführt. Dabei konnten neue Erkenntnisse, betreffend Gen- und Proteinregulationsnetzwerken, in der Pollenbiologie gewonnen, sowie neue Akteure in der Pollenentwicklung, Pollenkeimung und Fertilisation identifiziert werden. So wurde die Existenz einer neuen pollenspezifischen Proteinfamilie DUF1216, deren Mitglieder nach einer gemeinsamen Domäne mit unbekannter Funktion benannt sind, aufgezeigt. Während zehn der zwölf Familienmitglieder auf Proteinlevel in ausgereiften Pollenkörnern und auf mRNA-Level während früherer Entwicklungsstadien detektiert wurden, fand keine Identifikation von funktionalen Homologen statt. Dennoch haben theoretische Prognosen für die DUF1216 Proteine eine Rolle in der subzellulären Transportmaschinerie vorgeschlagen. Vorläufig durchgeführte Analysen lassen auf eine funktionale Redundanz innerhalb der Familie schliessen. Um die Funktion der DUF1216 Proteine aufzudecken, stellt die Anordnung der DUF1216 Gene, in Form eines kompakten Klusters auf Chromosom drei, eine technische Herausforderung für die Anwendung von Standard revers-genetischen Ansätzen, wie der Herstellung von multiplen *Knock-out*-Insertionsmutanten, dar.

Aus diesem Grund wurde für die Etablierung eines genetischen Systems zur funktionalen Charakterisierung der DUF1216 Mitglieder ein künstlicher microRNA (artificial microRNA, amiRNA) basierter revers-genetischer Ansatz gewählt. So konnten *Arabidopsis thaliana* Linien, die stabil amiRNA-Konstrukte gegen multiple DUF1216 Mitglieder exprimieren und eine Herunterregulierung von sechs Genen auf mRNA-Level aufwiesen, generiert werden. Die mutierten Linien zeigten eine Pollendegeneration, beginnend während der ersten mitotischen Teilung der Mikrogametogenese, sowie reduzierte männliche Fertilität. Die Herunterregulierung der Zielgene und die beobachteten phänotypischen Effekte waren jedoch hoch variabel und es konnte keine direkte Verbindung zwischen der DUF1216 Genexpression und den phänotypischen Effekten nachgewiesen werden.

Statistische Analysen grosser Datensets der Genexpression und die phänotypische Quantifizierung von einzelnen Individuen ergaben, dass der Unterschied in der Expression von verschiedenen DUF1216 Mitgliedern mit dem reproduktiven Phänotyp korreliert. Dennoch bleibt die Beteiligung der verschiedenen Gene unbekannt. Möglicherweise ist die Funktionsweise der DUF1216 Familie durch komplexe Interaktionen charakterisiert und die Einführung von amiRNA, die diese gerichtet angreift, interferiert mit dem komplexen biologischem System, woraus ein variables phänotypisches Ergebnis resultiert. Obwohl die in dieser Arbeit präsentierten Ergebnisse Beweise dafür darstellen, dass die Mitglieder der DUF1216 Proteinfamilie eine Rolle während der Pollenentwicklung spielen und eine Auswirkung auf die männliche Reproduktionsfunktion haben, wird die Entdeckung der exakten molekularen Funktion dieser neuen Proteingruppe Gegenstand weiterer Forschung sein.

2 Introduction

2.1 Plant sexual reproduction

Plant reproduction is a process of fundamental importance for sustaining life on Earth, since plants are the main primary producers in the global ecosystem, converting solar energy into chemical energy during the photosynthetic process. Plants play a central role in water and carbon dioxide-cycle regulation, which has a major impact on sustaining the climatic conditions. Apart from their ecological significance, plants have major social importance, providing essential food and medicine sources for the humankind.

The plant kingdom is dominated by the flowering plants (angiosperms), which is also the most diverse plant group (Davies et al., 2004). The evolution of the angiosperms has led to the development of the flower by the diploid sporophytic generation, containing the reproductive organs and the germ line (haploid gametophytic generation) of the plant (Fig. 2-1 A). Moreover, the morphology of the reproductive organs and that of the male and female gametophytes enables the process of double fertilization, resulting in both embryo and endosperm formation inside the female reproductive tract, where the initial development of the new sporophyte is ensured by the endosperm nutritive tissue.

The tricellular male gametophyte, called pollen, matures in the anthers of the flower (Fig.2-1 B). It develops from a diploid sporogenous cell, which differentiates into the pollen mother cell (microsporocyte) and divides by meiosis forming four haploid microspores in a process called microsporogenesis. The microspore undergoes two mitotic divisions during microgametogenesis forming mature pollen grains. In *A. thaliana* the second mitosis giving rise to two sperm cells takes place in the anthers, but in the majority of angiosperm species this final maturation step occurs after pollen germination (Brewbaker, 1967; McCormick, 2004). Pollen development will be discussed in more detail later in this chapter (see 2.2).

The female gametophyte is a complex multicellular structure enclosed by the ovule within the ovary of the flower. It develops within the ovule from a diploid megaspore mother cell that undergoes meiosis (megasporogenesis) and one of the resulting haploid megaspore cells gives rise to the female gametophyte (megagametogenesis). Further, the surviving megaspore undergoes several mitotic divisions without cytokinesis, followed by cellularization and cell specification (Schneitz et al., 1995; Webb and Gunning, 1994). The mature megagametophyte of *A. thaliana* is a result of the so-called *Polygonum*-type developmental pattern and consists of three antipodal cells, one central cell, two synergid cells, and one egg cell (Fig. 2-1 C). The

egg and the synergid cells form the filiform apparatus of the embryo sac, as the two synergids coordinate the signalling during of the pollen tube reception and fertilization of the egg (Higashiyama et al., 2001, Ngo et al., 2014). The diploid central cell is formed after the fusion of two polar nuclei during the cellularization process of the female gametophyte. The three antipodal cells have no reported functional specialization, but supportive role as nutrient transfer cells has been proposed (Drews and Koltunow, 2011).

After landing on the stigma, the mature pollen grain hydrates and germinates, forming a quickly growing cellular protrusion, the pollen tube (reviewed by Boavida et al., 2005). The pollen tube grows through the internal tissues of the pistil, penetrates the ovule and bursts, allowing the two sperm cells to enter the embryo sac with one of them fertilizing the egg cell and the other the central cell and giving rise, respectively, to the diploid sporophyte and the triploid endosperm. The pollen guidance to the ovule, as well as the fertilization, are highly organized processes, relying on coordinated gene expression and intra- and intercellular signalling events in both male and female reproductive tissue (Boisson-Dernier et al., 2013; Escobar-Restrepo et al., 2007; Kessler et al., 2010; Leydon et al., 2013; Lindner et al., 2015; Ngo et al., 2014; Schiøtt et al., 2004).

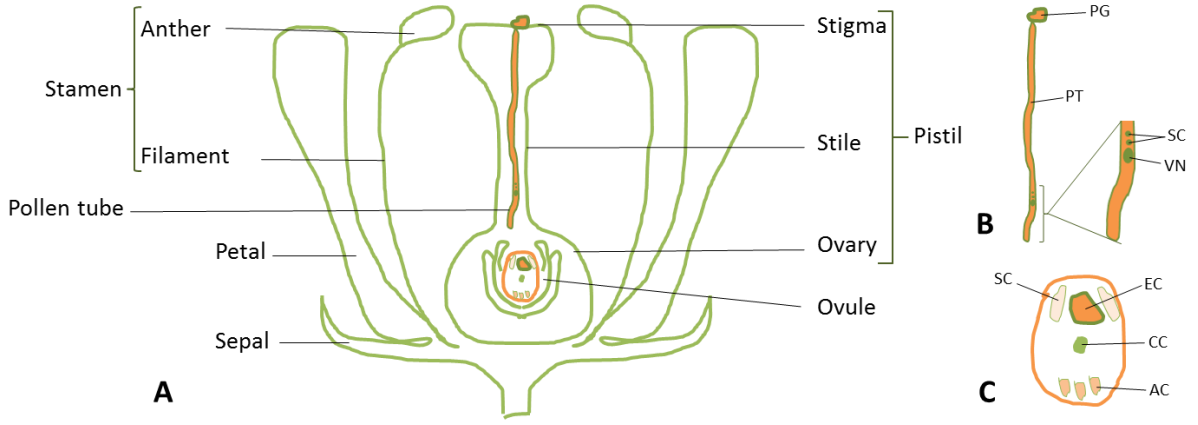

Figure 2-1 Schematic representation of an angiosperm perfect flower architecture and gametophyte morphology.

A – Angiosperm perfect flower containing both female (pistil) and male (stamen) reproductive organs. The petals and sepals form the outer parts of the flower. The anthers produce the pollen grains (PG), which germinate upon landing on the stigma and form quickly growing pollen tubes (PT). The PT delivers the male germ cells (sperm cells, SC) to the female gametophyte enclosed by the ovule and containing the haploid egg cell (EC) and the diploid central cell (CC), allowing the double fertilization to occur (not shown).

B – Pollen grain (PG) with growing pollen tube (PT) carrying the two sperm cells (SC) and the nucleus of the vegetative cell (VN).

C – Mature female gametophyte (embryo sac) containing three antipodal cells (AC), one central cell (CC), two synergid cells (SC), and one egg cell (EC).

2.2 Pollen development

The mature pollen grain (PG) of *Arabidopsis thaliana* is a tricellular structure consisting of a vegetative cell, which has incorporated the two generative (sperm) cells. The cell wall of the pollen grain is deposited over the course of pollen development and has a complex structure. The inner layer, or intine, is composed of cellulose and pectin and the thick outer layer, called exine, is composed of sporopollenine having cavities with species-specific architecture (Fig. 2-2). The exine's sculptured cavities are filled by pollen coat, which is a mixture of lipids, pigments, proteins, and aromatic compounds and is deposited on the pollen surface by the surrounding sporophytic tissue. It has been shown that the components of the pollen cell wall have an important protective function and are also playing a role in adhesion, hydration and germination on the stigma, as well as in male-female recognition processes (Edlund et al., 2004).

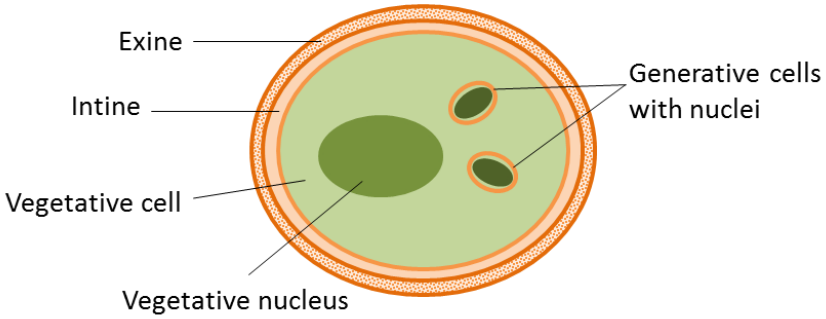

Figure 2-2 Schematic representation of the anatomy of the mature pollen grain in *Arabidopsis thaliana*. The large vegetative cell incorporates the two germ cells. The cell wall of the pollen grain consists of an inner cellulose layer (intine) and outer layer (exine) composed of sporopollenine.

As it was briefly introduced (2.1), the pollen grains develop within the pollen sacs of the anthers from a diploid sporogenous cell of sporophytic origin, which differentiates into a pollen mother cell (PMC), or microsporocyte. The microsporocyte undergoes further meiotic and mitotic divisions giving rise to the actual male germ line, the haploid sperm cells. The developing pollen is surrounded by a layer of cells with nutritive and structural function, the tapetum, which degenerates during pollen development providing cellular material for the pollen wall formation (Fig. 2-3). Pollen development depends on gametophytic and sporophytic gene expression and identifying the main players in the maturation process has been a subject of intense scientific effort in the last decades. Using different strategies, like

forward- and reverse-genetics screens, allowed the identification of multiple genes whose products are part of the cellular machinery driving key steps of the developmental process.

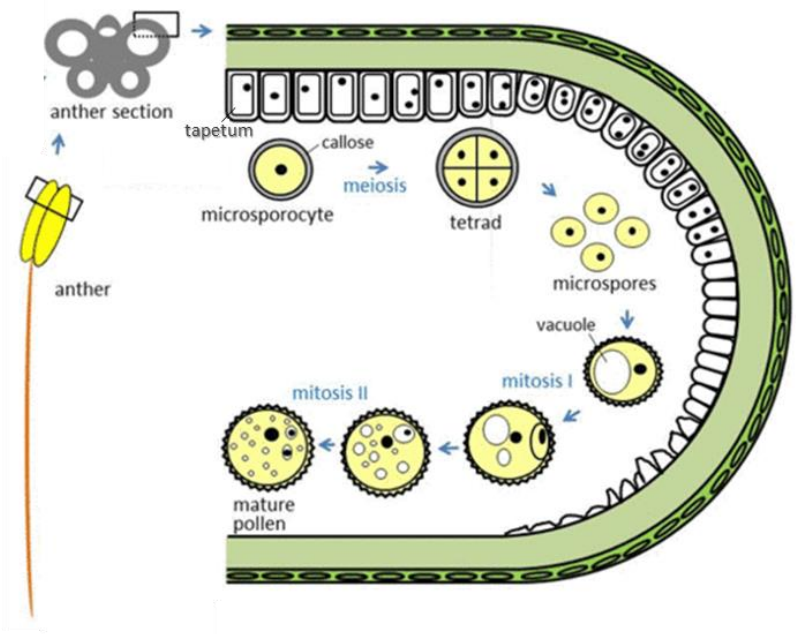

Figure 2-3 Pollen development within the anther.
The pollen develops within the pollen sacs of the anther from a diploid pollen mother cell (PMC) or microsporocyte and supported by the surrounding tapetal cells. The PMC undergoes meiosis forming four haploid microspore cells. The microspores divide asymmetrically through mitosis (mitosis I) to form the polar bicellular pollen grain containing vegetative nucleus and one generative cell. A second symmetric mitotic division (mitosis II) of the generative cell results in two haploid germ cells enclosed by the vegetative cell of the mature pollen grain.
Figure modified from: http://abrc.sinica.edu.tw/2010E/view2/faculty_E1.php?id=suendf

The pollen mother cells and the tapetum cells originate from the same type archesporial cells in the developing anther, which differentiate into sporogenous and parietal cells, respectively. Parietal cells differentiate further to give rise to the tapetal layer of cells and other cell types in the anther (Goldberg et al., 1993). The *A. thaliana sporocyteless* (*spl*) mutant is deficient for a nuclear protein expressed before the initial archesporial cell divisions and fails to form both male and female sporocytes (Schiefthaler et al., 1999).

During the first stage of the pollen developmental process, microsporogenesis, the diploid pollen mother cell undergoes meiosis forming four haploid microspores associated in a tetrad and surrounded by tapetum-derived callose. If the control of cell fate determination is disturbed during anther development, like in the Arabidopsis *excess microsporocytes1* (*ems1*)

mutant lacking tapetal cells and excessively producing microsporocytes, this also results in pollen developmental failure and male sterility, although the meiotic division of the PMC is normal (Zhao et al., 2002). In the mutant of the kinesin motor protein TETRASPORE (*tes*) the four microspores do not separate due to a failure in meiotic cytokinesis and the mature pollen grains contain variable number of nuclei with different cell identity resulting in fertilization defects (Spielman et al., 1997; Yang et al., 2003). The microsporogenesis is completed with breaking down the cell wall of the PMC by the action of tapetal enzymes and releasing the free microspores. If the degradation of the PMC cell wall is defective, like in the *quartet (qrt)* mutants, the four microspores are not separated and are released as a tetrad upon pollen maturation. The *QUARTET1/2/3* genes are expressed in the anther sporophytic tissue and encode for enzymes involved in cell wall loosening and degradation (Francis et al., 2006; Preuss et al., 1994; Rhee et al., 2003).

In later developmental stages the importance of the tapetal activity for pollen development has been demonstrated with the identification of several mutants in *A. thaliana* called *male sterile (ms)* with defective or prematurely degenerating tapetum. The gene products of *MALE STERILE1/7/9/15* genes are sporophytically expressed and are playing a role in the postmeiotic pollen development and their disruption leads to plant sterility due to tapetal cells defects (Taylor et al., 1998; Wilson et al., 2001a).

The microgametogenesis begins with enlargement of the free haploid microspore and the production of a large vacuole combined with migration of the nucleus to the cell periphery forming a polarized microspore. Further, the microspore undergoes an asymmetric mitotic division (pollen mitosis I, PMI) to form bicellular pollen grain with a germ cell engulfed by the large vegetative cell. The two cells resulting from PMI inherit different cytoplasmic content from the microspore and display a differential gene expression pattern, which is of major importance for establishing their cell fate (Twell et al., 1998). The polarization process and the consequent asymmetric cell division (PMI) depend on the proper cellular microtubule dynamics. The *gem1/mor1 Arabidopsis* gametophytic mutant, lacking the microtubule-associated GEM1/MOR1 MAP215 family protein, displays disturbed nuclear migration and division asymmetry during PMI. The defective cytokinesis leads to failure to establish the germ cell fate, pollen degeneration and transmission defects (Park et al., 1998; Whittington et al., 2001). Another mutant with defects in asymmetric cell division and cellular patterning during PMI is *sidecar pollen* (*scp*), whose gene product has been identified as a microspore-specific LATERAL ORGAN BOUNDARIES DOMAIN/ASYMMETRIC LEAVES 2-like

(LBD/ASL) protein putatively acting as a transcription factor (Chen and McCormick, 1996; Oh et al., 2010). In addition to the formation of WT-like pollen grains and prominent pollen degeneration, a proportion of *scp* microspores divide symmetrically and prematurely with only one of the resulting cells further forming one vegetative cell and the germ cells, thus forming four-celled mature pollen grains. If the PMI is blocked like in the *solo pollen* mutant, this results in one-celled mature pollen (Chupeau et al., 1998). In the case of the mutant *two-in-one* (*tio*), lacking a functional protein of the FUSED (FU) Ser/Thr protein kinase family, the nuclear asymmetric division is not disturbed, but cytokinesis does not complete, resulting in a binucleate pollen (Oh et al., 2005).

With the PMI completed, two morphologically and functionally different cells are formed: the vegetative cell and the germ cell. The vegetative cell exits the cell division cycle and is transcriptionally active accumulating transcripts and cellular reserves of proteins, lipids and other compounds needed for the development of the sperm cells, as well as for the germination and growth of the pollen tube (Pacini, 1996; Schwacke, 1999). The germ cell undergoes a symmetric mitotic division (PMII) to give rise to two haploid sperm cells. The *Arabidopsis* gametophytic mutants of the *duo pollen* class are defective in proteins involved in the regulation of the generative cell cycle, which leads to formation of only one sperm cell-like structure not able to complete fertilization (Durbarry et al., 2005).

It has been proposed that after the second pollen mitosis is completed the newly formed sperm cells and the vegetative nucleus form a physically associated structure called male germ unit (MGU) ensuring the proper spatial orientation of the functional elements of the male gametophyte (Dumas et al., 1985). In the MGU the two sperm cells are connected by common extracellular matrix and potentially through intracellular connections, and one of the sperm cells forms a microtubular cytoplasmic association to the vegetative nucleus. It has been shown that mutants with abnormal MGU are affected in their transmission through the pollen (Lalanne and Twell, 2002) and it is generally accepted that – apart of the structural stabilization of the male reproductive elements – the MGU plays a role during double fertilization and is important for cell-to-cell communication (McCue et al., 2011; Slotkin et al., 2009).

Male gametophyte development is a complex process, relying on the orchestrated expression of multiple genes, and it is precisely regulated by intra- and extracellular signals. Although the classical single-gene molecular characterization approach has provided researchers with valuable information about pollen biology and helped highlighting important structural and

regulatory factors during the pollen developmental process, it has limited resources in capturing the complexity of the biological system. In recent years, the technical advancements have made it possible to study the (pollen) developmental process at the whole-transcriptome and the whole-proteome level. This global view towards biological systems opens a different scientific perspective and helps identifying not just single players in a specific process but whole regulatory networks.

Pollen biology is a subject of intense research, and many scientific reports provide novel large-scale data about gene and protein expression in pollen of different species and under different experimental conditions (Becker et al., 2003; Lee and Lee, 2003; Borges et al., 2008; Wang et al., 2008a; Grobei et al., 2009; Mayank et al., 2012; Sarhadi et al., 2012; Loraine et al., 2013). Expression profiling during pollen development, however, is the subject of only a few studies, mainly because sample isolation and handling are technically challenging (Bokvaj et al., 2015; Honys and Twell, 2004; Ma et al., 2008; Wei et al., 2010).

According to the different expression studies (transcriptomics or proteomics) mature pollen of *Arabidopsis* exhibits a very distinctive expression profile compared to other plant tissues or organs. It has been reported that mature pollen expresses on average 6044 protein-coding genes (average number from the different studies), of which around 10% pollen-specific (Honys and Twell, 2003; Pina et al., 2005; Loraine et al., 2013). Compared to the sporophytic tissue (ca. 12 000 protein coding genes), mature pollen displays a reduction in expression complexity due to the advanced functional specification. In addition, the pollen-expressed genes show an all-over broader expression range compared to other tissues (Schmid et al., 2005). Mature pollen actively expresses cell wall and cytoskeletal structural genes/proteins, as well as genes/proteins involved in signalling and vesicular trafficking. This ensures that the dry pollen, although metabolically inactive, already contains the entire molecular machinery that is required for germination and initial tube growth. Underrepresented in dry pollen, however, are gene ontology categories connected to transcription and protein synthesis processes.

The *Arabidopsis* transcriptome during microgametogenesis (Honys and Twell, 2004) reveals major transcriptional changes over the course of pollen development. The number of expressed genes decreases from ca. 12 000 in the UCM to ca. 7000 in the mature pollen, but the number of pollen-specific transcripts increases from 7% to 9% in the two stages, respectively, reflecting the functional specialization during development. The study has also reported that a major switch of gene expression characterizes the transition from bi-cellular to

tri-cellular stage (pollen mitosis II) based on the identified distinctive gene co-regulation patterns before and after PMII. Overrepresented at the UCM and BCP stage are mRNAs involved in cell cycle regulation and transcription (indicated as "early" developmental program genes), whereas in TCP and MPG signalling and cell wall metabolism genes (indicated as "late" genes) are actively transcribed, which is consistent with the ongoing differentiation process.

In addition to multiplying greatly the available knowledge about pollen biology and giving a global view on the developmental process, the transcriptomics study (Honys and Twell, 2004) provided the scientific community with valuable data about previously unknown genes expressed during pollen development. Based on this findings novel players of the pollen molecular machinery were characterized (Gibalová et al., 2009; Leydon et al., 2013; Verelst et al., 2007).

2.3 Identification of DUF1216 novel protein family expressed during pollen development

Gene expression in *Arabidopsis* pollen has been the subject of multiple scientific studies, which are consistent in their major findings about the approximate number and the functional categories of the predominantly expressed genes in mature pollen grains (Honys and Twell, 2004; Loraine et al., 2013; Pina et al., 2005; Schmid et al., 2005). However, the expressed mRNA is not necessarily translated into protein and, therefore, several pollen proteomics studies have been conducted, aiming to complement the available transcriptomics data and further expand the knowledge about the pollen biology (Holmes-Davis et al., 2005; Grobei et al., 2009; Ge et al., 2011; Fu and Yang, 2014).

The study conducted by Grobei and colleagues (Grobei et al., 2009) used a shotgun proteomics approach to identify ca. 3500 unique proteins in the mature pollen of *A. thaliana*, including 530 previously undetected proteins. The general findings about the functional groups present in the mature pollen proteome were consistent with the available transcriptomics data, with a weak correlation between the protein and the corresponding mRNA abundance (Schmid et al., 2005). Overrepresented were Pfam domains related to signalling, vesicular trafficking, cytoskeleton, cell wall reorganization, and protein folding and stabilization, whereas categories connected to transcription, cell cycle progression and protein synthesis were underrepresented. These results reflect the metabolically inactive state

of the mature pollen, which already contains the necessary molecular machinery for the further developmental steps.

Among the overrepresented Pfam protein domains, the Domain of Unknown Function 1216 (DUF1216) was identified as being significantly overrepresented in the mature pollen proteome. Ten of the eleven known DUF1216 proteins were detected, and four of them were among the ten most abundant pollen proteins. In the course of the current study a twelfth member of the DUF1216 was identified and later added to the publically available resources. Table 2-1 represents the DUF1216 genes with their locus identifiers and the arbitrary names assigned to them for simplicity.

Table 2-1 Arbitrary names assigned to the DUF1216 members.

Arbitrary names	Gene
DUFF1/ D1	AT3G28770
DUFF2/ D2	AT3G28780
DUFF3/ D3	AT3G28790
DUFF4/ D4	AT3G28810
DUFF5/ D5	AT3G28820
DUFF6/ D6	AT3G28830
DUFF7/ D7	AT3G28840
DUFF8/ D8	AT3G28980
DUFF9/ D9	AT5G39870
DUFF10/ D10	AT5G48575
DUFF11/ D11	AT5G61720
DUFF12/ D12	AT3G28750

Not all DUF1216 members were detected by previous pollen transcriptome studies. *DUFF4* and *DUFF5*, which were presented by one ambiguous Affymetrix probeset, were identified as unique peptides by (Grobei et al., 2009). In contrary, *DUFF12*, which was the most abundant transcript in (Honys and Twell, 2004), was not detected at the protein level. A probeset for *DUFF10* was not present on the Affimetrix array and no peptide spectral counts were detected. Nevertheless, DUFF3/6/8/11 were among the top ten expressed proteins in the mature pollen, as well as among the highest expressed proteins in the sperm cells and growing pollen tube (Monica Schauer, unpublished data). Moreover, spectral counts for all members, except for DUFF1/10, were detected when studying the sperm cell proteome.

The proteins of the DUF1216 family share the Pfam DUF1216 in one or two copies (Fig. 2-4) and are characterised by low sequence identity within the family (below 30%) with the

exception of DUFF4/5/8, which share more than 75% sequence identity. Bioinformatic analysis of the DUF1216 domain neither revealed distant homologs nor a predicted structure for DUF1216 (Grobei et al., 2009). However, it has been reported that the *BcMF10* gene expressed in the tapetal cells and during the microspore stage of pollen development in *Brassica rapa ssp. chinesis* shares sequence similarity to the domain DUF1216 of *Arabidopsis* and plays a role during pollen intine formation (Huang et al., 2008).

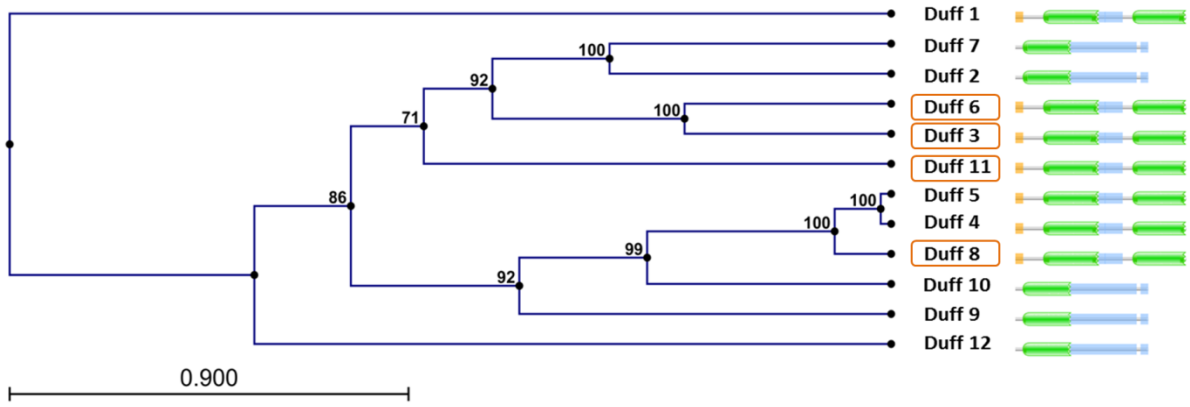

Figure 2-4 Phylogenetic tree and domain structure of the DUF1216 protein family.
The four most abundant proteins are highlighted using rectangles. The green shapes represent the domain DUF1216 within the protein sequence (light blue). The internal node numbers represent the result of the Bootstrap analysis. The domain structure representation is derived from (Finn et al., 2014)**.**

The potential interactor network of the DUF1216 members was analysed applying the sophisticated probabilistic functional algorithm AraNet, combining multiple "omics" data from different organisms (Grobei et al., 2009; Lee et al., 2010). The five DUF1216 genes present in the AraNet dataset were accounted to the functional category "endomembrane system" and the conducted *in silico* analysis predicted altogether 108 interaction partners for them. Solid evidence for co-expression in pollen was obtained for 67 of these potential interaction partners and around half of them were annotated to functional categories linked to cellular trafficking. For some of the predicted interactors, like SYP21 and SYP22 Qa-SNARE proteins, mutant phenotypes causing pollen defects were reported (Sanderfoot et al., 2001). Based on these theoretical findings, it was predicted that the DUF1216 family proteins are part of the cellular trafficking machinery (Grobei et al., 2009).

As it was introduced above, the DUF1216 family members were detected at the mRNA level in various transcriptome studies as being characteristic for the mature pollen grain (Winter et

al., 2007; Zimmermann et al., 2004), which is illustrated by Fig. 2-5. Nine of the DUF1216 family members have been found at the transcript level in earlier stages of pollen development (Honys and Twell, 2004). Studies describing the transcriptional profile of dry, hydrated, and germinated pollen (Wang et al., 2008b) confirm the expression pattern of the DUF1216 family genes in mature pollen and show that during germination and tube growth the *DUFF* transcript levels are decreasing.

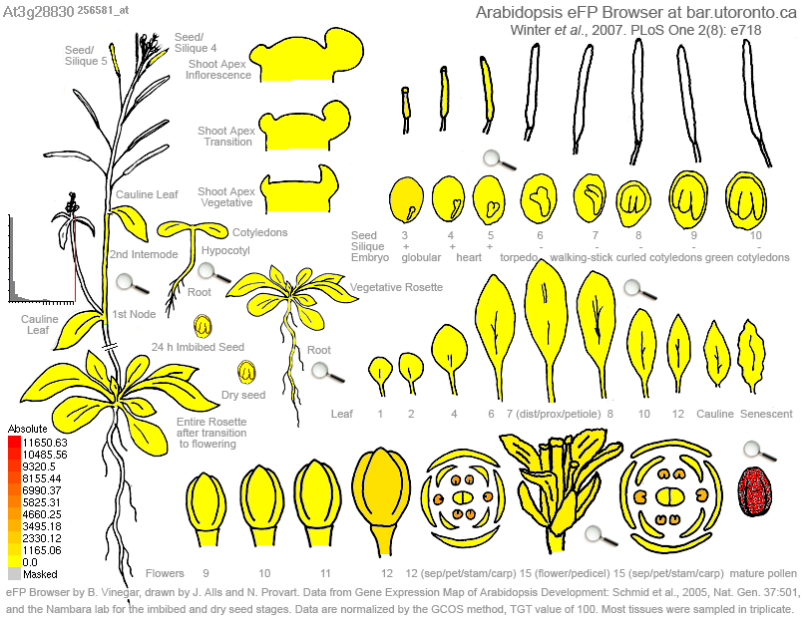

Figure 2-5 Graphical output of the *Arabidopsis* eFP Browser gene expression tool.
The pollen-characteristic gene expression pattern is shown on the example of *DUFF6* mRNA.

The physical location of the DUF1216 family genes in the *Arabidopsis thaliana* genome is shown in Fig. 2-6. Interestingly, nine of the twelve genes are located in a compact 198-kbp-cluster at the upper arm of chromosome 3, with eight of them (*DUFF12/1/2/3/4/5/6/7*) spanning the physical distance of 43 kbp and interrupted by only one gene, which is not a member of the family. *DUFF8* is separated from this cluster by other 30 genes located in between. The *DUFF9/10/11* are located at the lower arm of chromosome 5. The described location of the DUF1216 family genes represents a challenge for further experimental work aiming at the functional characterization of the DUF1216 family using a reverse-genetics approach like crossing insertion mutants of the individual genes to create a multiple knock-out mutants. Therefore, alternative approaches were considered, and two different strategies allowing overcoming this technical challenge were applied: studying *A. thaliana* mutants

presumably deficient in multiple *DUFF* genes, and designing artificial microRNA constructs targeting several of the DUF1216 members. The results of these experiments are described in chapter 4.

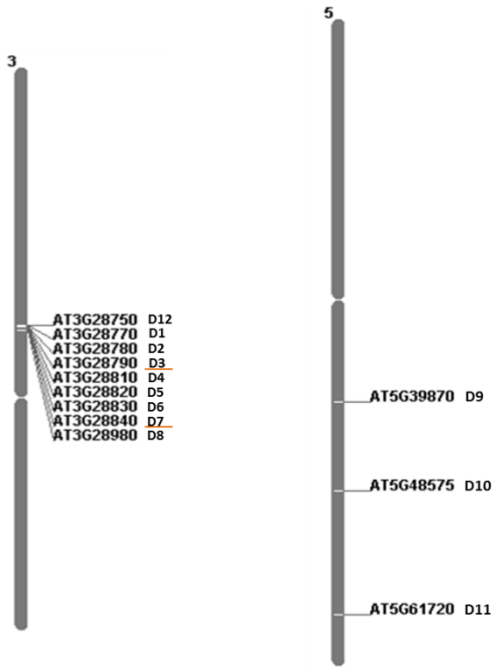

Figure 2-6 Chromosomal location of the DUF1216 family genes.
Eight of the genes (*DUFF12* to *DUFF7*) form a 43-kbp cluster on chromosome 3. The physical distance between *DUFF12* and *DUFF8* is 198 kbp and 30 other genes are located in between *DUFF7* and *DUFF8*. The red lines represent the loci of genes that do not belong to the DUF1216 family. Source of the image: TAIR Map Viewer tool.

2.4 Aims of this thesis

The aim of this work was the functional characterization of the newly discovered protein family DUF1216 in *A. thaliana* pollen, which would contribute to our understanding in the field of pollen biology.

The novel pollen-specific protein family DUF1216 has been identified in a previous study on pollen proteome and several of the twelve members of DUF1216 family have been detected among the most abundant proteins in the mature pollen grain. In addition, transcriptome data revealed the expression profiles of the DUF1216 family members during pollen development, germination, and pollen tube growth. Preliminary bioinformatics analysis could not identify functional homologs or make a structural prediction for the DUF1216 proteins. Taken

together, there were indications that the large DUF1216 pollen-specific protein family plays a role in the reproductive process, but any theoretical or functional evidence were still missing. The goal of this thesis was to establish a biological system using a reverse-genetics approach, allowing the functional characterization of the DUF1216 family proteins and trying to elucidate their contribution to the male gametophyte development and reproductive function. Considering the tandem chromosomal location of nine of the *DUFF* genes and the technical challenge to obtain multiple knock-out mutants by crossing individual T-DNA insertion lines, an artificial microRNA approach was chosen to help revealing the role of the DUF1216 members during male gametophyte development or later during the reproduction process. In the scope of this thesis was to design and clone amiRNA constructs targeting different members of the DUF1216 family and introduce them into *Arabidopsis thaliana*. Based on the protein expression data, three different promoters were chosen to drive the expression of the amiRNAs against the DUF1216 family members: the ubiquitously expressed Ubiquitin10, the pollen-specific LAT52, and the sperm cell specific H3.3 promoter. Further objectives were to extensively characterize the stable expression lines, quantifying the gene expression and screening for reproductive phenotypes. The detailed analysis of the potential pollen-related reproductive phenotype should have been complemented by information about the sub-cellular localization of the members of the DUF1216 protein family. Furthermore, a broader project goal was the identification of potential interactors of the DUF1216 family proteins using different methods to study the protein-protein interactions, which would provide valuable information about their molecular function.

Altogether, these data should give novel insights about the importance and the function of the pollen-specific DUF1216 proteins.

3 Material and Methods

3.1 Plant material, growth and transformation

Arabidopsis thaliana (L.) Heynh., ecotype Columbia (Col-0) was used for establishing stable mutant lines and as a control for all experiments.

Depending on the experimental purpose, *Arabidopsis* plants were grown on soil or on sterile 1x MS plates (Murashige and Skoog, 1962). In order to sterilize the seeds they were incubated in 70 % ethanol and 0.05 % Triton X-100 for 30 minutes, followed by incubation in 95% ethanol for 15 minutes and then sterile dried. The seeds were kept for 48 h at 4°C in darkness for stratification and then grown under long day conditions (16 h light, 8 h darkness), at a temperature of 22 °C and with a light intensity of 200 µmol/m^2s.

For establishing stable mutant lines approximately 12 weeks old *A. thaliana* plants were transformed via the floral dip transformation method (Clough and Bent, 1998).

For crossing procedures young closed floral buds were emasculated 2 days prior to pollination in order to prevent self-pollination. For transmission efficiency (TE) studies 5 to 12 flowers from at least two different plants were pollinated per single cross and at least 200 seeds were analysed to determine transmission rate. TE was calculated as percentage of F1 heterozygous mutant seedlings from the WT-scored F1 progeny of the cross.

The established stable *A. thaliana* mutant lines are listed in Appendix (IV).

Nicotiana benthamiana (L.) was used for transient gene expression assays. Single colonies of *Agrobacteria tumefaciens*, transformed with binary plasmids, were grown overnight in LB medium with appropriate antibiotics. The cultured bacteria were centrifuged (15 minutes at 4000 rpm) and resuspended in 10 mM MES-KOH (pH 5.6), 10 mM $MgCl_2$, 150 µM acetosyringon. The cell density was adjusted to 0.7-0.8. Each clone was mixed at 1:1 with *Agrobacteria* expressing the p19 viral silencing suppressor (Voinnet et al., 2003) and the mix was incubated at room temperature for 2-4 h. The leaves of well-watered *N. benthamiana* plants were infiltrated and the leaf material was analysed under the microscope within three days.

3.2 Standard pollen assays and imaging

In vitro pollen germination

Pollen grains from open *A. thaliana* flowers were germinated to *in vitro* on solid medium using a standard approach (Boavida and McCormick, 2007). The germinated pollen was analysed using phase contrast microscopy or fluorescence microscopy within 5 hours after transferring the pollen grains on solid medium.

Alexander staining of mature pollen grains and whole anthers

Pollen viability tests were performed using the Alexander staining method (Alexander, 1969). For differential staining of mature pollen grains open flowers of 4 to 5 weeks old *A. thaliana* plants were used. Pollen was fixed on a glass slide with 10% EtOH and imaged in a droplet of Alexander stain. At least 300 pollen grains were counted for every sample.

Whole anthers were incubated 12 hours in Alexander solution, which was exchanged with FPA 50 fixative (5:5:90 Formalin : Propionic acid : 50% EtOH) for another 12 hours. FPA 50 was replaced with 70% EtOH. The anthers were dissected and imaged in Herr clearing solution (Herr, 1971) using a Leica DMR light microscope (Leica Microsystems).

DAPI staining of pollen nuclei

Mature pollen grains were fixed on a glass slide with 10% ethanol and imaged in a droplet of DAPI solution (0.4 µg/ml DAPI, 0.1 M Sodium phosphate pH 7, 1 mM EDTA, 0.1 % v/v Triton X-100) using a fluorescence microscope DM6000 B (Leica Microsystems).

For imaging pollen from earlier developmental stages whole inflorescences were pre-fixed in an ethanol-acetic acid solution (3:1 v/v), which was exchanged with 70 % ethanol. Anthers were dissected on a glass slide in a droplet of DAPI solution and the released pollen was examined using an UV-light source (excitation wave length 358 nm, emmission peak at 470 nm).

Aniline blue staining of pollen tubes

A. thaliana siliques were fixed 2 days after pollination in a 9:1 (v/v) EtOH – acetic acid solution for 12h at 4°C. Further handling was performed as described in (Huck et al., 2003) and samples were analysed using an UV-light source.

Microscopy equipement is listed in Appendix (IV).

3.3 Bacterial strains, growth and transformations procedure

Escherichia coli DH5α (Hanahan, 1983)

Genotype: (φ80d lacZΔM15) Δ(lacZYA-argF) recA1 endA1 hsdR17 supE44 thi-1 gyrA96 relA1 deoR

Escherichia coli DB3.1 (Miki et al., 1992)

Genotype: F- gyrA462 endA1 glnV44 Δ(sr1-recA) mcrB mrr hsdS20(r_B^-, m_B^-) ara14 galK2 lacY1 proA2 rpsL20(Sm^r) xyl5 Δleu mtl1

DB3.1 cells were used to propagate plasmids containing the ccdB operon.

Agrobacterium tumefaciens GV3101 (Koncz and Schell, 1986)

Genotype: GV3101 carries the Ti-plasmid pMP90 (GV3101::pMP90). The strain has a chromosomal resistance to rifampicin; the Ti-plasmid mediates resistance to gentamicin.

Agrobacterium tumefaciens was used for stable transformation of *Arabidopsis thaliana* and for transient expression of recombinant proteins in *N. benthamiana*.

Escherichia coli and *Agrobacterium tumefaciens* cells were grown at 37°C and 28°C respectively, on LB plates or in LB liquid medium with appropriate antibiotics.

Standard heat shock transformation procedures were applied for competent bacterial cell transformation with plasmid DNA (Hellens et al., 2000; Inoue et al., 1990).

3.4 Standard molecular biology techniques and corresponding equipment

3.4.1 Preparation and handling of nucleic acids

Various laboratory applications like molecular cloning, plant or bacterial selection and expression studies require preparation and handling of nucleic acids. In this work the following molecular biology methods were used:

Extraction of plasmid DNA from bacteria

Extraction of genomic DNA from plants

Extraction of RNA from plants and cDNA synthesis

Gel electrophoresis and gel extraction of DNA-fragments

Polymerase chain reaction (PCR) and PCR-based techniques: RT-PCR, PCR-restriction fragment length polymorphisms/cleaved amplified polymorphic sequences (PCR-RFLP /

CAPS) (Konieczny and Ausubel, 1993), thermal asymmetric interlaced (TAIL-) PCR (Singer and Burke, 2003), restriction site extension (RSE-) PCR (Ji and Braam, 2010)
Molecular cloning
Southern blot analysis (Southern, 1975): non-radioactive and radioactive assay

All experimental procedures were performed using standard protocols (Sambrook and Russel, 2012) or following the manufacturers' manuals.
The Appendix section (IV) contains a table of used oligonucleotides and a list of used molecular biology reagents, kits, and equipment.

3.4.2 Cloning of DUFF fluorescent fusion proteins

Coding sequences of *DUFF3*, *DUFF7*, and *DUFF11* were PCR-amplified from genomic DNA (gDNA) template. attB recombination sites were incorporated into the amplification product to make use of the Gateway cloning technology (Life Technologies). BP reactions with the donor vector pDONR207 created the corresponding entry clones. LR reactions with the pMDC83 vector (Curtis and Grossniklaus, 2003) produced expression clones, in which GFP was C-terminally fused to the *DUFF*-ORFs under the control of the viral 35S promoter.
2000 bp upstream of the coding sequence of *DUFF7* were amplified using gDNA as a template. Primers were designed to introduce HindIII and BamHI cutting sites into the promoter sequence, which were used to replace the 35S promoter in the *DUFF7* expression clone with the native *DUFF7* promoter.
1000 bp upstream of the coding sequence of *DUFF11* were amplified from gDNA template. Primers were designed to introduce HindIII and SpeI cutting sites into the promoter sequence. The 35S promoter of the *DUFF11* expression clone was replaced with the native *DUFF11* promoter.
GFP-fusion protein expression was analyzed using a confocal microscope in the 500 to 560 nm emission range, using 488 nm argon laser to excite the fluorophore.
The primers used for cloning the C-terminal GFP-fusion versions of the *DUFF* genes are listed in Appendix (IV).

3.4.3 Semi-quantitative and quantitative PCRs

RNA for semi-quantitative or quantitative reverse transcription PCRs was extracted from the tissue of interest (flowers, anthers, leaves, stems) using standard phenol-chloroform extraction method, or with the help of the NucleoSpin® RNA Plant Kit (Macherey-Nagel). Efficient DNase treatment of the RNA was essential for further procedures. After quantification and quality control using the NanoDrop (Thermoscientific), the Agilent 2100 Bioanalyser (Agilent Technologis), and gelelectrophoresis the RNA was reverse transcribed into cDNA using oligo dT-, random hexamere-, or gene-specific primers. For performing the PCRs, cDNA was diluted to different extent depending on the quantity of starting plant material.

For the semi-quantitative approach the linear phase of the reaction for every primer pair was determined to ensure proper quantification results. PCR reactions were loaded on an agarose gel and the strength of the fluorescent signal was converted into a relative expression value.

Primers for qPCRs were designed following the SYBR® Green Assay Design requirements of Beacon Designer software and their specificity and amplification efficiency were determined.

Normalization using several internal reference genes (Ling and Salvaterra, 2011) was usually performed for both semi-quantitative and quantitative PCR experiments. The reference genes *POLYUBIQUTIN21* (Czechowski et al., 2005) and *ACTIN11* (Huang et al., 1997) used for data normalization in this work were validated for this particular quantification assay.

Primers used for semi-quantitative PCRs, quantitative PCRs, as well as the primers for reference genes are listed in the Appendix (IV).

3.4.4 Southern blot

The Southern blot technique was used for detecting and quantifying the number of T-DNA insertions present in different mutant plants/lines. Genomic DNA was isolated from leaves using standard phenol-chlorophorm extraction method and digested using restriction enzymes (XbaI, AscI, EcoRV, SacI were used in different experiments). After separation of the fragments on 0.8% agarose gel, the DNA was transferred on a positively charged nylon membrane (Nylon Membranes, positively charged, Roche Diagnostics) via capillary blotting. Probes detecting different parts of the T-DNA sequence were designed. Figure 4-11 illustrates the probe binding positions at the T-DNA and primers for the probe synthesis are listed in the Appendix IV.

DIG-dUTP-labeled probes were synthesized by PCR, detected with anti-digoxigenin-AP Fab fragments and visualized with the chemiluminiscence CDP-star substrate (The DIG System Labeling and Detection of Nucleic Acids, Roche Diagnostics). Detection was performed by exposing the membrane to an X-ray film Super RX (Fujifilm) or using the ChemiDoc™ XRS+ System (BioRad).

For the radioactive assay, probes were labeled using α-^{32}P dCTP using the Nick translation protocol (NEB) and probe visualization was performed by exposing the membrane to an X-ray film (Fujifilm).

3.4.5 Designing and cloning amiRNA constructs

An artificial microRNA (amiRNA) approach (Schwab et al., 2006) was chosen to downregulate the mRNA levels of the of DUF1216 family members. amiRNA are single-stranded small (21 nucleotide long) RNA species resembling the naturally expressed miRNAs in the plant, but specifically designed to target individual genes or groups of genes based on sequence similarity. The expression of amiRNAs depends on the endogenous miRNA molecular machinery to post-transcriptionally silence the genes of interest (Fig.3-1) (Sablok et al., 2011).

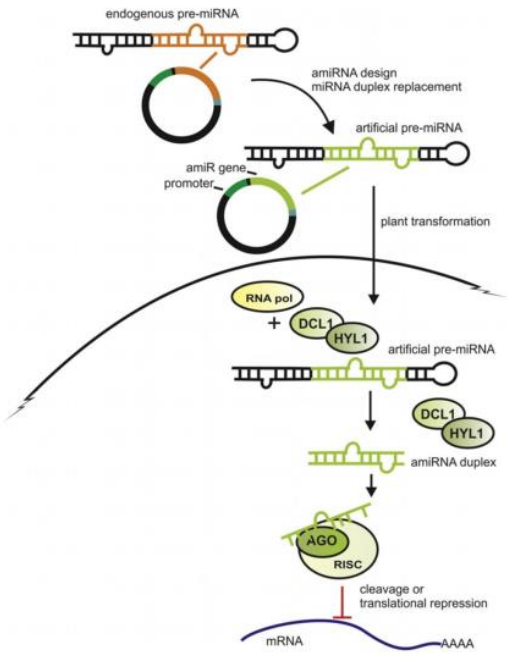

Figure 3-1 Molecular mechanism of generating and *in planta* processing of amiRNAs.
Derived from (Sablok et al., 2011).

The Web MicroRNA Designer (WMD) tool (Ossowski et al., 2008) version 3.1 was used to design the amiRNA molecules targeting multiple genes or single members of the DUF1216 family. Table 3-1 shows the sequences of the two constructs used in this work.

Table 3-1 amiRNA molecules and their targets in the DUF1216 family.

Name of the amiRNA	Sequence	Target genes
amiRNA2x	TAAACATTCTACAGGTCGCTG	AT3G28780 (*DUFF2*) AT3G28840 (*DUFF7*)
amiRNA5x	TAACGAATTGGGTTGTGACTT	AT3G28790 (*DUFF3*) AT3G28810 (*DUFF4*) AT3G28820 (*DUFF5*) AT3G28830 (*DUFF6*) AT3G28980 (*DUFF8*) AT5G48575 (*DUFF10*, potential target)

Site-directed mutagenesis was performed using the pRS300 plasmid carrying a miR319a precursor (Schwab et al., 2006) to introduce the amiRNA sequences of interest and generate the amiRNA containing precursor. The precursor was then introduced into the pDrive cloning vector (Qiagen PCR Cloning Kit) and attB sites were added by PCR in order to introduce the PCR fragment into pDONR207 vector via BP recombination reaction, generating entry clones (Gateway Cloning, Life Technologies).

Ubiquitin10 and LAT52 promoters were amplified from vectors pTKan and pGreenII-0179 (Krebs et al., 2012; Boisson-Dernier et al., 2008) and subsequently cloned into destination vectors of interest pHA1 and pQAN1, respectively, using AscI and XbaI restriction sites. pHA1 (Hiroko Asano, unpublished) and pQAN1 (Quy Ngo, unpublished) were generated by introducing the Gateway cloning cassette into the minimal binary pMOA vectors (Barrell and Conner, 2006) and display *in planta* kanamycin and basta resistance, respectively.

Performing LR recombination reactions with entry clones containing the amiRNA precursors and the destination vectors containing the promoters of interest, allowed to create different expression clones, which were used for stable *A. thaliana* transformation. Fig. 3-2 represents the T-DNA structure of two of the expression clones relevant for this work.

The primers used for engineering and cloning of the amiRNA constructs are listed in Appendix (IV).

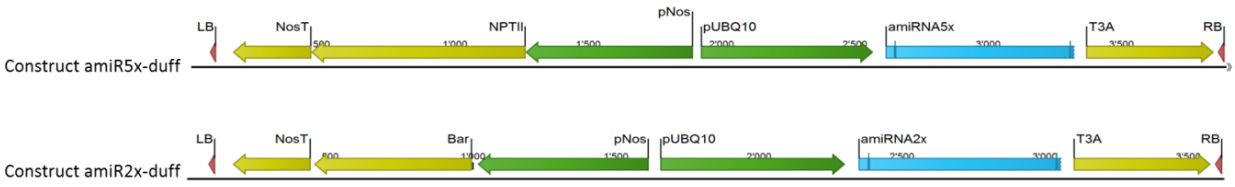

Figure 3-2 T-DNA structure of plant expression vectors carrying amiRNA5x (construct amiR5x-duff in pHA vector) and amiRNA2x (construct amiR2x-duff in pQAN vector).
The expression of both amiRNAs is driven by the Ubiquitin10 promoter.

3.5 Software tools

Data analysis and statistics were performed using MS Excel version 2010 (Microsoft) and R 3.2.1.

For sequence analysis the software CLC Main Workbench version 7 and previous, (Qiagen), as well as open source bioinformatics services (NCBI, Bioinfotmatics Toolkit by MPI Tuebingen) were used.

Genotyping primers for T-DNA lines were designed with the help of the T-DNA primer design tool provided by the SALK Institute Genomic Analysis Laboratory.

Analysis and processing of images were performed with ImageJ (version 1.49v and previous) and Imaris by Bitplane (version 7.6.5. and previous).

GENEVESTIGATOR Plant Biology gene expression platform (© NEBION / ETH Zurich) was used to identify and visualize DUF1216 gene expression patterns in different mutant backgrounds or experimental set-up.

Primers for qPCRs were designed using Beacon Designer™ software by PREMIER Biosoft.

3.6 Statistical tools

Chi-square statistical test (Yates, 1934) was performed to analyze whether there is a significant difference between the expected frequencies and the observed frequencies in one or more categories and therefore allow to test if a certain null hypothesis is true.

Analysis of variance (ANOVA) was performed using R to access the variability in gene expression among the amiRNA populations, as well as to study the effect of the gene expression levels on the phenotypic differences between the lines. We started with a multi-

way ANOVA, to test which factors (*DUFF* gene, inflorescence) influenced gene expression. We could not detect an influence of the inflorescence on gene expression and continued with one-way ANOVA in our analysis for each *DUFF* gene. The manual F was computed by dividing the mean sum of squares of the targeted factor (duff, line, or inflorescence) by the overall means square of its interaction terms (e.g. duff:line and duff:inflorescence) instead of the residuals term. The phenotype we analysed is proportion data and requires a binomial generalized linear model (GLM) with logit link function (Nelder and Wedderburn, 1972). We chose a quasibinomial GLM to account for overdispersion of the data. The *DUFF* genes differ in their gene expression. Therefore, we used the normalized linear gene expression data as fixed intercept (offset). Wild type data was used in several comparisons and we corrected for multiple testing in order to maintain the family-wise error rate at 5% (Gabriel, 1969).

For analysis of pollen abortion a principal component analysis (PCA) was conducted using the gene expression data of all amiR-duff lines. We evaluated the scree plots and tested for the influence of single *DUFF* genes expression on the principle components, or, in other words, we tested which genes are responsible for the variance depicted by the first two principal components.

Gene expression data were visualized in R by performing principal component analysis (PCA) and making clustered heat maps.

4 Results

4.1 The expression of the DUF1216 family genes is restricted to the male part of the flower

Proteomics findings and gene expression data (see section 2.3) about the male tissue-specific expression pattern of the DUF1216 members were confirmed by performing semi-quantitative PCR on cDNA derived from different plant parts and quantitative PCR (qPCR) on cDNA from emasculated flowers. Figure 4-1 shows that *DUFF*-gene expression was detected in the floral samples and only very low expression signal could be detected in the leaf- and stem samples. No gene expression signal could be detected when performing qPCR for the DUF1216 members on emasculated floral tissue (data not shown). Experiments were performed using Col-0 WT plants.

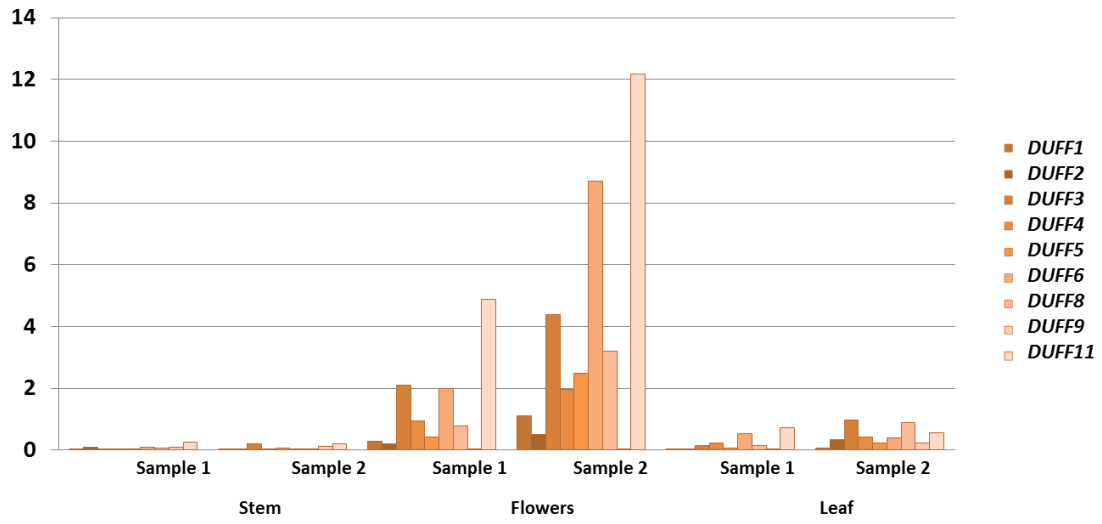

Figure 4-1 Relative DUF1216 gene expression in different plant tissues.
The Y-axis represents the relative signal of *DUFF* gene expression after 25 PCR cycles.

A standard reverse-genetics approach to reveal novel protein function is to disturb the sequence of the gene of interest and study the mutant phenotype. Helpful tools are the various existing T-DNA collections. Preliminary analysis of several individual T-DNA insertion lines for different *DUFF* genes did not show any abnormal phenotype (M. Grobei, A. Nestorova,

data not shown). This could be explained with functional redundancy within the family, since at least 10 of the members are expressed in the male reproductive tissues.

Considering the chromosomal location of the DUF1216 genes with eight of them clustering together on chromosome 3 (Fig. 2-6), generating multiple knock out (KO) mutants by crossing T-DNA lines with single insertions for the *DUFF* genes is challenging. Therefore, we used alternative approaches to address this issue, such as described in chapters 4.2 and 4.3.

4.2 Using different *Arabidopsis* mutant backgrounds as a tool to study DUF1216 protein function

4.2.1 The GENEVESTIGATOR gene expression platform and mutant line selection

The GENEVESTIGATOR gene expression platform offers the resources to investigate the gene expression patterns at various developmental stages, in different tissues or in specific mutant backgrounds and experimental contexts. The GENEVESTIGATOR Mutation tool search resulted in the identification of several *A. thaliana* mutants, displaying significant (more than 2-fold in the log2- expression scale) differential regulation of multiple DUF1216 members. Figure 4-2 shows a GENEVESTIGATOR Mutation Tool output image of different mutant backgrounds with reduced *DUFF* expression levels. Some of the mutants discovered in this analysis were male sterile, like *ms1* (Wilson et al., 2001b) and *ga1* (Tyler et al., 2004) and, therefore, they were not a subject of further experimental interest.

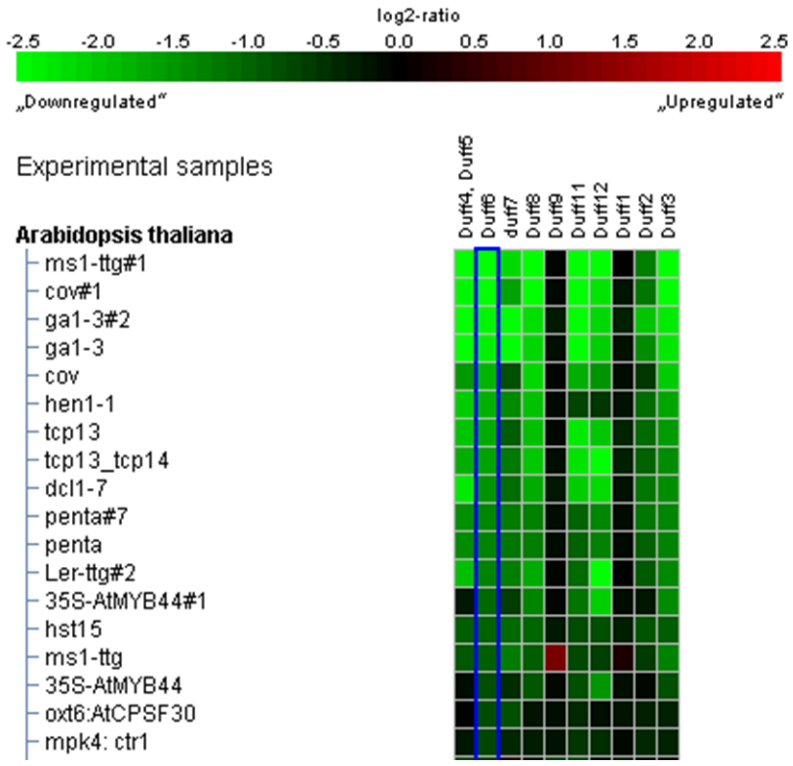

Figure 4-2 GENEVESTIGTOR Mutation Tool graphical output.
Several *A. thaliana* mutants with reduced *DUFF* gene expression levels compared to the corresponding control WT genotype in the experiments. *DUFF4* and *DUFF5* are presented by one ambiguous Affimetrix probeset, which is reflected by the GENEVESTIGATOR analysis.
Among the male sterile mutants like *ms1* (Wilson et al., 2001b) **and *ga1*** (Tyler et al., 2004)**, pollen-producing mutants with reduced *DUFF* gene expression levels were identified, like *dcl1-7, cov1, hen1-1* (see the text).**

Several of these mutants with no known severe male reproductive defects were obtained, including *dcl1-7* (Golden et al., 2002), *cov1* (Parker, 2003), *hen1-1* (Chen et al., 2002a) where the *DUFF* genes were predicted to be downregulated (nine out of twelve in *dcl1-7*, ten out of twelve in *cov1*, and eight out of twelve in *hen1-1*), and *atmyb44* (Jung et al., 2008) with expected upregulation of at least seven of the DUF1216 members (GENEVESTIGATOR graphical representation not shown). Table 4-1 shows the predicted *DUFF* gene expression in the mutants. As a control, the expression pattern of the pollen specific oleopollenin genes (Mayfield et al., 2001) in these *A. thaliana* mutants was analysed, showing no differential regulation compared to WT.

Based on the preliminary data, the *DUFF* genes were expressed in the pollen grains. Therefore, in case of reduced *DUFF* gene expression, a pollen-related reproductive phenotype could be expected. In order to test this hypothesis, DAPI staining of the mature pollen grains of *dcl1-7*, *hen1-1*, and *cov1* mutants was performed allowing detecting the effects of

presumed *DUFF* genes downregulation on pollen nuclear architecture, but no mature pollen defects were identified (data not shown).

In an attempt to account for these experimental observations, the expression levels of the *DUFF*s were analysed using a semi-quantitative PCR approach (cDNA derived from floral tissue) and compared to the corresponding WT background. The results are presented in Figure 4-3. The *dcl1-7* and *myb44* mutants did not show the expected changes in their *DUFF* gene expression compared to Col-0 WT (downregulation and upregulation, respectively), and from both mutant genotypes in Ler WT background, *cov1* and *hen1-1*, only *hen1-1* plants showed the expected reduction in the *DUFF* gene expression. Therefore, *hen1-1* mutant plants were taken for further characterization.

Table 4-1 *DUFF* gene expression in different *A. thaliana* mutants according to the GENEVESTIGATOR Mutation Tool.

Mutant background	*DUFF* genes with predicted differential expression
dcl1-7	*DUFF2, DUFF3, DUFF4,5, DUFF6, DUFF8, DUFF9, DUFF11, DUFF12*
cov1	*DUFF1, DUFF2, DUFF3, DUFF4,5, DUFF6, DUFF7, DUFF8, DUFF11,DUFF12*
hen1-1	*DUFF2, DUFF3, DUFF4,5, DUFF6, DUFF7, DUFF8, DUFF9*
myb44	*DUFF2, DUFF3, DUFF4,5, DUFF6, DUFF8, DUFF9*

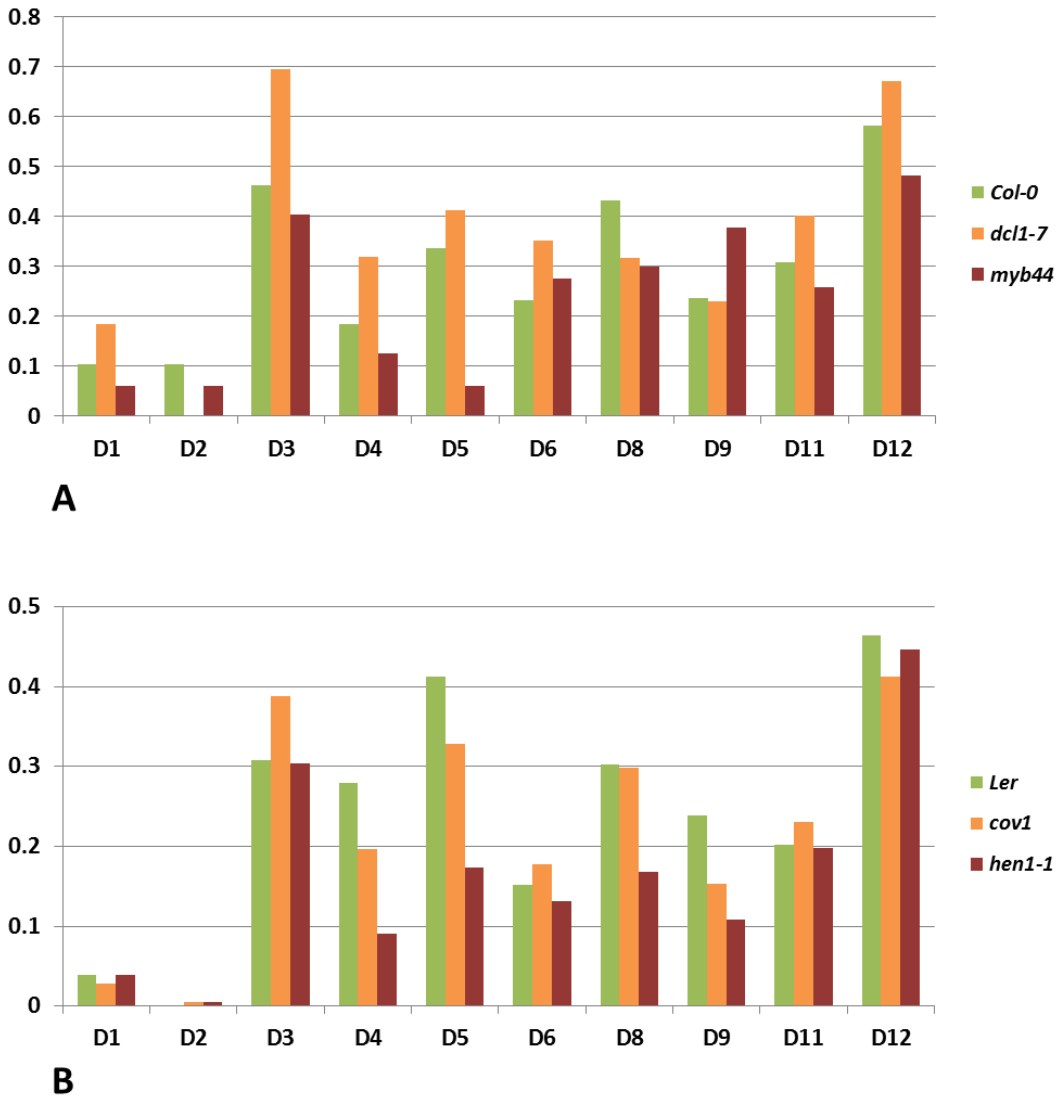

Figure 4-3 Relative DUF1216 gene expression in different mutant backgrounds.
A – *dcl1-7* (expected reduction in *DUFF* expression levels) and *myb44* (expected up-regulation) are in Col-0 background. The expression pattern of the *DUFF* genes does not correspond to the GENEVESTIGATOR data base prediction (see Table 4-1).
B – *cov1* and *hen1-1* (expected downregulation of *DUFF* expression) are in Ler genetic background. In *hen1-1* reduced expression levels for several of the *DUFF* genes can be measured.

The gene expression analysis on floral cDNA using semi-quantitative PCR approach was repeated and the predicted differential regulation of several *DUFF* members could be confirmed for the *hen1-1* mutant background (Fig. 4-4).

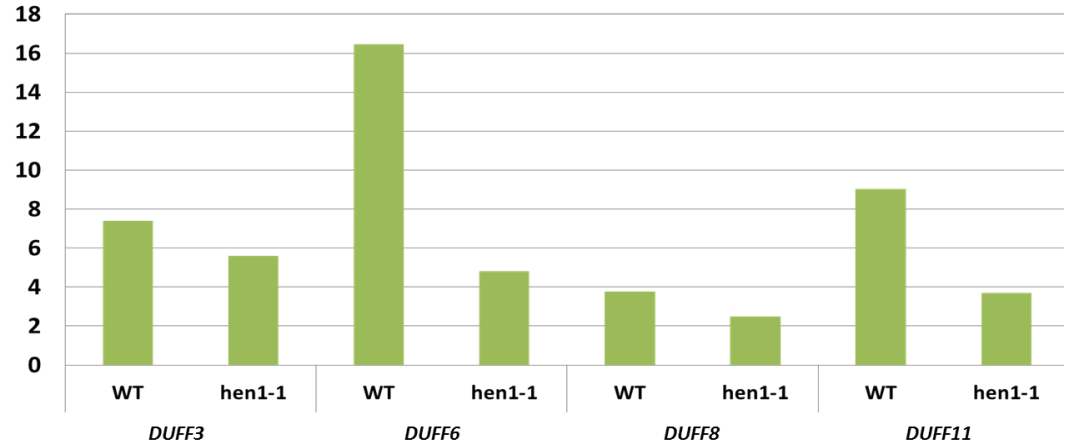

Figure 4-4 Relative DUF1216 gene expression in *hen1-1*.
Several of the *DUFF* genes showed reduced expression levels compared to the WT.

4.2.2 *hen1-1* shows reduced transmission efficiency of the mutant allele

HEN1 is a methyltransferase involved in the post-transcriptional modification of small RNAs. Plants carrying the *hen1-1* allele display pleiotropic phenotypes, including reduced fertility (Chen et al., 2002a). However, exact data about the male transmission efficiency in the mutant were not reported. Since it was confirmed that *DUFF* gene expression is reduced in *hen1-1*, it was important to show that the male reproductive function is disturbed in this mutant. This would support the hypothesis that the pollen-specific DUFF proteins are playing a role in the reproduction process. Quantification the transmission efficiency of the *hen1-1* mutant plants was performed and Table 4-2 summarizes the results of the reciprocal crosses. It was found that both male and female transmission efficiency are reduced in *hen1-1*.

Table 4-2 Transmission efficiency result *hen1-1*.
Both male and female transmission efficiency is reduced.

Cross (female x male)	HeZ	WT	TE
hen1-1+/- x Ler	77	99	76.23 %
Ler x *hen1-1*+/-	66	110	60.0 %

4.3 amiRNA reverse genetics approach to target the DUF1216 members

4.3.1 amiRNA: method of choice to study DUF1216

Ten of the DUF1216 proteins have been detected at protein level in the mature pollen and eight of the *DUFF* genes are located in a compact cluster on the upper arm of chromosome 3, as it was introduced in section 2.3. T-DNA insertion lines for several of these genes were analysed and no abnormal phenotype was detected (data not shown), which suggests that the proteins carrying the DUF1216 could act redundantly in the pollen. Generating a knock out insertional mutants for multiple members of the family via crossing T-DNA mutants for the different *DUFF* genes would help to elucidate the biological function of the proteins. However, the tandem chromosomal location of the *DUFF*s makes this approach not applicable for the DUF1216 family.

Therefore, an artificial microRNA reverse genetics approach was chosen to address the question about the biological function of the DUF1216 protein family. Multiple gene products can be targeted by using a single amiRNA construct making the method suitable for studying large gene families and/or several genetically linked loci.

4.3.2 Construct design, cloning, and transformation scheme

Four different amiRNAs (amiR-duff) were designed with the help of the Web MicroRNA Designer Tool (see 3.4.5) to target 10 of the DUF1216 family members. All amiRNAs have their binding site within the ORF of the mRNA molecules (Fig. 4-5).

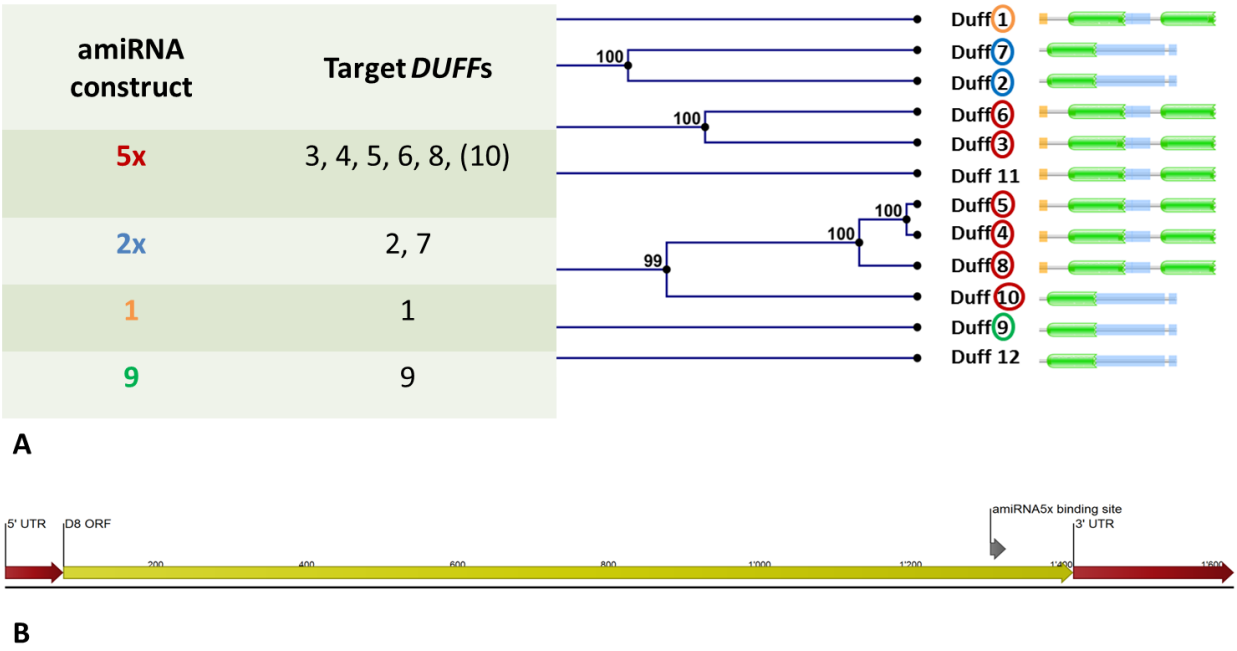

Figure 4-5 amiRNA constructs targeting different *DUFF* genes.
A – amiRNAs designed to target the DUF1216 family.
B – Binding position of amiRNA5x at the *DUFF8* mRNA open reading frame.

The amiR-duff precursors were cloned (see 3.4.5) under the control of the ubiquitously active UBQ10 promoter, the pollen specific LAT52 promoter (Twell et al., 1991), and under the sperm sell specific H3.3 promoter (Okada et al., 2005). The H3.3 promoter was chosen, since proteomics studies showed that DUF1216 proteins are characteristic not only for mature pollen, but are also present in the sperm cell proteome (Monica Schauer, unpublished data). A schematic summary of the generated constructs is presented on Figure 4-6.

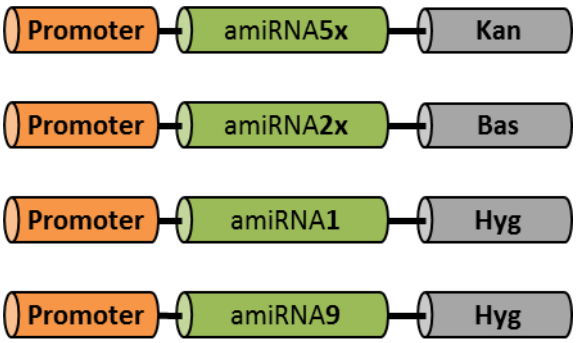

Figure 4-6 Graphical representation of the amiRNA constructs.
The four amiRNA (green) were cloned behind UBQ10, LAT52, and H3.3 promoters (orange) into plant expression vectors harbouring different selection markers (grey).

Cloning different amiRNA constructs under the same promoters into expression vectors carrying different selection markers *in planta*, allowed introducing multiple constructs into the same T0 plant. Such a transformation approach could help addressing assumed functional redundancy or synergistic effects of DUF1216 members. Based on this assumption, amiR-duff constructs were introduced into the *DUFF11* homozygous knock out line N653197 (*duff11*) in order to enhance the expected phenotypic effect. Three types of stable Col-0 *duff11*-transformants were generated: double transformants, carrying amiRNA5x and amiRNA2x constructs, single transformants carrying miRNA5x, and single transformants carrying amiRNA2x. This transformation scheme was applied to generate amiR-duff mutants, expressing pUBQ10 or pLAT52 driven amiRNA.

4.3.3 T1-transformant phenotype screen and line selection

Following the T0 *A. thaliana* transformation, T1 stable lines were obtained (double and single transformants under the UBQ10, or LAT52 promoter). Preliminary work conducted with these lines included gene expression analysis and phenotype screen.

To confirm the functionality of the introduced amiRNA constructs, semi-quantitative PCRs for the target *DUFF* genes were performed using floral tissue from T1 amiR-duff plants. Downregulation of the target genes to different degrees was detected in the single T1 lines. In total, *DUFF* gene expression was analysed in eight T1 UBQ10-driven double amiR-duff lines, five T1 LAT52-driven double amiR-duff lines, and three T1 UBQ10-driven single amiR5x-duff lines, all of them showing downregulation of the target genes in the range of 10 to 80 %. An example of the experimental findings is presented in Figure 4-7.

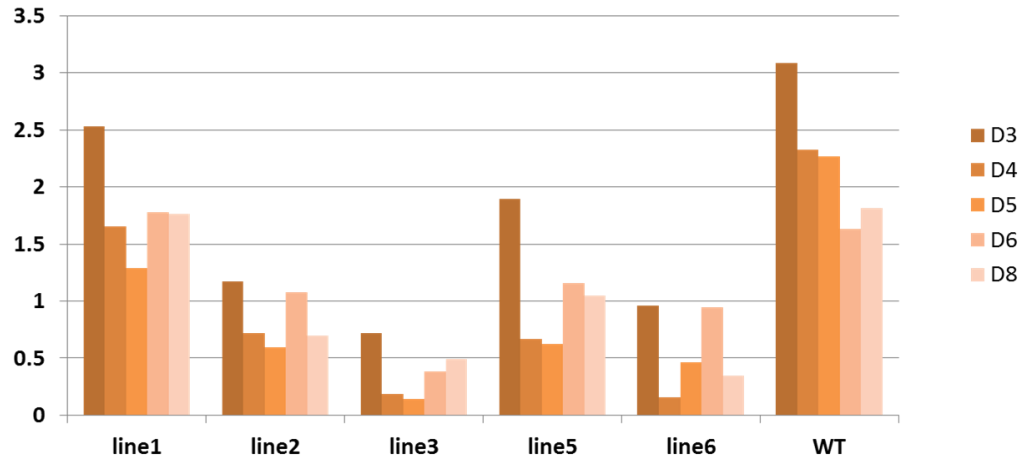

Figure 4-7 Relative DUF1216 gene expression in amiRNA pUBQ T1 double transformant plants.
Target *DUFF* genes are downregulated in lines expressing amiR5x and amiR2x under the UBQ10 promoter.

Since DUFF proteins are pollen-specific, T1 lines were subjected to a phenotype screen designed to identify pollen-originating reproductive defects.

Mature pollen grains from open flowers of T1 amiR-duff plants and Col-0 WT were stained with DAPI to visualize the nuclear architecture (Fig 4-8). Although viable mature pollen grains in amiR-duff plants did not display any defects in the nuclear constitution, a proportion (not quantified during these experiment) of non-viable pollen grains was observed in 10 out of 13 analysed lines.

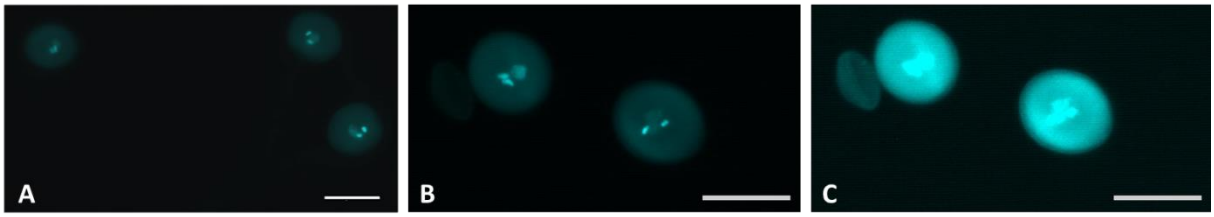

Figure 4-8 DAPI staining of mature pollen grains
A – Col-0 WT mature pollen with DAPI-visualized two sperm cell nuclei and a bigger vegetative cell nucleus.
B, C – amiR5x-duff (pUBQ10) Line 3 mature pollen. Nuclear constitution of mature mutant pollen grains is normal, but aborted pollen grains can be observed. Scale bar 25 µm.

In vitro pollen germination tests were performed with the T1 heterozygous amiR-duff lines and no significant difference in the proportion of non-germinated grains was measured (Fig.

4-9). The measured pollen abortion percentage in the mutants accounts for the differences in the percentage of germinated pollen grains.

In the later stages of the project the *in vitro* germination experiments were repeated with homozygous amiR-duff mutant plants in the T3 generation, but no differences compared to WT pollen germination rate was observed (data not shown).

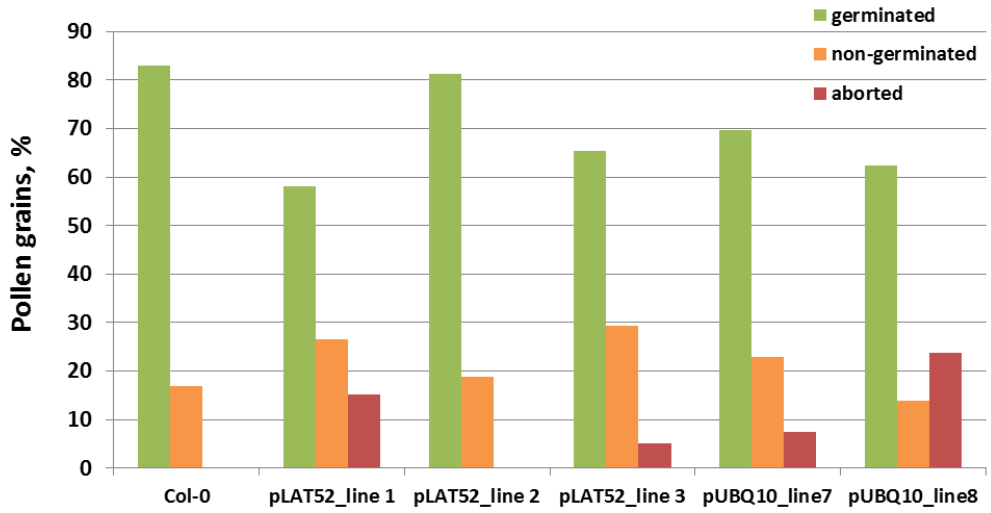

Figure 4-9 *In vitro* pollen germination of amiR-duff lines.
T1 double transformant amiR-duff lines (plants heterozygous for both amiR2x-duff and amiR5x-duff constructs) *in vitro* pollen germination rates are comparable to WT germination rate. The higher proportion of non-germinated pollen grains in the mutant lines is due to the presence of degenerated pollen grains.

DAPI staining of amiR-duff mature pollen grains revealed that plants expressing these constructs are affected in their pollen development. In order to better visualize and quantify this defect, Alexander differential staining of aborted and viable pollen grains was applied. Figure 4-10 illustrates the Alexander staining approach and Figure 4-11 summarizes the quantification of pollen abortion observed among T1 amiR-duff plants. In total, 18 out of 24 analysed T1 amiR-duff lines showed between 5 and 50% of aborted pollen grains, while pollen abortion in WT was only about 2%. The SALK line (*duff11*) used as T0 to generate the amiR-duff lines did not display pollen developmental defects when evaluated using the Alexander staining method (data not shown).

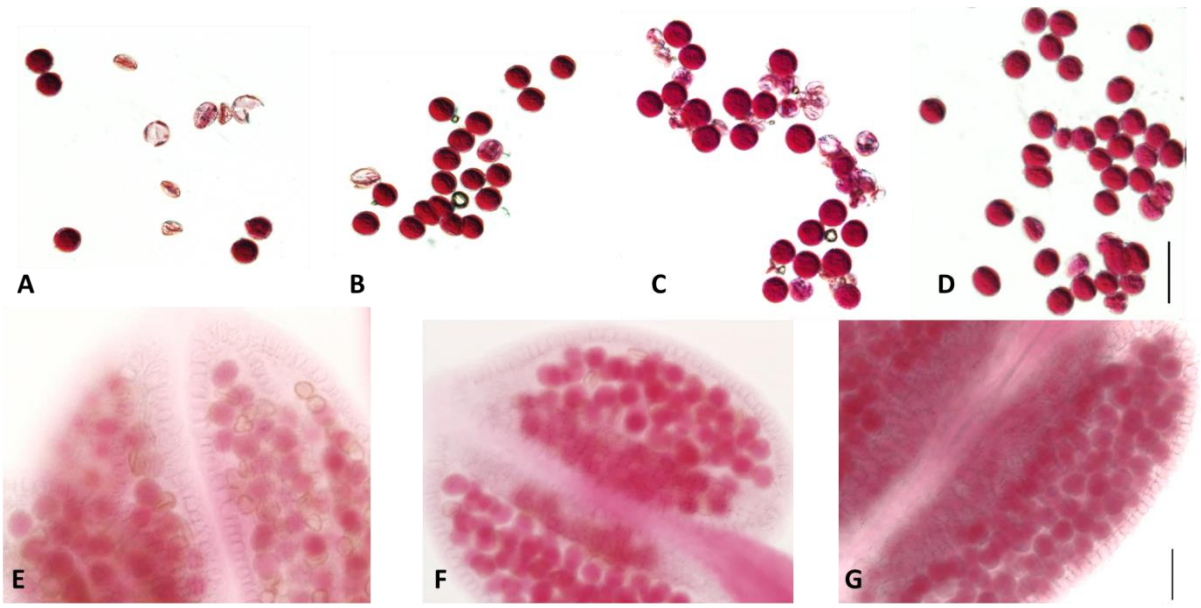

Figure 4-10 Alexander staining of T1 amiR-duff lines.
A, B, C, E, F – Alexander stained pollen and anthers of double amiR-duff mutant T1 plants.
A – pLAT52 line 1
B – pLAT52 line 3
C – pUBQ10 line 8
E – pUBQ10 line 8
F – pLAT52 line 1
D, G – Alexander stained pollen and anthers of Col-0 WT plants. Scale bar 50 µm.

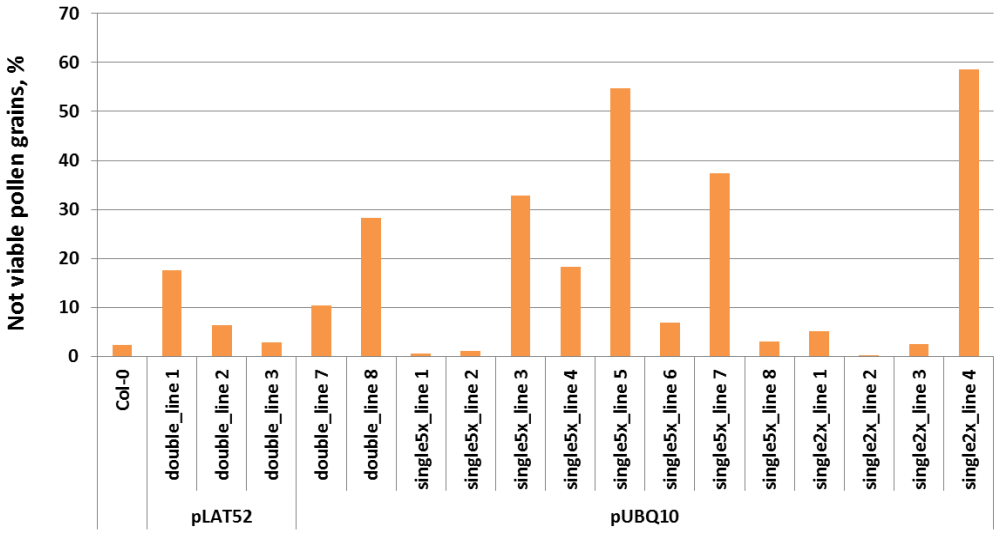

Figure 4-11 Pollen lethality among T1 amiR-duff *A. thaliana* lines.
Independent lines display different proportion of aborted pollen grains.

4.3.4 Single T-DNA insertion events are rare among amiR-duff populations

It has been reported that T-DNA insertions in *A. thaliana* genome are associated with chromosomal rearrangements, which can lead to misinterpretation of T-DNA-related phenotypes (Curtis et al., 2009). Moreover, chromosomal rearrangements (e.g. translocations) are often associated with gamete developmental failure in heterozygote state, since the rearrangements during meiosis result in genetically unbalanced gametes (Clark and Krysan, 2010; Curtis et al., 2009). On the other hand, multiple T-DNA copies can lead to transcription-dosage effects, which often can trigger silencing of the introduced transgene (Schubert, 2004).

In an attempt to identify mutant lines carrying single amiR-duff construct insertions and to minimize the possible effects of multiple inserts, T2 segregation analysis of the amiR-duff lines was combined with extensive Southern blot analysis.

In case of a single insertion it was expected that the mutant allele (due to the selection marker) would segregate in a Mendelian 3:1 (mutants : WT) ratio in the T2 generation of plants. Gametophytic effects would be reflected by a segregation distortion in T2 with a prevalence of plants not carrying the mutant allele (transmission defect). A prevalence of mutant plants (> 75%) indicates multiple T-DNA insertions in the segregating plant population. Altogether, 34 independent amiR-duff lines were subjected to segregation analysis in the T2 generation

and in 24 of them the mutant allele segregated either in a Mendelian manner (20), or there was a sign for a gametophytic defect (in four lines the WT individuals outnumbered the mutant ones).

Furthermore, to complement the segregation analysis of the amiR-duff lines, a Southern blot method was applied. As it was introduced in section 3.4.4., the Southern blot allows the quantification of the T-DNA insertion number based on the detection of gDNA fragments with a sequence-specific probe.

Probes for Southern blot recognizing different parts of the T-DNA sequence were designed to count the insertion number in the genome of amiR-duff lines (Fig. 4-12).

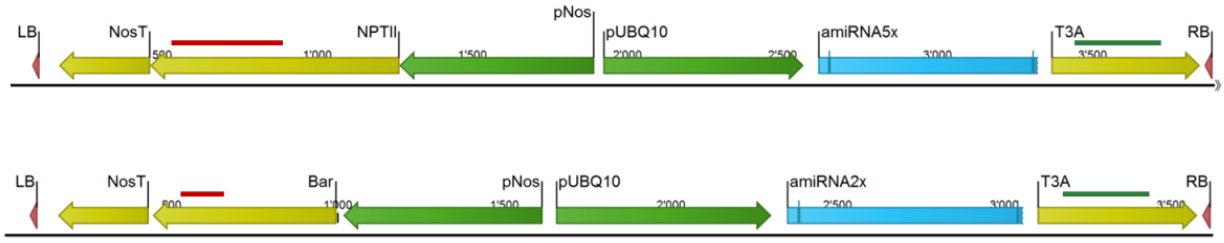

Figure 4-12 Probes for Southern blot and their binding sites in the T-DNA sequence.
Probes were designed to bind within the coding sequence of the selection markers, NPTII or Bar for vectors pHA1 and pQAN, respectively, which is schematically shown by the red lines in the figure. Additional probe was designed to recognize the T3A terminator sequence in both vectors used (green lines).

The Southern blot analysis revealed that nine out of twenty-seven single amiR-duff and three out of twelve double amiR-duff lines carried single copies of the introduced T-DNA (Fig. 4-13). Moreover, four T-DNA insertions were identified in the *duff11* T0 background line where the NPTII gene was silenced (picture not shown).

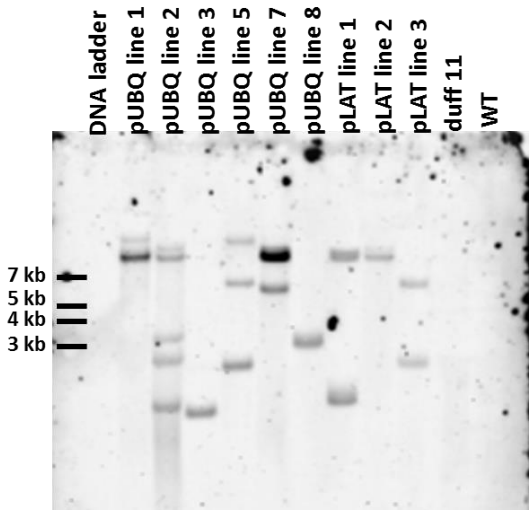

Figure 4-13 Southern blot analysis of amiR-duff lines.
Detection of T-DNA copy number in double amiR-duff lines with a probe against the Bar selection gene of pQAN. Two of the lines carry single T-DNA insertions.

The Southern blot findings were compared to the results of the T2 segregation experiment in order to select lines for further analysis. A line was selected if the following criteria were fulfilled: single T-DNA insertion in the plant genome or a tandem insertion combined either with a Mendelian 3:1 segregation pattern or segregation distortion potentially caused by a gamete failure. Based on these findings 15 amiR-duff lines were selected for more precise further characterization.

4.3.5 Homozygous amiR-duff expressing plant populations show strong variability in pollen abortion rates and reduced expression levels of amiRNA target genes

The characterization of gametophytic mutants is hampered if the mutation is in a heterozygous state, since half of the gametes are carrying the WT allele. Therefore, we performed segregation analysis with the 15 previously selected lines, allowing identifying homozygous for the amiRNAs individuals in the T3 generation. Homozygous plants were obtained for nine out of the eleven single amiR-duff lines and also for all four double amiR-duff lines analysed. For two of the single amiR-duff lines, no homozygous plants could be identified in the T3 screen.

The expected proportion of homozygous individuals in case of single insertion locus in the double transformant amiR-duff lines was 1/16. However, three of these lines showed a much higher rate of homozygosity based on the segregation of the mutant allele in T3:

- 23 homozygous individuals out of 40 analysed plants from line 8 (pUBQ10);
- 34 homozygous individuals out of 40 analysed plants from line 2 (pLAT52);
- 7 homozygous individuals out of 40 analysed plants from line 5 (pLAT52).

Characterising lines displaying segregation distortion is rather challenging and, therefore, further work was focused on single transformant amiR-duff lines.

Homozygous single transformant amiR-duff lines, carrying single T-DNA insertion or a tandem insertion in a single locus, and displaying a higher proportion of aborted pollen in T1 compared to WT, were again analysed for pollen degeneration phenotype in the T3 generation.

The pollen abortion phenotype was accessed individually for every identified homozygous T2 mother plant, based on the T3 segregation. The proportion of aborted pollen grains was quantified by pooling pollen from two T3 individuals originating from the same T2 mother plant. The experiment was performed twice using different T3 plants originating from the same T2 mother plants (Fig. 4-14). Pollen abortion rates were significantly different between individual lines carrying the same amiR-duff construct (lines 25- carrying amiR5x-duff, and lines 27- carrying amiR2x-duff). Furthermore, significant variability within the same line and also between the experimental replicates was observed.

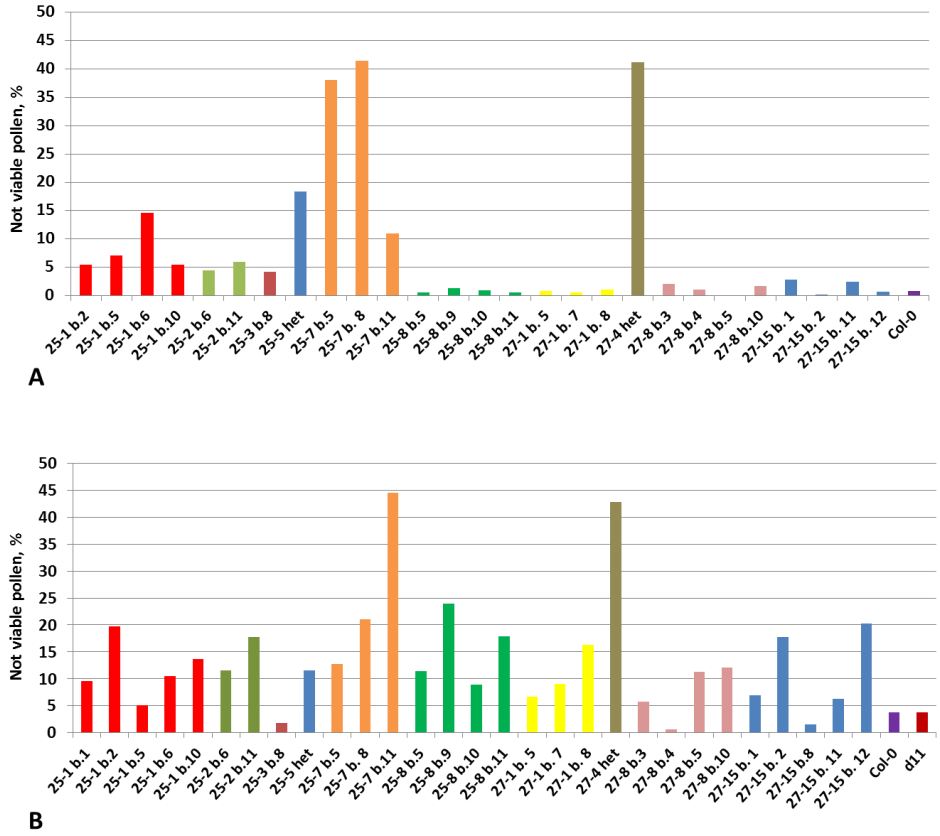

Figure 4-14 Pollen lethality in T3 amiRNA lines.
Every bar corresponds to an independent homozygous from individual line (indicated by different colours). For two lines, 25-5 and 27-4, no homozygous plants could be identified in the T3 screen. At least 350 pollen grains from two plants were counted to evaluate the pollen abortion in the independent homozygous plants. Lines are carrying either amiR5x-duff (25) or amiR2x-duff (27). The quantification was performed twice (A and B) using different T3 plants originating from the same T2 mother plant. *duff11* T0 background line shows WT-levels of non-viable pollen (B). Large variability in the pollen abortion phenotype can be noticed.

Flowers from the same individuals used for quantifying the pollen abortion in the amiR-duff homozygous lines were collected. The synthesized cDNA was used to perform qPCRs measuring the expression levels of the *DUFF* genes in the mutant lines. Figure 4-15 represents the gene expression results as a clustered heat map combined with the pollen abortion phenotype data (mean value of pollen abortion for every line was calculated) for the two independent experiments.

The quantitative PCR approach confirmed the findings from chapter 4.3.3 (Fig. 4-7) that the target genes of the amiR5x-duff construct are downregulated in the mutants (20-80% residual transcript). On the contrary, the amiR2x-duff construct turned out not to be functional in reducing the mRNA levels, since the target genes *DUFF2* and *DUFF7* were not

downregulated in these lines. An exception was line 27-4, where most of the *DUFF*s were significantly downregulated, which is probably linked to the severe pollen abortion phenotype in this line. It is possible that amiR2x-duff acts by blocking the translation process instead of depleting the mRNA of the target genes, but this hypothesis was not experimentally proved. Testing this possibility would require designing an antibody recognizing an epitope within the DUFFs protein structure and quantifying the protein levels of the targets of the amiR2x-duff in the mutant lines and comparing the results with the WT expression levels..

Expression of *DUFF4* could not be detected by qPCRs, although several different primer pairs were tested. Detection of *DUFF4* mRNA in the semi-quantitative PCR assay (see 4.3.3) could be explained by using primers, which are not specific for *DUFF4*, but could also detect *DUFF5*, since the two genes share 95.4 % sequence identity. However, DUFF4 was identified at the protein level (Grobei et al., 2009), indicating that the unique *DUFF4* mRNA could not be detected in this work.

Furthermore, we tried to correlate the data of this first quantitative measure of *DUFF* gene expression with the phenotypic data of the same individuals. The result showed that the downregulation of the target *DUFF* genes does not clearly correlate with the observed pollen abortion phenotype (e.g. homozygous line 25-3 harbours a functional amiR5x-duff construct, but displays a low pollen abortion percentage. In comparison, the same line in the T1 heterozygous generation showed 30% aborted pollen grains, see Fig. 4-11). Nevertheless, one can see that prominent downregulation of most of the *DUFF*s (including *DUFF*s, which are not targets) is associated with a pollen abortion phenotype (e. g. Fig. 4-15 B, lines 25-5, 25-7, 27-4).

Based on the findings in this experiment five amiR-duff lines were chosen for more precise characterization: 25-1, 25-2, 25-5, 25-7, all carrying amiR5x-duff, and 27-4 carrying amiR2x-duff construct.

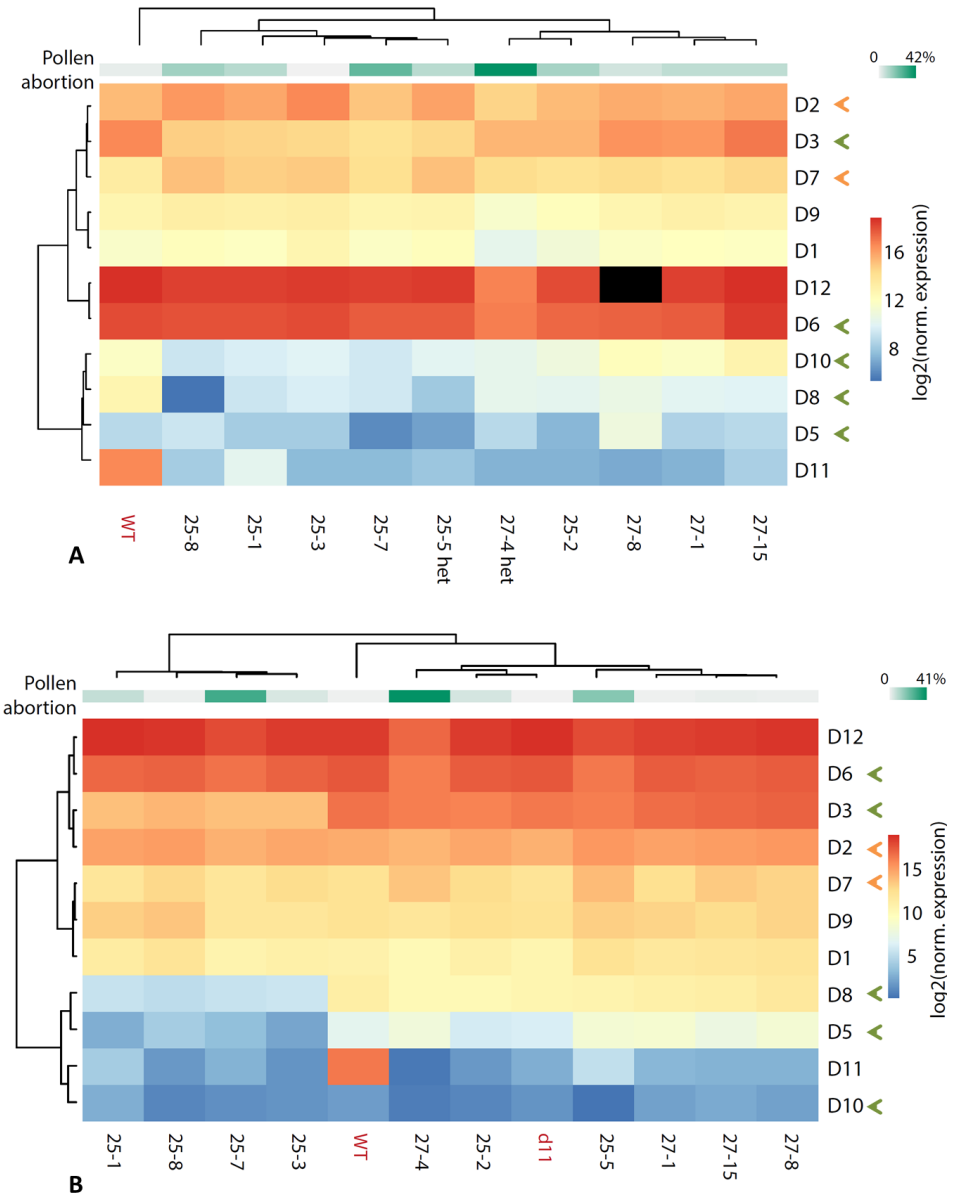

Figure 4-15 Pollen viability quantification and gene expression analysis of amiR-duff lines.
Gene expression results of pooled flowers from homozygous plants used for phenotyping are presented as clustered heat map. The bar above represents the pollen abortion percentage (mean value from experimental data presented on Fig. 4-14) and does not contribute to the clustering. The clustering is performed based on normalized gene expression data and clearly separates the genes in a low- and higher expressed ones (on the left). The line clustering (top) does not clearly separate WT from mutants, or independent lines carrying different constructs from each other, indicating gene expression variability.
Target genes of amiR5x-duff indicated with green arrows are downregulated compared to WT-expression levels, and the targets of amiR2x-duff are indicated by orange arrows (amiR2x-duff construct is not functional). *DUFF11* is absent in amiR-duff lines, but strongly expressed in WT. Black box: expression signal N.A.
For further explanation see the text. A and B are experimental replicates.

4.3.6 Mapping the position of the T-DNA insertions in amiR-duff single transformant lines

In order to facilitate the handling of the amiR-duff lines, as well as to be able to exclude positional effects of the T-DNA insertion on the phenotype, an extensive mapping of the T-DNA flanking genomic sequences was undertaken. Applying thermal asymmetric interlaced PCR and restriction site extension PCR the positions of the T-DNA in the genome of three of the selected single amiR-duff lines were successfully mapped (Table 4-3). Line 25-5 carries two insertions about 27 kbp apart from each other, corresponding to 0.135 % recombination probability.

All three mapped loci and the genes in those regions are not extensively studied and no functional data or reports about related phenotypes were found.

Table 4-3 Mapping the T-DNA flanking genomic sequence in amiR-duff lines

amiR-duff line	Chromosomal position of the T-DNA	Genomic locus
25-2	Ch. 1 pos. 25310150	ORF of At1g67530, ARM repeat superfamily protein (Coates, 2003)
25-5	Ch. 4 pos. 9757486	Intragenic region of At4g17440, DUF1639 and At4g17450, transposable element
	Ch. 4 pos. 9730497	
27-4	Ch4 pos. 900783	600 bp upstream of At4g02050, Sugar transporter protein 7 (Büttner, 2010)

To rule out the possibility that any observed reproductive phenotype in the amiR-duff mutants is caused by the position of the T-DNA in the genome, standard SALK lines bearing insertions in the same genomic loci or in close proximity to them, were obtained (Table 4-4). Homozygous individuals of these SALK mutants were examined for general vegetative and reproductive phenotypes. All plants displayed normal vegetative growth and development and the siliques elongated normally, indicating full seed set. Alexander staining of mature pollen grains and aniline blue staining of pollen tubes of the SALK mutant lines did not show any phenotypic deviations compared to the WT control plants (data not shown). Nevertheless, testing the transmission efficiency of the mutant allele through pollen and egg cells of the SALK mutants will strengthen the observation that T-DNA insertions in the loci of interest do not cause any reproductive defects in the plant. Therefore, reciprocal crosses of the T-DNA insertion mutants to WT, followed by evaluation of the mutant allele transmission in the F1 generation should be performed.

Table 4-4 SALK T-DNA mutant lines harbouring insertions in the loci of the amiR-duff lines

amiR-duff line	Chromosomal position of amiR-duff T-DNA	SALK line	Chromosomal position of SALK T-DNA	Genomic locus of SALK T-DNA
25-5	Ch. 4 pos. 9757486	SALK_069 118.38.35.x	C/9755042-9755284	Intragenic region of At4g17490 and At4g17500
		SALK_036 267.36.05.x	C/9759209-9759260	At4g17500, 3` UTR
	Ch. 4 pos. 9730497	SALK_135 750.15.20.x	W/9730713-9730868,9731081-9731124	Intragenic region of At4g17440 and At4g17450
		SALK_042 247.25.55.x	C/9729526-9729629	Intragenic region of At4g17440 and At4g17450
27-4	Ch 4 pos. 900783	SALK_087 232.35.95.x	W/900891-900955	Intragenic region of At4g02050 and At4g02055
		SALK_203 906C	W/900420-900559	Intragenic region of At4g02050 and At4g02055
		SALK_206 531	W/900894-901126	Intragenic region of At4g02050 and At4g02055

Multiple amiR-duff mutant lines were generated and their preliminary analysis included quantification of the gene expression, screening for pollen related phenotypes, and extensive insertion analysis and mapping. This allowed narrowing down the number of lines for further analysis and choosing lines harbouring functional amiR-duff construct in a single genomic locus, which would facilitate further experimental handling of the mutants. Moreover, the amiR-duff lines displayed moderate to strong pollen developmental phenotype, potentially due to amiR-duff action. The selected lines are listed in Table 4-5.

Table 4-5 amiR-duff lines selected based on preliminary analysis.

Line name	Target *DUFF* mRNA downregulation	Pollen abortion %	T-DNA insertions
25-1	+	5-20	2 linked, mapping unsuccessful
25-2	+	5-18	1 mapped
25-5	+	12-18	2 linked, mapped
25-7	+	12-40	2 linked, mapping unsuccessful
27-4	global *DUFF* transcript downregulation	40	1 mapped

4.3.7 Single-plant approach to reduce biological variability

A. thaliana lines, expressing amiR-duff functional constructs display pollen developmental defects. Preliminary screening and line characterization was performed using Alexander staining, which is a fast and easy to handle method to differentiate viable from non-viable grains. Regardless of these advantages, the quantitative outcome of Alexander staining strongly depends on biological factors like physiological state of the plant and flower developmental state. Additional noise is added to the system since amiRNA expression and silencing activity is not uniform in different lines (experimental observation Fig. 4-15) and also in different plants from the same line (assumed from data Fig. 4-14). Moreover, Alexander staining gives valuable information about pollen developmental defects, but is not informative if other stages of the reproductive process are affected (pollen germination, pollen tube growth and guidance). Analysis of the mutant allele transmission efficiency (TE) would give a better general indication whether the reproductive process is disturbed in amiR-duff lines. To address these issues, an alternative experimental approach was designed (Fig 4-16). Anthers from the first (1 to 14) opening flowers on the primary and secondary inflorescences of heterozygous amiR-duff were sampled to analyse *DUFF* gene expression levels. The pollen from the next (11 to 24) opening flowers from the same inflorescences was used to pollinate *dde2*$^{-}$ (von Malek et al., 2002) male sterile plants and calculate the amiR-duff male transmission efficiency in F1. This approach allowed correlating gene expression data with reproductive phenotype data within the same organism.

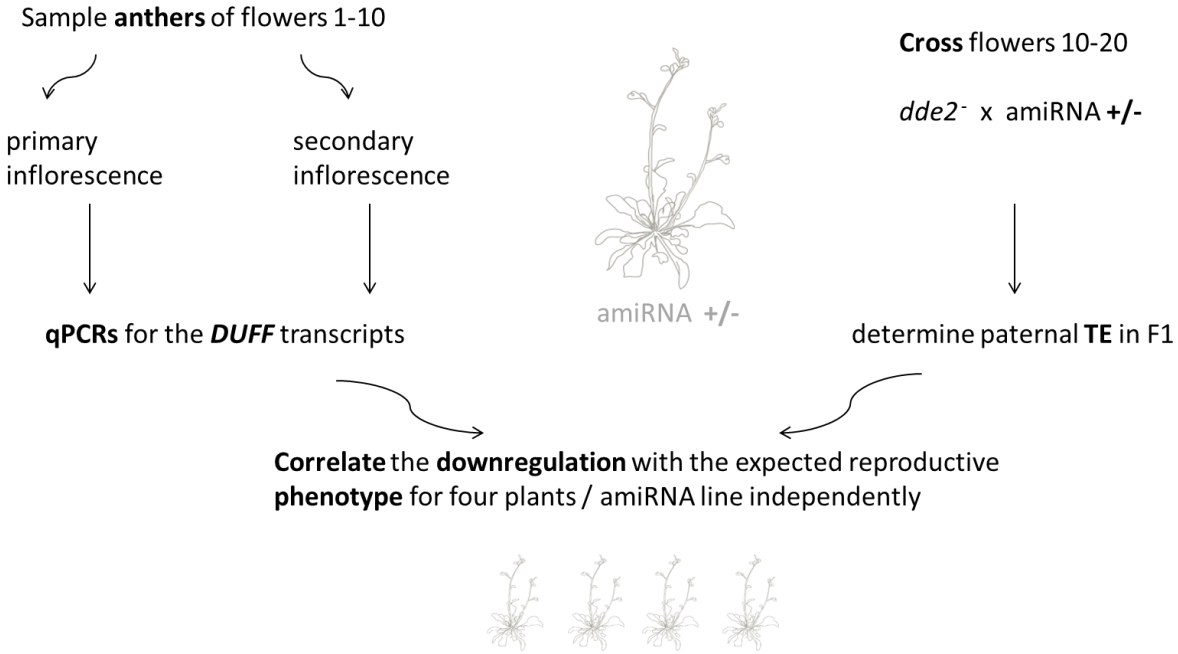

Figure 4-16 Gene expression and phenotype analysis of single amiR-duff plants.
Anther material to study *DUFF* gene expression from seven independent plants per amiR-duff line was sampled. Pollen from the same plants was used for crosses to *dde2*⁻ flowers to determine amiR-duff male transmission efficiency. Correlation study of the gene expression levels and the observed reproductive phenotype in four individual plants per amiR-duff line was performed, corresponding to eight biological replicates per line. Illustration source: (Weiss and Buchanan, 2009)

Figure 4-17 shows the results from the transmission efficiency crosses performed with the five chosen amiR-duff lines. Male transmission efficiency for the amiR-duff construct is reduced in all lines except 25-2. Primary and secondary inflorescences of seven individuals per amiR-duff line were crossed and F1 analysis delivered consistent between all replicates results.

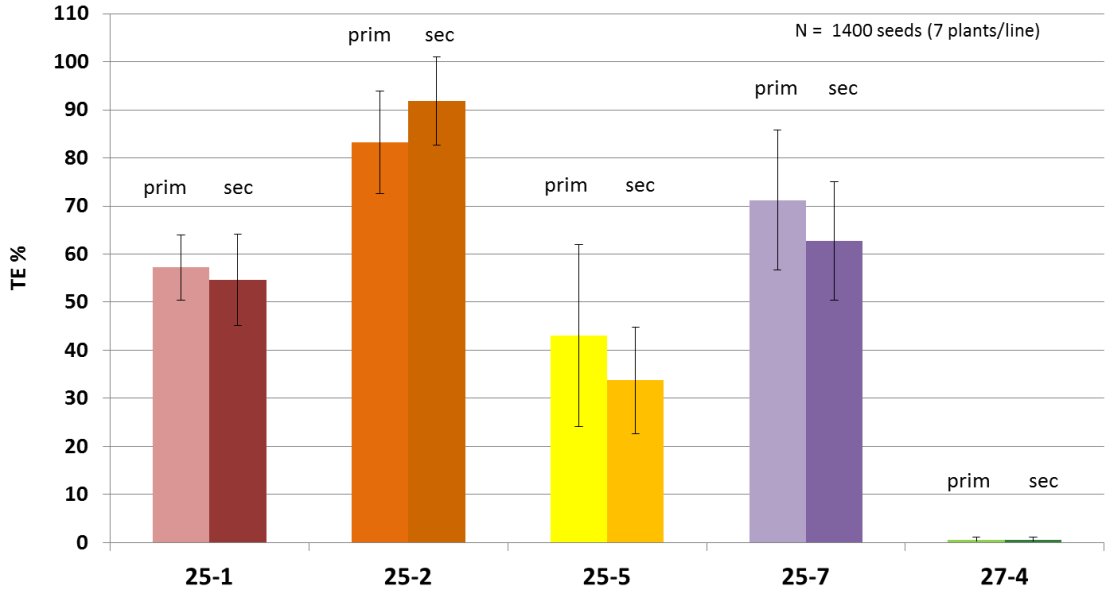

Figure 4-17 Male transmission efficiency (TE) of amiR-duff lines.
Pollen from the primary (prim) and the secondary (sec) inflorescences of seven individual plants for every amiR-duff lines was used for crosses to *dde2*$^{-}$. In total, the genotype of at least 1400 seeds per inflorescence was analysed to create this bar diagram. The error bars represent the standard deviation.

DUFF gene expression analysis was performed on anther material from four of the individual plants (primary and secondary inflorescence each) used to determine the male TE. The results for all five lines are shown in Figure 4-18. As expected from previous gene expression analyses, the target genes of the amiR5x-duff are downregulated in the corresponding lines and *DUFF* transcript levels are globally reduced in line 27-4 carrying the amiR2x-duff. Performing the experiment with eight biological replicates for each studied line gave a better insight into the transcriptional state of the DUF1216 family genes. Wild type replicates displayed a high variability in expression levels of most of the *DUFF* genes, some of them up to 16-fold (*DUFF6*, *DUFF2*, *DUFF1*, *DUFF7*, *DUFF12*). The expression pattern of others (*DUFF9*) was more homogenous. The expression of the other members *DUFF3*, *DUFF5*, *DUFF8*, and *DUFF10* varied up to four fold in different WT plants. This prominent biological variability in the *DUFF* gene expression was also reflected in the amiR-duff expression data, despite clear evidence of target gene downregulation in all mutant lines. In addition, the reduction of the male transmission efficiency in the mutants cannot be directly attributed to amiR-duff action, since line 25-2 carries a functional amiR5x-duff, but does not show a significant reduction in TE.

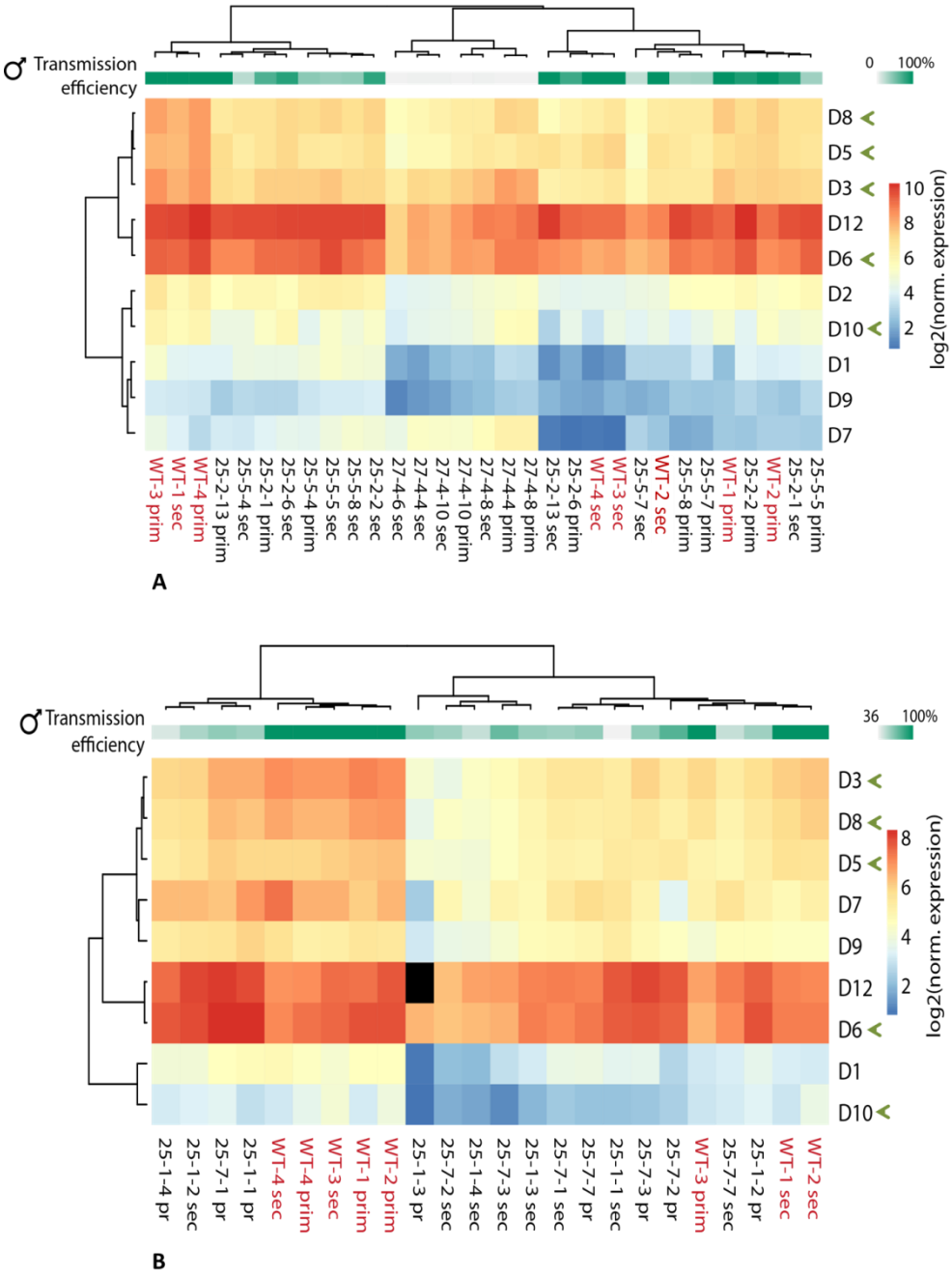

Figure 4-18 Male transmission efficiency and gene expression analysis of amiR-duff lines.
Eight biological replicates for each line were analysed for their gene expression and phenotyped (cDNA was synthetized from anther material from the primary and secondary inflorescences of four plants per line; flowers from the same inflorescences were taken for TE crosses to *dde2*). The bar above the heat maps showing the measured TE percentage does not contribute to the clustering. Clustering is performed based on normalized gene expression data and clearly separates the genes in low- and higher expressed ones (on the left). The line clustering (top) does not clearly separate WT from mutants, or different mutant lines from each other, indicating gene expression variability. Target genes of amiR5x-duff indicated with green arrows are downregulated compared to WT-expression levels. Global downregulation of *DUFF* transcripts was observed in line 27-4 carrying amiR2x-duff. Black box: expression signal N.A.
A – Lines 25-2, 25-5, 27-4
B – Lines 25-1 and 25-7

The complexity of the experimental design and the variable outcome required more sophisticated analysis of the transmission efficiency and gene expression data. Multi-way analysis of variance (ANOVA) was performed in an attempt to explain the effects of gene expression on the observed phenotype. The different amiR-duff lines had distinctive gene expression and primary and secondary inflorescence differed from each other as well (Table 4-6). However, conservative testing (manual F in the Table 4-6) revealed that primary and secondary inflorescences are equal. In other words, the amiR-duff lines differ from each other based on their *DUFF* expression pattern. In contrast, the gene expression of the two inflorescences of the same plant does not differ. Further in depth analysis of each *DUFF* gene revealed that the expression of *DUFF6*, *DUFF12*, and *DUFF7* genes had a major influence on transmission efficiency. The analysis also concluded that the biological variability in *DUFF* genes expression is significant and the interpretation of experimental results is hampered. In line 25-2 *DUFF* gene expression was not related to the phenotype.

Table 4-6 ANOVA analysis result table.
The predictive variables (factors with a potential impact on the TE phenotype) were tested independently and in connection to each other to determine their impact on the transmission efficiency phenotype. The results of the test statistic (F-value and manual F) indicate that the amiR-duff lines differ from each other based on their *DUFF* expression pattern and that the two inflorescences do not differ from each other in their gene expression pattern. Further explanation of the ANOVA analysis results: see the text.
DF (degrees of freedom), Sum Sq (sum of squares), Mean Sq (mean squares) – parameters needed to calculate the test statistics F. P-values – indicate the significance of the test statistics.

Predictive variable	DF	Sum Sq	Mean Sq	F-value	P (F)	manual F	P (manual F)
DUFF	10	12'765'403.2	1'276'540.3	319.7	0.0000	13.1016	0.0000
Line	4	1'844'255.1	461'063.8	115.5	0.0000	4.2000	0.0065
Inflorescence	1	42'348.4	42'348.4	10.6	0.0013	4.2911	0.0588
DUFF:Line	34	4'116'437.9	121'071.7	30.3	0.0000		
DUFF:Inflorescence	9	73'225.3	8'136.1	2.0	0.0350		
Line:Inflorescence	4	55'070.9	13'767.7	3.4	0.0089		
Residuals	311	1'241'914.8	3'993.3	NA	NA		

4.3.8 amiR-duff lines T4 analysis: phenotype instability and gene expression analysis

The aim of the approach applied above, where the gene expression pattern and the phenotype of individual plants were studied and the data was analysed statistically, was to reduce the system complexity and variability and to highlight genes with major effects on the phenotype. Based on the results from 4.3.7, experimental efforts were restricted to characterize lines 25-5, 25-7, and 27-4, displaying a prominent relationship between their *DUFF* gene expression pattern and the measured reduction in male transmission efficiency. Quantification of pollen viability applying Alexander staining was chosen as a phenotyping approach in order to facilitate the phenotype screening.

The pollen viability test was performed with homozygous T4 plants from lines 25-5 and 25-7 and heterozygous 27-4 (no homozygous plants were identified for this line). Flowers for *DUFF* gene expression analysis were collected from the same individuals. Flowers four to ten from the main inflorescence of eight plants per line were screened and quantification was done for three plants per line. All 27-4 plants displayed a prominent pollen abortion phenotype. None of the plants from line 25-7 showed the expected phenotype (pollen abortion rates between 10 and 40 % based on previous analysis, see Fig. 4-14) and only one plant from line 25-5 displayed the expected pollen defect (previous analysis identified 10 to 20 % aborted grains, see Fig. 4-14). Gene expression analysis was performed on flower tissue from the phenotypically characterized plants (Fig. 4-19). As in the previous gene expression experiments, it was found that the targets of the amiR5x-duff are downregulated compared to WT gene expression levels and global downregulation of *DUFF* transcripts characterizes line 27-4. Strong variability in *DUFF7* expression was detected. It was observed that in plants with pollen developmental defects, simultaneous downregulation of *DUFF6* and *DUFF12* transcripts occurred in addition to the downregulation of amiR-duff target genes. This observation is consistent with the conclusions from the ANOVA analysis that the two genes significantly contribute to the transmission efficiency defect (see 4.3.7).

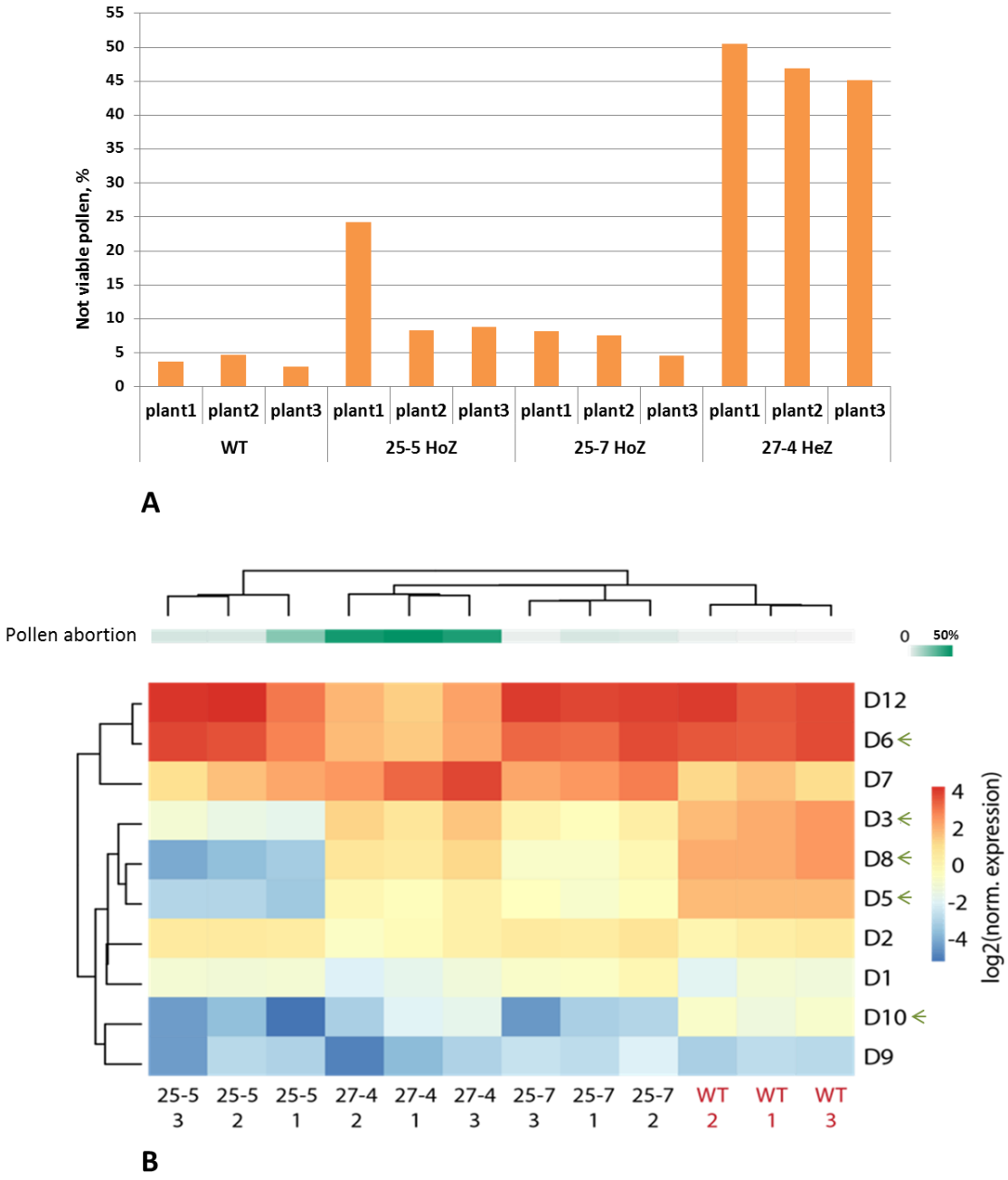

Figure 4-19 Pollen viability quantification and gene expression analysis of T4 amiR-duff lines 25-5, 25-7, and 27-4.

Pollen viability and *DUFF* gene expression were quantified for three individual plants per line. A proportion of non-viable pollen was observed in all plants from line 27-4 and in one individual from line 25-5. Gene expression results are presented as clustered heat map. The bar above the heat map showing the pollen abortion percentage does not contribute to the clustering which is based on gene expression only. Clustering successfully separates WT from mutants, as well as different amiR-duff lines. Target genes of amiR5x-duff indicated with green arrows are downregulated compared to WT-expression levels. Global downregulation of *DUFF* transcripts is measured in line 27-4 carrying amiR2x-duff. Plants with scored higher pollen abortion display downregulation of *DUFF12*, which is not a target of amiR-duff.

A – Pollen viability quantification.

B – Gene expression analysis.

4.3.9 Multiple *DUFF* genes contribute to the reproductive defects in the amiR-duff lines

Since T4 plants carrying amiR5x-duff did not display a pollen developmental phenotype, the same experimental procedure as in 4.3.8 was applied for screening through populations of amiR-duff lines 25-7 and 25-5 in the T3 and T4 generations in parallel. Mutant individuals with strong (35-40 % for line 25-7 and 18-20 % for line 25-5), moderate (8-10 %), or no phenotype, were selected together with WT control plants for gene expression analysis. In line 25-5 no homozygous plants with a strong pollen abortion phenotype were identified and, therefore, heterozygous plants were selected for the experiment. The expression analysis was restricted to a subset of *DUFF* genes to reduce the experimental load. The expression of target genes *DUFF3*, *DUFF5*, *DUFF6*, and *DUFF8*, as well as *DUFF12*, was examined based on conclusions from the previous analysis. *DUFF9* and *DUFF7*, which are not targets of amiR5x-duff construct, were included in the experiment. As expected, target genes were downregulated in the mutant plants and non-targets showed relatively stable expression pattern in all plants (Figures 4-20 A and 4-21 A). The expression data were analysed statistically applying ANOVA in order to explain the phenotypic differences in the amiR-duff populations. Phenotype- and gene expression data for the two analysed lines are visualised in Figure 4-20 and Figure 4-21 as clustered heat maps and biplots of principal component analysis (PCA).

PCA of *DUFF* gene expression in line 25-7 separated WT plants from amiR-duff mutants mainly due to *DUFF8* and *DUFF3* expression with contribution of *DUFF6* and *DUFF12* (Fig. 4-20 B). Another PCA conducted only with amiR-duff plants, separated mutants with strong pollen abortion from ones showing weak phenotype due to *DUFF6, DUFF12*, and *DUFF3* expression (Fig 4-20 C). ANOVA analysis using the principal components from PCA revealed *DUFF6* ($F = 29.8$, $P = 0.0003$), *DUFF3* ($F = 29.8$, $P = 0.0003$), and *DUFF12* ($F = 8.9$, $P = 0.0136$) as responsible for the pollen developmental defect. Additionally, one-way ANOVA showed that expression of *DUFF6, DUFF3*, and *DUFF12* explained the pollen abortion phenotype, which is also consistent with the PCA findings.

PCA of *DUFF* gene expression in line 25-5 separated WT plants from amiR-duff mutants mainly due to *DUFF8, DUFF5*, and *DUFF3* expression (Fig. 4-21 B). However, a PCA conducted with amiR-duff mutants only, could not separate mutants displaying strong abortion from the other mutants (Fig. 4-21 C), very likely because of the low number of plants in the experiment. One-way ANOVA analysis did not find any of the *DUFF* genes to influence the pollen abortion phenotype.

In summary, the statistical analysis of the gene expression and phenotype data of amiR-duff single transformant lines found that at least five of the DUF1216 family members contribute significantly to the observed reproductive phenotype, namely, *DUFF3*, *DUFF5*, *DUFF6*, *DUFF8*, and *DUFF12*.

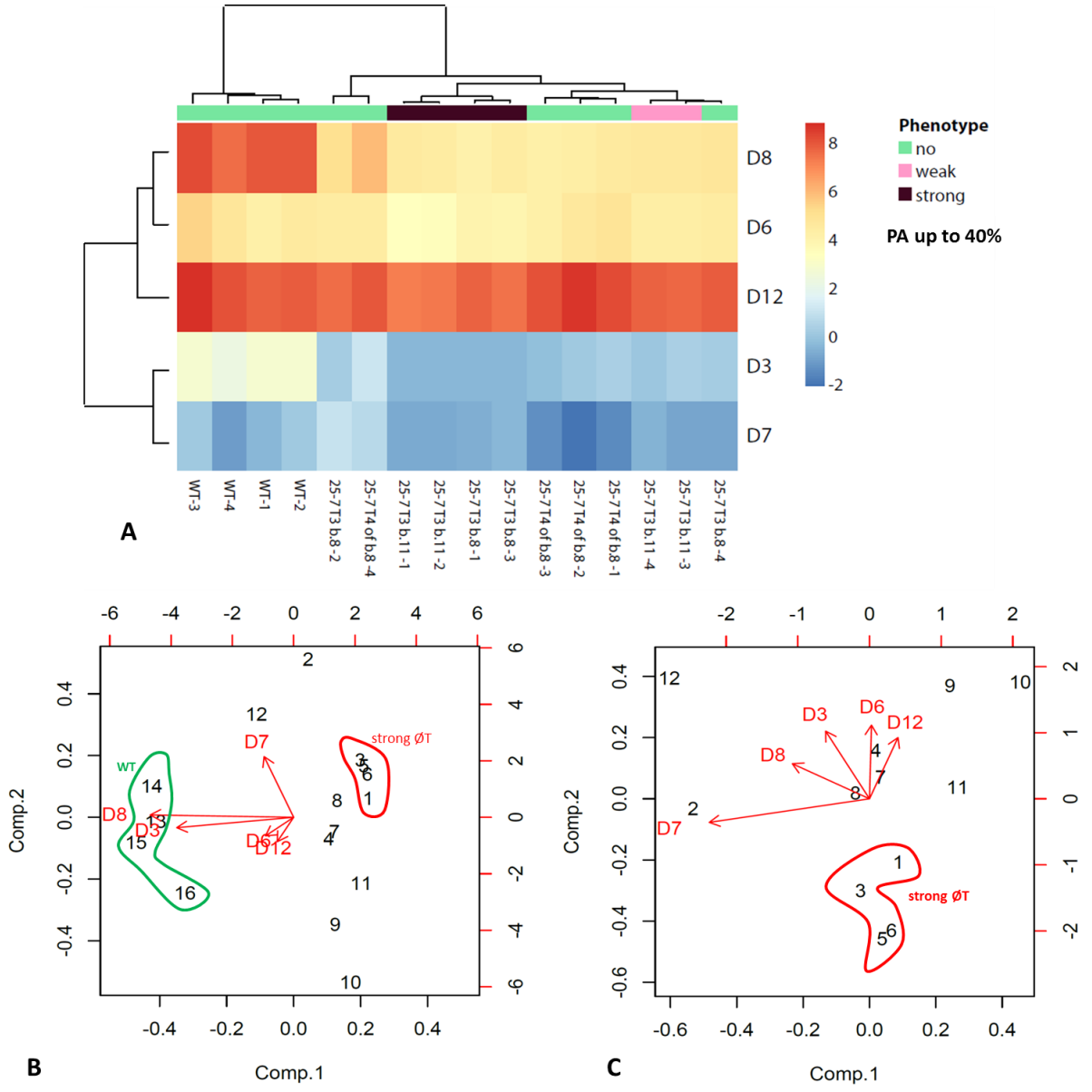

Figure 4-20 Statistical analysis of gene expression and pollen abortion quantification in amiR-duff line 25-7.

A – Clustered heat map of *DUFF* gene expression and pollen abortion quantification bar.

B – Principal component analysis (PCA) separates WT plants (green shape) from amiR-duff mutants. The first principal component explains 81.8% (PC1, *DUFF8* and *DUFF3*, and in part *DUFF6* and *DUFF12*) and the second principal component explains 12.6% (PC2, *DUFF7*) of the observed variance. Gene expression contributing to the principal components is presented as red arrows pointing in the direction of change. If an arrow is parallel to one PC axis, then gene expression solely contracts to this PC. The length of the arrow is proportional to its contribution to the PC. The black numbers in the plot correspond to the arbitrary numbers assigned to the individual plants in the raw dataset.

C – PCA of amiR-duff mutants only, separates plants with a strong phenotype (red shape) from plants with a weak phenotype due to *DUFF6*, *DUFF12*, and *DUFF3* expression. PC1 and PC2 explain 61.1% and 32.5% of the variance, respectively.

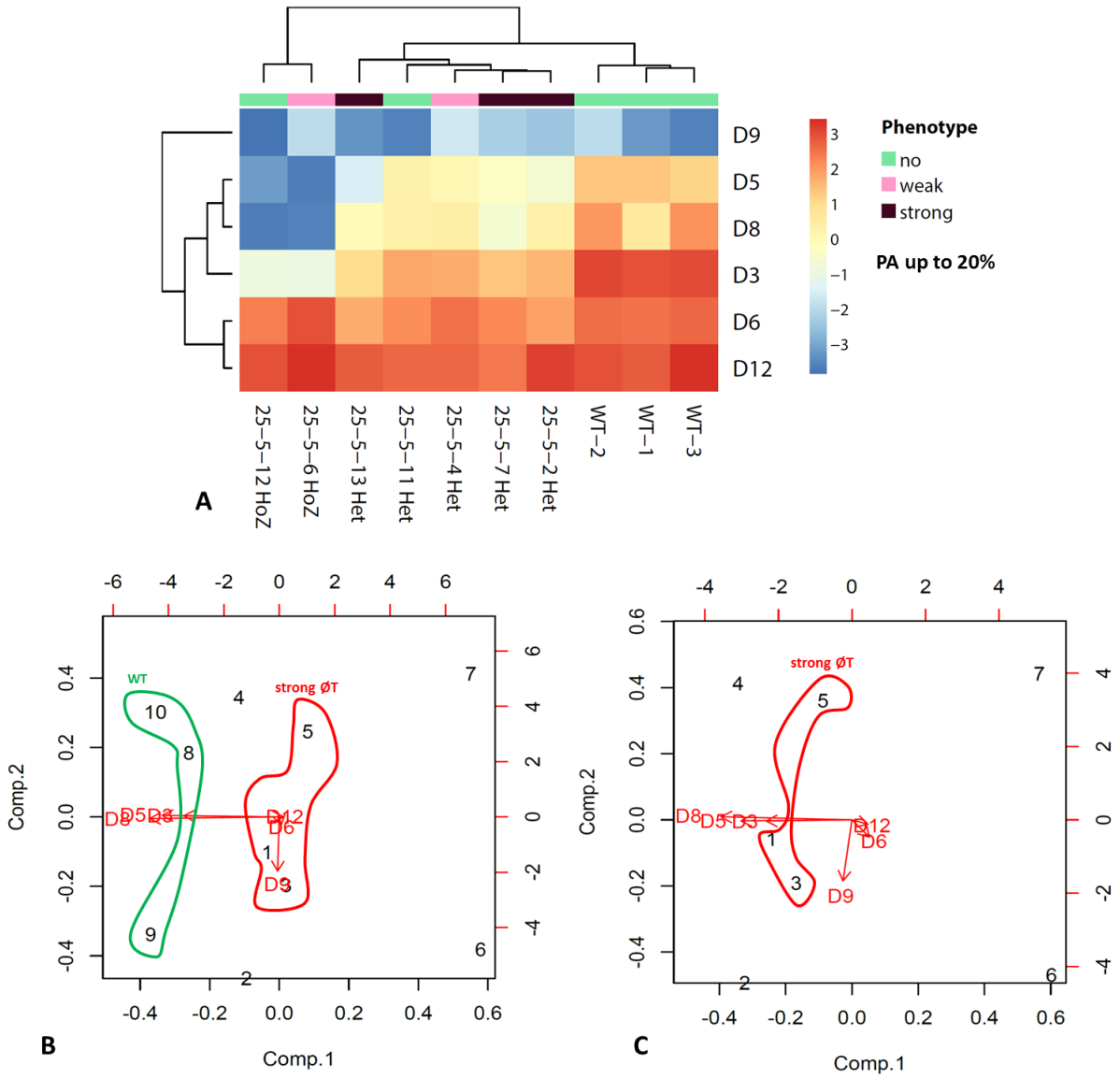

Figure 4-21 Statistical analysis of gene expression and pollen abortion quantification in amiR-duff line 25-5.

A – Clustered heat map of *DUFF* gene expression and pollen abortion quantification bar.

B – Principal component analysis (PCA) separates WT plants (green shape) from amiR-duff mutants. The first principal component explains 88.5% of the variance (PC1, *DUFF8*, *DUFF5*, and *DUFF3*). Gene expression contributing to the principal components is presented as red arrows pointing in the direction of change. If an arrow is parallel to one PC axis, then gene expression solely contracts to this PC. The length of the arrow is proportional to its contribution to the PC. The black numbers in the plot correspond to the arbitrary numbers assigned to the individual plants in the raw dataset.

C – PCA of amiR-duff mutants only, cannot separate plants with a strong phenotype (red shape) from plants with a weak phenotype.

4.3.10 DUF1216 gene expression affects plant fertility: transmission analysis

Male transmission efficiency of five of the single transformant amiR-duff lines was extensively analysed (see 4.3.7). It was found that plants expressing amiR-duff constructs display consistent male reproductive defect (Fig. 4-17).

In order to investigate in detail the reproductive phenotype of amiR-duff mutants, reciprocal crosses for lines 25-5, 25-7, and 27-4 were performed. Three to four heterozygous mutant plants were used for the reciprocal crossing procedure; the resulting F1 seeds from the same type of cross were pooled, and the genotype of the F1 seedlings was determined (data not shown). For lines 25-5 and 25-7 no reduction in male or female transmission efficiency was detected, since the F1 population segregated in approximately 1:1 (heterozygous : WT) ratio. A significant reduction of both male and female transmission was detected for line 27-4 (< 0.5 %) and further work was performed only with lines 25-5 and 25-7.

Strong biological variability in *DUFF* gene expression characterizes amiR-duff mutant lines, which has a potential impact on phenotypic output. Therefore, the transmission efficiency reciprocal measurement was repeated with prior phenotyping of the heterozygous mutants used for the crosses. Pollen abortion was quantified in heterozygous plants from lines 25-5 and 25-7 and these plants were used for reciprocal crosses. F1 seeds from individual crosses were not pooled for the analysis. The screen for pollen abortion did not reveal any plants displaying the phenotype in the heterozygous line 25-7 population. The results from this experiment are presented in Table 4-7. Two out of five analysed plants (plant 11 and plant 13) from line 25-5 and two out of three analysed plants (plant 1 and plant 2) from line 25-7 showed reduced male transmission efficiency. In one plant from line 25-7 mild reduction in female transmission was detected (plant 3). Moreover, no obvious relationship between the pollen developmental defect and reduction in transmission efficiency was found. In conclusion, the reciprocal transmission efficiency analysis identified male reproductive defects in amiR-duff lines, but the distinct transmission efficiency reduction detected and described in 4.3.7 could not be confirmed.

Table 4-7 Results from reciprocal crosses of amiR-duff lines 25-5 and 25-7.

Non-viable pollen grains in the mutant plant	Cross (female x male)	HeZ	WT	Total	TE, %
18%	25-5 plant 2 x WT	125	84	209	100
	WT x 25-5 plant 2	134	84	218	100
3%	25-5 plant 4 x WT	150	76	226	100
	WT x 25-5 plant 4	185	115	300	100
18%	25-5 plant 7 x WT	145	83	228	100
	WT x 25-5 plant 7	129	138	267	93.48
none	25-5 plant 11 x WT	121	124	245	97.58
	WT x 25-5 plant 11	100	214	314	46.73
21%	25-5 plant 13 x WT	89	51	140	100
	WT x 25-5 plant 13	127	184	311	69.02
4%	25-7 plant 1 x WT	126	110	236	100
	WT x 25-7 plant 1	104	155	259	67.10
none	25-7 plant 2 x WT	171	153	324	100
	WT x 25-7 plant 2	113	178	291	63.48
none	25-7 plant 3 x WT	146	185	331	78.92
	WT x 25-7 plant 3	129	139	268	92.81

4.3.11 Pollen degeneration onset characterizes the transition from polarized microspore to bicellular pollen in the amiR-duff lines

Despite the strong inter- and intra-line variability, it was observed that amiR-duff expressing plants are affected in their pollen development. Characterizing the pollen developmental defect can help elucidating the function of DUF1216 family members.

Inflorescences of four independent plants from Col-0 WT and lines 25-5 and 25-7 displaying prominent phenotype were analysed to determine the pollen abortion time point during pollen development. Dissected pollen from different developmental stages was stained with DAPI to visualize pollen nuclear constitution (Fig. 4-22). Quantification of the pollen grains in different developmental stages was performed for three of the four plants analysed, all of them showing a similar phenotype. Figure 4-23 shows the quantification results from single inflorescences of lines 25-5 and 25-7 and the corresponding WT control. In both lines the pollen abortion process begins in late vacuolar stage (polarized microspore) at the transition to binucleate pollen. This is the time point of the first pollen mitotic division. In later developmental stages the pollen degeneration in the mutants severely progresses and in mature stage the proportion of aborted pollen grains is ca. 20% in line 25-5 and ca. 40% in line 25-7 (Fig. 4-23).

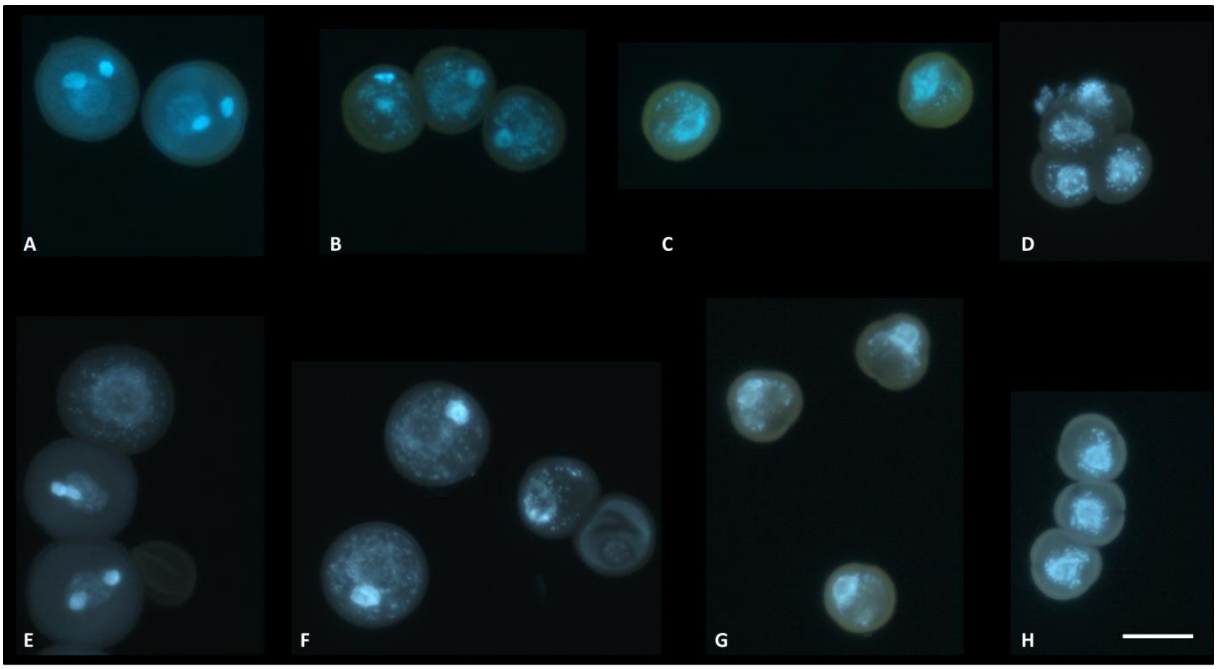

Figure 4-22 DAPI stained pollen grains in different developmental stages.
A to E – WT pollen in different developmental stages: tricellular pollen (A), bicellular pollen (B), polarized microspores (C), and unicellular microspores (D).
E to H – amiR-duff 25-7 pollen in different developmental stages: tricellular pollen (E), bicellular pollen (F), polarized microspores (G), and unicellular microspores (H). Pollen degeneration can be observed from later polarized microspore stage and progresses in later developmental stages. Scale bar 15 µm.

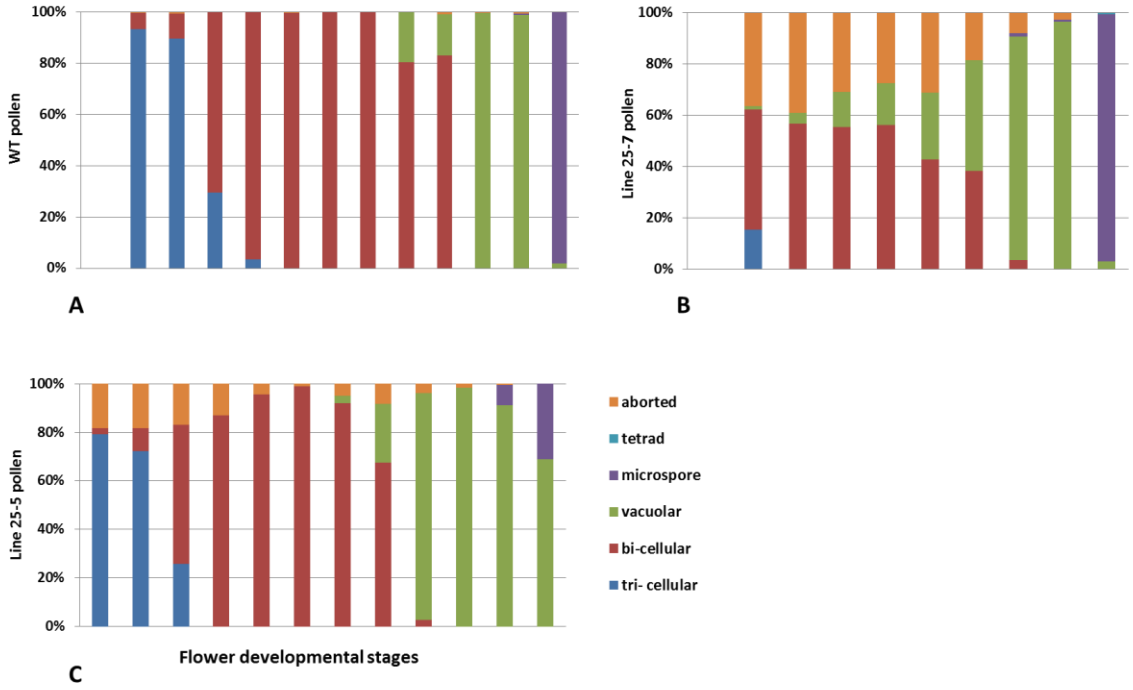

Figure 4-23 Quantification bar diagram of pollen developmental stages and degeneration advancement in amiR-duff lines.
Bars correspond to different flower developmental stages (buds) in the inflorescence.
A – WT pollen developmental advancement.
B, C – amiR-duff lines 25-7 and 25-5 pollen developmental advancement accompanied by pollen degeneration. In both lines pollen abortion starts at the transition between vacuolar and bicellular stages and accumulates with developmental advancement.

4.4 DUF1216 protein localization

In the scope of this study was to determine the sub-cellular localization of the DUF1216 proteins, since this information could help understanding their molecular function. With the advancement of the study it became clear that several of the DUF1216 family members could play a more prominent role for pollen reproductive function. Extensive experimental efforts were invested to clone fluorescent protein fusion constructs for *DUFF3*, *DUFF5*, *DUFF6*, *DUFF7*, *DUFF8*, *DUFF11*, and *DUFF12*. The aim was to perform transient expression assays and establish stable *A. thaliana* lines. However, to the current time point, functional constructs were obtained for three of these genes (*DUFF3*, *DUFF7*, and *DUFF11*) and their

analysis is described below. The cloning procedure is described in 3.4.2. The cloning of the gDNA-fluorescent protein fusion versions of the other DUF1216 family members of interest is a subject of current experimental work.

4.4.1 Transient expression in *N. benthamiana*

C-terminal GFP fusion versions of DUFF3, DUFF7, and DUFF11 (DUFF-GFP) were transiently expressed in *N. benthamiana* leaves and the fluorescent protein expression pattern was observed using confocal microscopy (Fig. 4-24). Two of the fusion proteins displayed cytosolic localization of the GFP signal (DUFF3- and DUFF7-GFP) and DUFF11-GFP localized to quickly moving granulate structures in the periphery of the cells. In order to confirm and further investigate the observed sub-cellular localization of the DUFF proteins expressed under the control of the viral 35S promoter, co-localization assays with fluorescent constructs of known localization are needed.

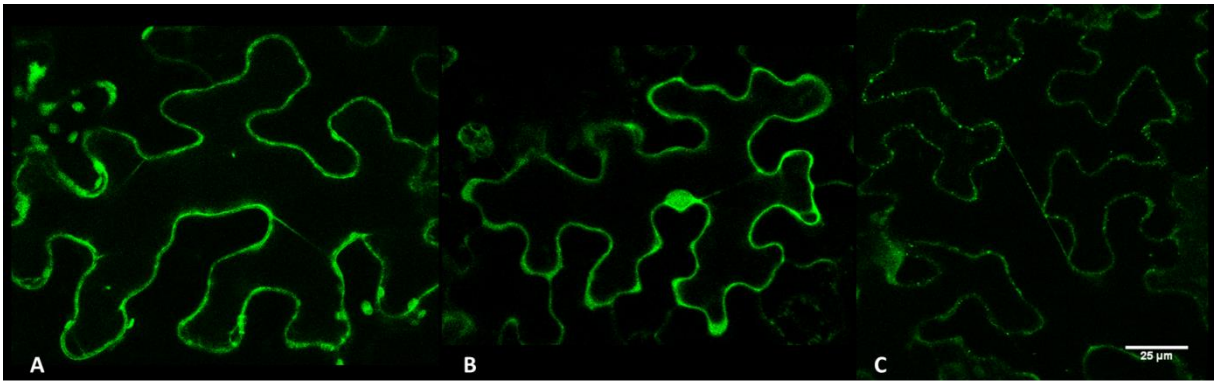

Figure 4-24 Transient expression of DUFF-GFP constructs in *N. benthamiana* leaves
A – DUFF3-GFP is expressed in the cytosol of tobacco leaf-cells.
B – DUFF7-GFP also localizes cytosolically in tobacco cells.
C – DUFF11-GFP forms highly mobile granules localizing to the cellular periphery in *N. benthamiana*.

4.4.2 Stable expression in *A. thaliana*

Arabidopsis thaliana lines stably expressing C-terminal fusion versions of DUFF7 and DUFF11 under the control of their native promoters (pDUFF-GFP) were analysed using confocal microscopy (Fig. 4-25). Four independent T1 pDUFF7-GFP lines of different expression strength displayed strong plasma membrane localization and weaker cytosolic

signal. Three stable *Arabidopsis* T1 pDUFF11-GFP lines expressing GFP at different strength showed that DUFF11 protein is associated with mobile cable-like structures, as well as to highly mobile vesicular structures in the growing pollen tube. These findings confirmed and further extended the knowledge obtained from analysing the transiently expressed fluorescent versions of the DUFFs. However, the exact sub-cellular localization of DUFF7 and DUFF11 should be confirmed. The cable-like structures visualized by pDUFF11-GFP might be associated with the cytoskeleton and the nature of the observed endomembrane structures needs further investigation. In order to identify the precise sub-cellular localization of both proteins, co-localization studies with known sub-cellular structures are needed. Crossing the pDUFF7-GFP and pDUFF11-GFP lines to fluorescent (fluorophore other than GFP) marker lines for different cellular compartments and analysing the expression pattern in the progeny should help answering these questions.

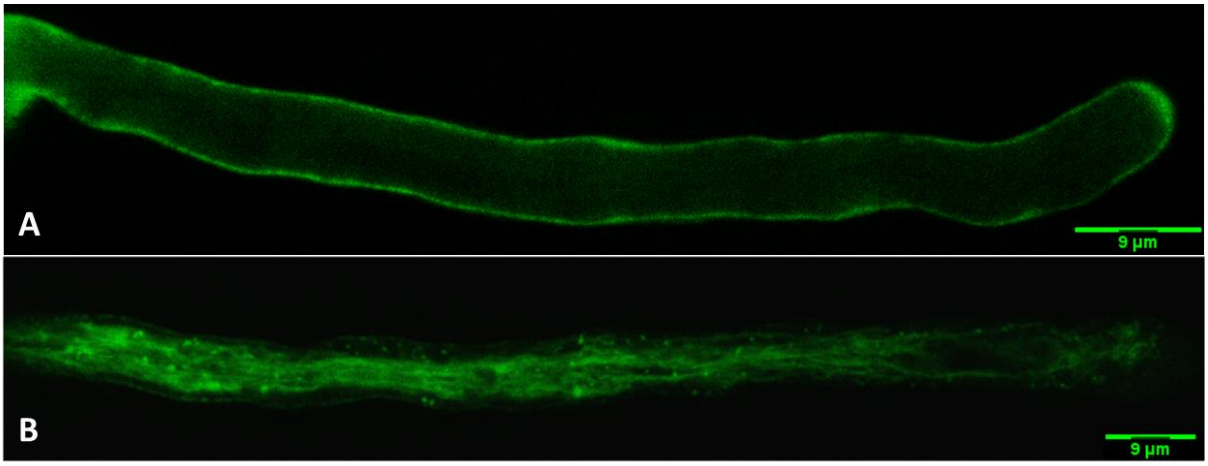

Figure 4-25 Stable expression of DUFF-GFP in *A. thaliana* pollen tubes
A – pDUFF7::DUFF7-GFP is expressed at the plasma membrane and in the cytosol in growing pollen tubes.
B – pDUFF11::DUFF11-GFP is expressed in cable-like structures and highly-mobile endomembrane structures within the pollen tube.

5 Discussion and future directions

5.1 Plants expressing amiRNA-constructs targeting the DUF1216 family members display fertility defects

5.1.1 Pollen developmental defects

It was observed that pollen developmental defects occur among *A. thaliana* populations expressing amiR-duff. 18 out of the 24 analysed T1 lines showed a proportion of aborted pollen between 5 and 50 %. Pollen abortion varied greatly from WT level to up to 40 % among the daughter plants of an individual T1 line (see 4.3).

If a pollen abortion phenotype is observed in a mutant line, this is an indication that the introduced transgene is affecting the pollen developmental process. This could be a primary effect of the transgene expression (e.g. amiRNA targeting genes important for pollen development) or of the disruption of an essential pollen gene by the T-DNA. Nevertheless, the T-DNA integration into the genome is a random event (Krysan, 1999) and often, multiple copies are inserted, causing secondary phenotypic effects.

It has been reported that pollen development is affected in around 10 % of the transgenic *A. thaliana* populations (Xing and Zachgo, 2007) and this phenomenon is often associated with chromosomal translocation events caused by T-DNA insertion into the plant genome (Clark and Krysan, 2010). A reciprocal translocation event could lead to the formation of genetically unbalanced gametes, failing to maturate. In a heterozygous state these plants would produce around 50 % viable pollen, since the other half lacks essential developmental genes due to the rearrangement. In a homozygous state the full pollen viability will be restored, because the gametes are genetically balanced (Curtis et al., 2009). The individual amiR-duff lines display different level of pollen abortion (e.g. line 25-5 plants show maximal 20 %, and plants of line 25-7 about 40 %). More importantly, this proportion varies significantly between the single individuals, independent of the genotype (homozygous or heterozygous).

Other mechanisms for the occurrence of pollen lethality are chromosomal deletions induced by the transgene integration or simply T-DNA positional effect in case important developmental genes are lost or disrupted. In these cases the lethality phenotype would not be due to the transgene action, but will be a persistent characteristic of the line (Xing and Zachgo, 2007). In contrast, the pollen abortion phenotype among amiR-duff populations is

highly variable. In addition, experiments in 4.3.6 showed that T-DNA insertions in the amiR-duff lines integration loci do not lead to pollen developmental defects.

It is also possible that amiR-duff target other genes and their downregulation affects pollen development in amiR-duff lines. The mechanism of action of amiRNAs, where only one effective small RNA of imperfect complementarity to the target is produced, reduces the possibility to target undesired genes. Moreover, the automated amiRNA designer tool WMD allows to introduce mismatches at the 3` end of the amiRNA sequence to avoid off-targets, which was implemented for designing the amiR-duff (Schwab et al., 2006).

The collected data suggest that the observed pollen developmental defect is caused by amiR-duff action rather than being an experimental artefact. Nevertheless, only extensive genome mapping of amiR-duff lines, as well as analysis of scrambled amiR-duff *A. thaliana* mutant lines, combined with gene-expression profiling, can help excluding chromosomal rearrangements and amiR-duff off-target effects as causative for the phenotype.

The pollen abortion process starts in the late vacuolar stage of pollen development in amiR-duff lines and coincides with the first mitotic division. The proportion of degenerated pollen grains increases with developmental advancement and reaches its maximum at tricellular stage. Later, the abortion quantification at mature grain stage delivers similar results. The onset and progression of the pollen degeneration correlate with the active accumulation of *DUFF* transcripts in the developing pollen grains, although some of the *DUFF* genes are expressed at low levels already at the microspore stage (Fig. 5.1, based on Honys and Twell, 2004 and findings of this work). The expression patterns of *DUFF3*, *DUFF6*, *DUFF8*, and *DUFF12* imply that they are playing a role in the early proliferative stages of pollen development, but their action is also required in the later differentiation phase. These are also the DUF1216 members identified in this work being the most important players for the reproductive phenotype in the amiR-duff lines. Effects of *DUFF11* expression were not analysed, since amiR-duff lines are in the *duff11* KO background. After pollen mitosis II (in bicellular stage, BCP) the expression of additional *DUFF* genes is activated (*DUFF1*, *DUFF2*, *DUFF7*, *DUFF9*). Curiously, these four genes have their expression peak in BCP and their expression strongly decreases in mature pollen (MP), whereas the already mentioned *DUFF3*, *DUFF6*, *DUFF8*, *DUFF11*, and *DUFF12* transcripts accumulate until the MP stage. *DUFF4*, *DUFF5* and *DUFF10* mRNA transcripts were not detected in earlier pollen developmental stages (probesets not present on the ATH1 microarray), but mRNA of *DUFF5*

and *DUFF10* genes was detected in MP in this study and DUFF4 and DUFF5 proteins were detected by Grobei and colleagues.

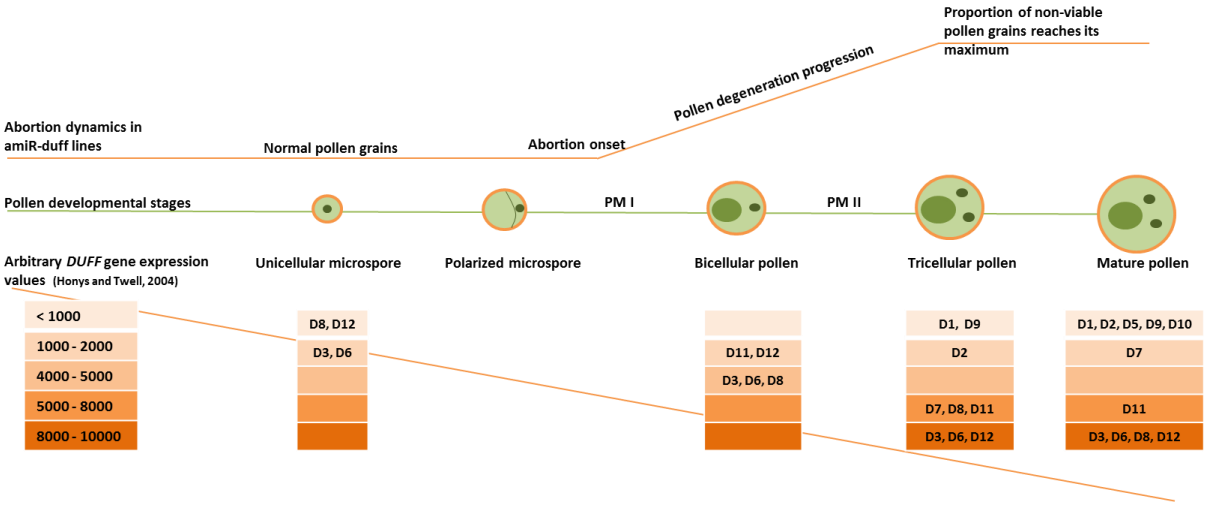

Figure 5-1 Dynamics of DUF1216 members gene expression during pollen maturation and pollen degeneration processes in amiR-duff lines.
Pollen abortion onset and progression in amiR-duff lines coincide with the accumulation of *DUFF* transcripts during microgametogenesis.

The differential expression dynamics of *DUFF* genes over time suggest functional separation during pollen development. Moreover, in this study it was shown that the individual *DUFF* genes are expressed in a very broad dynamic range in mature pollen grains in WT plants (see Fig 4-18) and it can be assumed that fine tuning of the transcriptional regulation and mRNA turn-over of these genes is important for the proper functioning of the corresponding proteins. Introducing the amiR-duff into the plant disturbs this potentially complex network by depleting individual *DUFF* transcripts more or less efficiently, probably depending on different amiRNA-target site pairing characteristics, but also depending on the overall molecular concentrations of target transcripts (Arvey et al., 2010). In addition, in some cases potential synergistic downregulation action on non-target *DUFF* transcripts could not be excluded (*DUFF12* in Fig. 4-15, Fig. 4-19, and Fig. 4-20). If the amiR-duff molecules interfere with the precisely regulated transcript concentrations of the DUF1216 members, the orchestrated action of the corresponding proteins ensuring proper maturation process could be disturbed, resulting in pollen abortion. Since the described scenario is a dynamic process with

complex kinetics and regulation, the phenotypic outcome strongly varies not only between different amiR-duff lines, but also between plants from the same amiR-duff line.

Further characterization of the amiR-duff *A. thaliana* lines should dissect the pollen abortion mechanism. During microgametogenesis the developing pollen undergoes significant morphological and metabolic changes, which can be visualized using various cytochemical stains. Proper vacuole formation and re-absorption prior PMI can be visualized using neutral red (Mahlberg, 1972). The accumulation of pollen storage contents like starch (iodine and potassium iodide), lipids (Fluorol staining (Brundrett et al., 1991)) and proteins (Amido black) can be assessed in order to identify possible role of DUF1216 members in synthesis or deposition/degradation of basic cell storage compounds. Proper formation and deposition timing of the pollen cell wall, which starts with exine development in early microspore stage and is followed by intine deposition accumulating until PMI (Regan and Moffatt, 1990), can be visualized using dyes binding specifically cellulose or sporopollenine. Understanding the mechanism of pollen abortion will not directly reveal the molecular function of DUF1216 family members, but will provide valuable information about the cellular processes they are involved in.

5.1.2 Reduced male fertility

Male fertility is reduced among the amiR-duff mutant populations. This means that pollen grains carrying the mutant allele partially fail to fulfil their physiological function. In amiR-duff line 25-5 (TE = 35%) this proportion is around 65% and for line 25-7 (TE = 65%) around 35%. However, not all analysed mutant lines displayed reduced male transmission and also, individual plants from the same mutant line showed variable results (see 4.3.10). The observed pollen degeneration in amiR-duff lines does not necessarily contribute to the reduction in transmission efficiency, since plants with fully viable pollen show reduced transmission of the mutant allele, indicating post-germination defects in the mutant pollen interfering with the fertilization process. Moreover, plants with a significant proportion of aborted pollen (ca. 20%) display normal transmission efficiency meaning that the remaining 30% mutant pollen successfully competes with WT grains (Table 4-7). These results indicate possible differential effect of the amiR-duff on *DUFF* genes playing a role during the pollen development, and, possibly later on during pollen germination and tube growth. If the expression balance (dosage and timing) within the DUF1216 family network is disturbed by

introducing amiR-duff transgene, the processes controlled by the targeted genes are affected. Depending on the amiR-duff directed gene expression output, the mutant plants display different reproductive defects. Although the experimental results quantifying the transmission defects of amiR-duff lines are variable, they seem to be consistent with the already discussed variability of the pollen developmental phenotype and the underlying complex gene expression pattern in these lines.

The hypothesis that members of the DUF1216 family are important for pollen tube growth through the transmitting tract is supported by the observation that in selfed homozygous amiR-duff lines a proportion of ovules remain unfertilized and abort, although multiple pollen tubes grow normally through the transmitting tract (Aniline blue staining in line 25-5, data not shown). Since maternal fertility defects were not detected in reciprocal crosses, it can be assumed that the ovule abortion occurs prior to fertilization as a result of failed gamete recognition. Transcriptome data derived from mature pollen grains, hydrated pollen grains and germinated pollen (Wang et al., 2008c) shows that *DUFF* genes transcript levels drop significantly during imbibition, with only *DUFF12* strongly expressed in the growing pollen tube, followed in abundance by *DUFF11*, *DUFF3* and *DUFF6* expression. However, the hypothesis about the importance of DUF1216 family genes in later reproductive stages needs further examination and quantification.

The results from the transmission efficiency analysis conducted in the *DUFF*-deficient genetic background of the *hen1-1 Arabidopsis* mutant (see chapter 4.2 and Table 4-2) is consistent with the transmission analysis of the amiR-duff lines, because reduced transmission through the male gametophyte was observed in both experiments. Nevertheless, the results obtained using the *hen1-1* mutant should be interpreted cautiously, since its genetic defect is causing a complex pleiotropic phenotypic response in the plant (Chen et al., 2002b).

5.1.3 Linking the genotype to the observed phenotype

We found that plants expressing amiR-duff constructs show reduced levels of *DUFF* gene expression, but display highly variable reproductive phenotypes. Therefore, it is difficult to define a direct relationship between the phenotypic defects of the mutant plants and the gene silencing action of the introduced amiRNA. A functional complementation assay would provide this link, but establishing a proper genetic system to functionally rescue the unstable phenotypic effects observed in the amiR-duff lines represents a further challenge.

As it has been shown for endogenous miRNAs (Palatnik et al., 2003), designing a target gene version carrying a silent mutation in the amiRNA-complementary site and introducing it in the amiRNA-plants would complement the mutant phenotype. In the case of the DUF1216 family it was demonstrated that the expression of multiple genes contributes to the phenotype occurrence, but the contribution of single *DUFF* expression is not known. In order to demonstrate and properly quantify the functional contribution of the DUF1216 members to the occurrence of reproductive defects in the amiR-duff lines, amiRNA-resistant versions of different target *DUFF* genes should be re-introduced in the amiR-duff plants. Possibly, lines carrying resistant versions of multiple *DUFF* genes in different combinations should be generated in order to obtain significant phenotypic effect and quantify the contribution of the different members. Subsequently, phenotypic traits like pollen abortion and transmission efficiency of the resulting transgenic lines should be precisely quantified and compared to the reproductive phenotypes among amiR-duff populations. Ideally, the plants carrying amiR-resistant versions of the DUFF proteins will show reduced levels of pollen abortion and transmission efficiency defects. However, the prominent phenotype variability among the amiR-duff populations could make it difficult to interpret the results. In addition, as it was already discussed in section 4.3.4, multiple insertions can lead to phenotypic outcome, which is not caused solely by the action of the introduced amiRNA. Supertransforming the amiR5x-duff lines, which carry two amiR-duff T-DNAs and at least four SALK T-DNA insertions (vector backbone pBIN-pROK2) originating from the *duff11* line, will make the genetic background of the complementation mutant lines even more complex and will increase the chances for undesirable phenotypic outcome.

In order to overcome these issues, an alternative to a functional complementation approach was designed (personal communication Prof. Niko Geldner) and is a subject of ongoing work. Homozygous T-DNA lines for several members of the DUF1216 family were selected based on results from this work considering the contribution of the different *DUFF* gene expression to the reproductive phenotype occurrence, and the line availability by the NASC Stock centre. Wild type Col-0 and plants from the chosen T-DNA mutant lines (*duff3*, *duff6*, and *duff11*) were used to transform a construct carrying amiR5x-duff under the control of pUBQ10, as well as a RFP fluorophore under the control of a seed specific promoter (Melamed-Bessudo et al., 2005). Thus, the silencing action of the amiR5x-duff could be further analysed independently or combined with a null genetic background of *DUFF3*, *DUFF6*, and *DUFF11*, whose absence could potentially increase the expected phenotypic effects. The

obtained T1 transformants would be homozygous for the SALK T-DNA insertion in the locus of the corresponding *DUFF* gene, but will be hemizygous for the newly introduced T-DNA (amiRNA5x-duff +/- RFP +/-), which would make these plants suitable for a transmission efficiency analysis. Pollinating WT stigmas with mutant pollen will allow the quantification of the male transmission efficiency based on seed fluorescence signal within the same plant generation and the results from this analysis will represent a measurement for the effect of the amiR5x-duff on the plant reproductive performance. Ideally, the male transmission efficiency of the transformants would be affected and this phenotypic effect would be stronger if the amiR5x-duff construct was introduced into *DUFF*-deficient mutant background. Comparing the experimental results for multiple crosses using independent T1 lines would generate statistically significant result allowing drawing conclusions about the importance of the DUF1216 family members for the proper male reproductive function.

5.2 Multiple members of the DUF1216 family act together to fulfil their biological function

5.2.1 Complexity within DUF1216 family

In the previous parts of this work the reproductive defects of the amiR-duff mutant lines were described. Using sophisticated statistical analysis of gene expression and phenotype quantification data, it was found that several of the DUF1216 family members (*DUFF3*, *DUFF5*, *DUFF6*, *DUFF8*, *DUFF12*, see 4.3.9) significantly contribute to the phenotype. Combined with the knowledge about the *DUFF* expression over pollen developmental stages where most of the members are co-expressed, these data supports the hypothesis that multiple DUFF proteins act together to fulfil their cellular function. However, it is not clear what kind of molecular interactions are characteristic for the DUFF proteins.

Since no other functional domains were identified within the family, it can be assumed that the protein function is based on the DUF1216 domain. In addition, the overall sequence similarity within the family is below 30% with the exception of *DUFF4*, *DUFF5* (> 95 % identical sequences), *DUFF3*, *DUFF6* (48 % identical to each other), and *DUFF8* (ca. 78 % identity to *DUFF4* and *DUFF5*). The assumption about the common molecular function based on the domain DUF1216, together with the evidence from single *duff* KO mutants showing no visible phenotype, suggests that functional redundancy exists among the proteins.

Functional redundancy is a well-known phenomenon in plants, which can hinder studying large protein families. Members of the F-box family proteins, which are involved in protein degradation, are also highly expressed in pollen according to available transcriptomics data. Confirmed T-DNA mutants for multiple members of the family were extensively studied, but none of them showed reproductive defects, suggesting functional redundancy and/or a high proportion of pseudogenes among these F-box protein genes (Ikram et al., 2014). On the other hand, most of the *DUFF* genes are transcribed and translated displaying characteristic expression patterns, suggesting that they all could have unique function in the reproductive process. As already mentioned above, based on the gene expression patterns during pollen development one can hypothesize that some of the DUFFs are important during whole microgametogenesis, whereas expression of others is restricted to the later stages of pollen maturation (see Fig. 5-1). The co-expression of multiple genes combined with potential overlapping molecular function could indicate cooperative mode of action for the DUF1216 proteins. Protein-protein interactions are commonly observed between the members of the same family (Park et al., 2001). For the members of AtMIKC* transcription factor family expressed during late pollen developmental stages, it was shown that the formation of different, partially functionally redundant heterodimeric protein complexes is required for DNA-binding (Verelst et al., 2007). Within the DUF1216 family functional co-regulation at transcriptional or protein level is also possible. Supporting this hypothesis are the observed synergistic effects of *DUFF6* and *DUFF12* gene expression downregulation (*DUFF12* as a potential off-target of the amiR-duff) on the pollen abortion phenotype occurrence (4.3). However, the putative associations between different DUFF proteins to fulfil their biological function need further extended analysis.

Although one can suspect functional association of DUFF proteins (redundancy or cooperative action) based on the temporal co-expression during pollen development, information about the spatial co-occurrence of the DUFF proteins will strengthen this hypothesis. Moreover, knowing the cellular localization can help elucidating the molecular function of the DUFF proteins. For example, localization studies combined with functional assays of integrin-like proteins in *Lilium* and *Nicotiana* pollen tubes revealed that these receptors are localized in the tip and periphery of the pollen tube and presumably play roles in tip growth and interaction with the extracellular matrix of the style (Sun et al., 2000). Similarly, studying the fluorescent protein fusion localization and dynamics of Pra2 and Pra3 (small GTPases from Ypt3/Rab11 family) revealed their localization to Golgi stacks and

TGN, respectively, indicating functional diversification within Ypt3/Rab11 family (Inaba et al., 2002). Cloning fluorescent protein fusion versions of the DUFFs to study their sub-cellular localization represents a valuable tool to study the protein dynamics *in vivo*. Data gained until now suggests that DUFF7 is strongly expressed at the plasma membrane of the pollen tube and DUFF11 expression signal represents cable-like structures potentially corresponding to cytoskeletal proteins, as well as highly mobile granules in the growing pollen. Gaining more data about the spatio-temporal subcellular dynamics of different DUFF proteins during pollen development, germination and pollen tube growth will improve the understanding of the role of DUF1216 family during plant reproduction.

In order to investigate putative interactions within the family, bimolecular fluorescence complementation (BiFC) can be applied by cloning truncated FP fusion versions of the *DUFF* genes (Kodama and Hu, 2012). More importantly, identifying the interaction partners of the DUF1216 proteins will be very informative about their physiological role, since it will reveal the molecular pathway they are acting in. As it was described in part 2.3 of this work, *in silico* analysis of DUF1216 protein structure identified several putative interactors associated with cellular trafficking. Based on the results from this analysis it was predicted that DUFF proteins are part of the vesicular trafficking machinery in pollen. Large screening of yeast-expressed libraries (Fields and Song, 1989) can be useful to identify putative interactors and possibly confirm this prediction. In addition, for further investigation of this hypothesis, expression studies in *DUFF*-deficient genetic background can be conducted. If the expression pattern of well-known markers for studied sub-cellular pathways or the expression of the predicted interactors is disturbed in *DUFF*-mutant background (e.g. amiR-duff lines), these results will strengthen the current hypothesis for DUF1216 cellular function.

5.2.2 Targeting DUF1216 family members with amiRNA generates genetically and phenotypically variable system

The characterization of amiR-duff lines included gene expression analysis and quantification of reproductive phenotypes presumably caused by *DUFF* gene downregulation. Although, extensive statistical analysis of these data concluded that the phenotype occurrence depends on *DUFF* gene expression, the analysis also inferred that strong biological variability is characteristic for DUF1216 family expression and no direct correlation between the plant *DUFF* expression pattern and measured phenotype could be specified. Moreover, the two quantified reproductive defects in amiR-duff populations, pollen degeneration and male

transmission efficiency, varied in their occurrence and strength between the individual lines, but also between individuals from the same line. We assume that the strong phenotypic variability reflects the fluctuations in DUF1216 gene expression resulting from our attempt to interfere with the complexity of this functional network.

There are two sources of variability, probably resulting in phenotypic diversity in the amiR-duff lines. One comes from the natural variability of *DUFF* gene expression and is also a result from the amiR-duff interference with the presumably complex system of interacting proteins. Second, the technical aspects of applying amiRNA knock down approach, as well as measuring gene expression in bulk tissue containing multiple cells in different developmental or cell cycle stage also contributes to all-over system variability.

Steady-state mRNA level, measured in this work, is determined by gene transcription and mRNA degradation rates, which are multi-step processes, having many different regulation points. The observed differences in the *DUFF* transcript levels suggests fast changes in mRNA abundance and tight regulation of the mRNA turnover, which is characteristic for regulatory genes like those involved in the cell cycle (Kim and Chen, 2011; Wang et al., 2002). This observation would support the prediction of a role of DUF1216 family members in sub-cellular trafficking, since the highly dynamic nature of transport processes requires fast changes in the supporting protein machinery. However, data about DUF1216 protein abundance – rather than mRNA levels – during pollen development is required to support this hypothesis.

In section 5.2.1 it was discussed that the members of the DUF1216 protein family are potentially functionally interconnected. It was also found that multiple DUFFs contribute to the phenotype, but the interaction context is not clear. Either functional redundancy or/and a cooperative mechanism were assumed. In favour of this hypothesis is the observed variability among amiR-duff line populations. It was shown that introducing a mutation to components of an interconnected regulatory network leads to large variation of expression of downstream genes, resulting in high phenotypic variation (Raj et al., 2010). In this work the authors mutated different components of the transcription factor network regulating intestinal specification in the nematode *Caenorhabditis elegans*, which resulted in high phenotype diversity of the mutant populations (WT-like formation of intestinal cells or failure in intestinal precursor development). Measuring the expression levels of the genes in the transcriptional network led to the discovery that disturbing the gene expression balance in the network results in a strong gene expression variability of functionally redundant downstream

players. Further, the authors demonstrated that this variation in gene expression is subjected to a threshold, which regulates an ON/OFF expression pattern of the master regulator gene in the intestinal formation regulatory network thus yielding alternative cell fates in genetically identical organisms. In addition, this study supports the hypothesis that systems controlled by interconnected elements are more robust against genetic and environmental variation, since the components of the network have a buffering effect on expression variability, especially if functional redundancy is characteristic for the system (Jeong et al., 2001; Levy and Siegal, 2008). It is not clear what is the functional interconnection of the members of DUF1216 family and if they play a role in the same cellular processes similar to the above described regulatory network, but the evidence summarized in the current work suggests that this is a highly probable scenario.

The described potentially complex interactions of the DUF1216 family members are not the single source of biological variability in the amiR-duff lines. The mRNA was quantified using RNA extracted from bulk material (whole flowers from single plants or anthers from several flowers of individual plants, depending on the experiment). Although the pollen grains undergo synchronized development within the anthers (Ishiguro, 2001; Wilson et al., 2011), it is possible that slight variations in the developmental timing have an impact on the amount of detected *DUFF* mRNA, especially considering the assumed fast changes in the transcriptional status of these genes during pollen development.

The amiRNA technique has been established as a reliable approach to supress genes of interest acting at both post-transcriptional and translational level (Yu and Pilot, 2014). Nevertheless, it was shown that the efficiency of the downregulation and the phenotypical effects can vary depending on the amiRNA structure and binding position within the target molecule (Schwab et al., 2006), on the regulation of the amiRNA abundance and activity within the single organism (Deveson et al., 2013; Fujii et al., 2014), as well as on the amount of the target transcript (Arvey et al., 2010). The function of *MONOGALACTOSYLDIACYLGLYCEROL SYNTHASE1* (*MGD1*) gene was studied expressing amiR-MGD1 in *A. thaliana* (Fujii et al., 2014). Since monogalactosyldiacylglycerol is an important structural part of thylakoid membranes and is essential for chloroplast development, the mutant plants with strongly reduced MGD1 transcript levels showed a wide range of phenotypes related to chloroplast development, even within the same line. However, the severity of the observed phenotypes correlated with the amount of the residual transcript of the target gene. Nevertheless, this example shows that the

regulation of an amiRNA is highly specific and can significantly differ even in plant populations of the same genetic background (lines). Applying amiRNA technique to target five of the ten pollen-expressed DUF1216 members also resulted in high phenotypic variability, including within the same line, but it did not clearly correlate with the *DUFF* gene expression pattern. The expression and the silencing action of the amiRNA differ in every individual plant, which interferes with the presumably complex interactions within the DUF1216 protein network. Therefore, it could be assumed that the observed phenotypic variability is the physiological response of the individual plant to the differential level of downregulation of the target (and possibly off-target) genes by the amiR-duff.

The generation of an efficient amiRNA knock down system targeting six of the DUF1216 members to a different extent did not result in a stable phenotypic outcome, suggesting that multiple factors contribute to this result. On the one side, as it was already discussed, are the potentially complex interactions of the members of DUF1216 family, whose precisely regulated expression might be important for proper pollen development and/or reproduction processes, and, on the other side is the line- and organism-specific silencing action of amiR-duff interfering with the DUF1216 network.

Although the chosen amiRNA approach provided evidence about the role of DUF1216 family members in pollen development and reproduction processes, the exact function of the proteins remains unknown. Studying their function in detail would be greatly facilitated by establishing a genetic system with distinct phenotypic output, which is easy to quantify.

Since the efficiency of the amiRNA depends on the structure of the amiRNA molecule and its binding position within the target sequence (Yu and Pilot, 2014), cloning and analysing alternative amiRNA sequences could be considered. Moreover, based on the knowledge gained during this work, amiRNAs targeting *DUFFs* that are significantly connected to the phenotype (*DUFF12*, *DUFF8*, *DUFF6*, and *DUFF3*) can be designed.

In the recent years, the advancement of genome editing techniques using sequence-specific DNA nucleases led to the development and application of the CRISPR/Cas system in plants (Feng et al., 2013). The method takes advantage of the bacterial adaptive immune system (Jinek et al., 2012), where the components were genetically modified to fulfil the requirements of different eukaryotic organisms, allowing targeted genome editing through either error-prone nonhomologous end joining or homology-directed repair after sequence-specific cleavage. The introduced mutations disrupting the coding sequence of interest are heritable and stable in the following generations (Feng et al., 2014) and the technique was

applied to target multiple genes of interest (Wang et al., 2015). The advantage of applying targeted genome editing to the members of the DUF1216 family is that null mutants for several of the genes could be generated. Possibly, this will result in distinct phenotypic response and will facilitate further analysis. Furthermore, the examination of mutants for different subsets of *DUFF* genes could help understanding the potential interplay and the complexity within the family.

III. Bibliography

Alexander, M.P. (1969). Differential staining of aborted and nonaborted pollen. Stain Technol. *44*, 117–122.

Arvey, A., Larsson, E., Sander, C., Leslie, C.S., and Marks, D.S. (2010). Target mRNA abundance dilutes microRNA and siRNA activity. Mol. Syst. Biol. *6*, 363.

Barrell, P.J., and Conner, A.J. (2006). Minimal T-DNA vectors suitable for agricultural deployment of transgenic plants. Biotechniques *41*, 708–710.

Becker, J.D., Boavida, L.C., Carneiro, J., Haury, M., and Feijó, J.A. (2003). Transcriptional profiling of Arabidopsis tissues reveals the unique characteristics of the pollen transcriptome. Plant Physiol. *133*, 713–725.

Boavida, L.C., and McCormick, S. (2007). Temperature as a determinant factor for increased and reproducible in vitro pollen germination in Arabidopsis thaliana. Plant J. *52*, 570–582.

Boavida, L.C., Ana Maria, V., Jörg D., B., and José A., F. (2005). Int J Dev Biol - Gametophyte interaction and sexual reproduction: how plants make a zygote.

Boisson-Dernier, A., Frietsch, S., Kim, T.-H., Dizon, M.B., and Schroeder, J.I. (2008). The peroxin loss-of-function mutation abstinence by mutual consent disrupts male-female gametophyte recognition. Curr. Biol. *18*, 63–68.

Boisson-Dernier, A., Lituiev, D.S., Nestorova, A., Franck, C.M., Thirugnanarajah, S., and Grossniklaus, U. (2013). ANXUR receptor-like kinases coordinate cell wall integrity with growth at the pollen tube tip via NADPH oxidases. PLoS Biol. *11*, e1001719.

Bokvaj, P., Hafidh, S., and Honys, D. (2015). Transcriptome profiling of male gametophyte development in Nicotiana tabacum. Genomics Data *3*, 106–111.

Brewbaker, J.L. (1967). The Distribution and Phylogenetic Significance of Binucleate and Trinucleate Pollen Grains in the Angiosperms.

Brundrett, M.C., Kendrick, B., and Peterson, C.A. (1991). Efficient Lipid Staining in Plant Material with Sudan Red 7B or Fluoral Yellow 088 in Polyethylene Glycol-Glycerol. Biotech. Histochem. *66*, 111–116.

Büttner, M. (2010). The Arabidopsis sugar transporter (AtSTP) family: an update. Plant Biol. (Stuttg). *12 Suppl 1*, 35–41.

Chen, Y.C., and McCormick, S. (1996). sidecar pollen, an Arabidopsis thaliana male gametophytic mutant with aberrant cell divisions during pollen development. Development *122*, 3243–3253.

Chen, X., Liu, J., Cheng, Y., and Jia, D. (2002a). HEN1 functions pleiotropically in Arabidopsis development and acts in C function in the flower. *1094*, 1085–1094.

Chen, X., Liu, J., Cheng, Y., and Jia, D. (2002b). HEN1 functions pleiotropically in Arabidopsis development and acts in C function in the flower. Development *129*, 1085–1094.

Chupeau, Y., Caboche, M., and Henry, Y. (1998). Androgenesis and Haploid Plants (Springer Science & Business Media).

Clark, K.A., and Krysan, P.J. (2010). Chromosomal translocations are a common phenomenon in Arabidopsis thaliana T-DNA insertion lines. Plant J. *64*, 990–1001.

Clough, S.J., and Bent, A.F. (1998). Floral dip: a simplified method for Agrobacterium-mediated transformation of Arabidopsis thaliana. Plant J. *16*, 735–743.

Coates, J.C. (2003). Armadillo repeat proteins: beyond the animal kingdom. Trends Cell Biol. *13*, 463–471.

Curtis, M.D., and Grossniklaus, U. (2003). A Gateway Cloning Vector Set for High-Throughput Functional Analysis of Genes in Planta [w]. *133*, 462–469.

Curtis, M.J., Belcram, K., Bollmann, S.R., Tominey, C.M., Hoffman, P.D., Mercier, R., and Hays, J.B. (2009). Reciprocal chromosome translocation associated with TDNA-insertion mutation in Arabidopsis: genetic and cytological analyses of consequences for gametophyte development and for construction of doubly mutant lines. Planta *229*, 731–745.

Czechowski, T., Stitt, M., Altmann, T., Udvardi, M.K., and Scheible, W.-R. (2005). Genome-wide identification and testing of superior reference genes for transcript normalization in Arabidopsis. Plant Physiol. *139*, 5–17.

Davies, T.J., Barraclough, T.G., Chase, M.W., Soltis, P.S., Soltis, D.E., and Savolainen, V. (2004). Darwin's abominable mystery: Insights from a supertree of the angiosperms. Proc. Natl. Acad. Sci. U. S. A. *101*, 1904–1909.

Deveson, I., Li, J., and Millar, A.A. (2013). MicroRNAs with analogous target complementarities perform with highly variable efficacies in Arabidopsis. FEBS Lett. *587*, 3703–3708.

Drews, G.N., and Koltunow, A.M.G. (2011). The female gametophyte. Arabidopsis Book *9*, e0155.

Dumas, C., Knox, R.B., and Gaude, T. (1985). The spatial association of the sperm cells and vegetative nucleus in the pollen grain ofBrassica. Protoplasma *124*, 168–174.

Durbarry, A., Vizir, I., and Twell, D. (2005). Male germ line development in Arabidopsis. duo pollen mutants reveal gametophytic regulators of generative cell cycle progression. Plant Physiol. *137*, 297–307.

Edlund, A.F., Swanson, R., and Preuss, D. (2004). Pollen and stigma structure and function: the role of diversity in pollination. Plant Cell *16 Suppl*, S84–S97.

Escobar-Restrepo, J.-M., Huck, N., Kessler, S., Gagliardini, V., Gheyselinck, J., Yang, W.-C., and Grossniklaus, U. (2007). The FERONIA receptor-like kinase mediates male-female interactions during pollen tube reception. Science *317*, 656–660.

Feng, Z., Zhang, B., Ding, W., Liu, X., Yang, D.-L., Wei, P., Cao, F., Zhu, S., Zhang, F., Mao, Y., et al. (2013). Efficient genome editing in plants using a CRISPR/Cas system. Cell Res. *23*, 1229–1232.

Feng, Z., Mao, Y., Xu, N., Zhang, B., Wei, P., Yang, D.-L., Wang, Z., Zhang, Z., Zheng, R., Yang, L., et al. (2014). Multigeneration analysis reveals the inheritance, specificity, and patterns of CRISPR/Cas-induced gene modifications in Arabidopsis. Proc. Natl. Acad. Sci. U. S. A. *111*, 4632–4637.

Fields, S., and Song, O. (1989). A novel genetic system to detect protein–protein interactions. Nature *340*, 245–246.

Finn, R.D., Bateman, A., Clements, J., Coggill, P., Eberhardt, R.Y., Eddy, S.R., Heger, A., Hetherington, K., Holm, L., Mistry, J., et al. (2014). Pfam: the protein families database. Nucleic Acids Res. *42*, D222–D230.

Francis, K.E., Lam, S.Y., and Copenhaver, G.P. (2006). Separation of Arabidopsis pollen tetrads is regulated by QUARTET1, a pectin methylesterase gene. Plant Physiol. *142*, 1004–1013.

Fu, Z., and Yang, P. (2014). Proteomics Advances in the Understanding of Pollen–Pistil Interactions. Proteomes *2*, 468–484.

Fujii, S., Kobayashi, K., Nakamura, Y., and Wada, H. (2014). Inducible knockdown of MONOGALACTOSYLDIACYLGLYCEROL SYNTHASE1 reveals roles of galactolipids in organelle differentiation in Arabidopsis cotyledons. Plant Physiol. *166*, 1436–1449.

Gabriel, K.R. (1969). Simultaneous Test Procedures--Some Theory of Multiple Comparisons. Ann. Math. Stat. *40*, 224–250.

Gibalová, A., Renák, D., Matczuk, K., Dupl'áková, N., Cháb, D., Twell, D., and Honys, D. (2009). AtbZIP34 is required for Arabidopsis pollen wall patterning and the control of several metabolic pathways in developing pollen. Plant Mol. Biol. *70*, 581–601.

Goldberg, R.B., Beals, T.P., and Sanders, P.M. (1993). Anther development: basic principles and practical applications. Plant Cell *5*, 1217–1229.

Golden, T.A., Schauer, S.E., Lang, J.D., Pien, S., Mushegian, A.R., Grossniklaus, U., Meinke, D.W., and Ray, A. (2002). SHORT INTEGUMENTS1/SUSPENSOR1/CARPEL FACTORY, a Dicer homolog, is a maternal effect gene required for embryo development in Arabidopsis. Plant Physiol. *130*, 808–822.

Grobei, M. a, Qeli, E., Brunner, E., Rehrauer, H., Zhang, R., Roschitzki, B., Basler, K., Ahrens, C.H., and Grossniklaus, U. (2009). Deterministic protein inference for shotgun

proteomics data provides new insights into Arabidopsis pollen development and function. Genome Res. *19*, 1786–1800.

Hanahan, D. (1983). Studies on transformation of Escherichia coli with plasmids. J. Mol. Biol. *166*, 557–580.

Hellens, R., Mullineaux, P., and Klee, H. (2000). Technical Focus:a guide to Agrobacterium binary Ti vectors. Trends Plant Sci. *5*, 446–451.

Herr, J.M.J. (1971). A New Clearing-Squash Technique for the Study of Ovule Development in Angiosperms. A New Clear. Tech. Study Ovule Dev. Angiosperms *58*, 785–790.

Higashiyama, T., Yabe, S., Sasaki, N., Nishimura, Y., Miyagishima S, Kuroiwa, H., and Kuroiwa, T. (2001). Pollen tube attraction by the synergid cell. Science *293*, 1480–1483.

Holmes-Davis, R., Tanaka, C.K., Vensel, W.H., Hurkman, W.J., and McCormick, S. (2005). Proteome mapping of mature pollen of Arabidopsis thaliana.

Honys, D., and Twell, D. (2003). Comparative analysis of the Arabidopsis pollen transcriptome. Plant Physiol. *132*, 640–652.

Honys, D., and Twell, D. (2004). Transcriptome analysis of haploid male gametophyte development in Arabidopsis. Genome Biol. *5*, R85.

Huang, L., Cao, J., Zhang, A.-H., Zhang, Y.-C., and Ye, Y.-Q. (2008). Characterisation of BcMF10 , a novel gene involved in pollen wall development of Brassica rapa ssp. chinensis. Funct. Plant Biol. *35*, 1194.

Huang, S., An, Y.Q., McDowell, J.M., McKinney, E.C., and Meagher, R.B. (1997). The arabidopsis ACT11 actin gene is strongly expressed in tissues of the emerging inflorescence, pollen, and developing ovules.

Huck, N., Moore, J.M., Federer, M., and Grossniklaus, U. (2003). The Arabidopsis mutant feronia disrupts the female gametophytic control of pollen tube reception. Development *130*, 2149–2159.

Ikram, S., Durandet, M., Vesa, S., Pereira, S., Guerche, P., and Bonhomme, S. (2014). Functional redundancy and/or ongoing pseudogenization among F-box protein genes expressed in Arabidopsis male gametophyte. Plant Reprod. *27*, 95–107.

Inaba, T., Nagano, Y., Nagasaki, T., and Sasaki, Y. (2002). Distinct localization of two closely related Ypt3/Rab11 proteins on the trafficking pathway in higher plants. J. Biol. Chem. *277*, 9183–9188.

Inoue, H., Nojima, H., and Okayama, H. (1990). High efficiency transformation of Escherichia coli with plasmids. Gene *96*, 23–28.

Ischebeck, T., Valledor, L., Lyon, D., Gingl, S., Nagler, M., Meijón, M., Egelhofer, V., and Weckwerth, W. (2014). Comprehensive cell-specific protein analysis in early and late pollen

development from diploid microsporocytes to pollen tube growth. Mol. Cell. Proteomics *13*, 295–310.

Ishiguro, S. (2001). The DEFECTIVE IN ANTHER DEHISCENCE1 Gene Encodes a Novel Phospholipase A1 Catalyzing the Initial Step of Jasmonic Acid Biosynthesis, Which Synchronizes Pollen Maturation, Anther Dehiscence, and Flower Opening in Arabidopsis. PLANT CELL ONLINE *13*, 2191–2209.

Jeong, H., Mason, S.P., Barabási, A.L., and Oltvai, Z.N. (2001). Lethality and centrality in protein networks. Nature *411*, 41–42.

Ji, J., and Braam, J. (2010). Restriction site extension PCR: a novel method for high-throughput characterization of tagged DNA fragments and genome walking. PLoS One *5*, e10577.

Jinek, M., Chylinski, K., Fonfara, I., Hauer, M., Doudna, J.A., and Charpentier, E. (2012). A programmable dual-RNA-guided DNA endonuclease in adaptive bacterial immunity. Science *337*, 816–821.

Jung, C., Seo, J.S., Han, S.W., Koo, Y.J., Kim, C.H., Song, S.I., Nahm, B.H., Choi, Y. Do, and Cheong, J.-J. (2008). Overexpression of AtMYB44 enhances stomatal closure to confer abiotic stress tolerance in transgenic Arabidopsis. Plant Physiol. *146*, 623–635.

Kessler, S.A., Shimosato-Asano, H., Keinath, N.F., Wuest, S.E., Ingram, G., Panstruga, R., and Grossniklaus, U. (2010). Conserved molecular components for pollen tube reception and fungal invasion. Science *330*, 968–971.

Kim, E.-D., and Chen, Z.J. (2011). Unstable transcripts in Arabidopsis allotetraploids are associated with nonadditive gene expression in response to abiotic and biotic stresses. PLoS One *6*, e24251.

Kodama, Y., and Hu, C.-D. (2012). Bimolecular fluorescence complementation (BiFC): A 5-year update and future perspectives. Biotechniques *53*, 285–298.

Koncz, C., and Schell, J. (1986). The promoter of TL-DNA gene 5 controls the tissue-specific expression of chimaeric genes carried by a novel type of Agrobacterium binary vector. MGG Mol. Gen. Genet. *204*, 383–396.

Konieczny, A., and Ausubel, F.M. (1993). A procedure for mapping Arabidopsis mutations using co-dominant ecotype-specific PCR-based markers. Plant J. *4*, 403–410.

Krebs, M., Held, K., Binder, A., Hashimoto, K., Den Herder, G., Parniske, M., Kudla, J., and Schumacher, K. (2012). FRET-based genetically encoded sensors allow high-resolution live cell imaging of Ca^{2+} dynamics. Plant J. *69*, 181–192.

Krysan, P.J. (1999). T-DNA as an Insertional Mutagen in Arabidopsis. PLANT CELL ONLINE *11*, 2283–2290.

Lalanne, E., and Twell, D. (2002). Genetic control of male germ unit organization in Arabidopsis. Plant Physiol. *129*, 865–875.

Lee, J.-Y., and Lee, D.-H. (2003). Use of serial analysis of gene expression technology to reveal changes in gene expression in Arabidopsis pollen undergoing cold stress. Plant Physiol. *132*, 517–529.

Lee, I., Ambaru, B., Thakkar, P., Marcotte, E.M., and Rhee, S.Y. (2010). Rational association of genes with traits using a genome-scale gene network for Arabidopsis thaliana. Nat. Biotechnol. *28*, 149–156.

Levy, S.F., and Siegal, M.L. (2008). Network hubs buffer environmental variation in Saccharomyces cerevisiae. PLoS Biol. *6*, e264.

Leydon, A.R., Beale, K.M., Woroniecka, K., Castner, E., Chen, J., Horgan, C., Palanivelu, R., and Johnson, M.A. (2013). Three MYB transcription factors control pollen tube differentiation required for sperm release. Curr. Biol. *23*, 1209–1214.

Lindner, H., Kessler, S.A., Müller, L.M., Shimosato-Asano, H., Boisson-Dernier, A., and Grossniklaus, U. (2015). TURAN and EVAN mediate pollen tube reception in Arabidopsis Synergids through protein glycosylation. PLoS Biol. *13*, e1002139.

Ling, D., and Salvaterra, P.M. (2011). Robust RT-qPCR data normalization: validation and selection of internal reference genes during post-experimental data analysis. PLoS One *6*, e17762.

Loraine, A.E., McCormick, S., Estrada, A., Patel, K., and Qin, P. (2013). RNA-seq of Arabidopsis pollen uncovers novel transcription and alternative splicing. Plant Physiol. *162*, 1092–1109.

Ma, J., Skibbe, D.S., Fernandes, J., and Walbot, V. (2008). Male reproductive development: gene expression profiling of maize anther and pollen ontogeny. Genome Biol. *9*, R181.

Mahlberg, P. (1972). Localization of neutral red in lysosome structures in hair cells of Tradescantia virginiana. Can. J. Bot. *50*, 857–859.

Von Malek, B., van der Graaff, E., Schneitz, K., and Keller, B. (2002). The Arabidopsis male-sterile mutant dde2-2 is defective in the ALLENE OXIDE SYNTHASE gene encoding one of the key enzymes of the jasmonic acid biosynthesis pathway. Planta *216*, 187–192.

Mayfield, J.A., Fiebig, A., Johnstone, S.E., and Preuss, D. (2001). Gene families from the Arabidopsis thaliana pollen coat proteome. Science *292*, 2482–2485.

McCormick, S. (2004). Control of male gametophyte development. Plant Cell *16 Suppl*, S142–S153.

McCue, A.D., Cresti, M., Feijó, J.A., and Slotkin, R.K. (2011). Cytoplasmic connection of sperm cells to the pollen vegetative cell nucleus: potential roles of the male germ unit revisited. J. Exp. Bot. *62*, 1621–1631.

Melamed-Bessudo, C., Yehuda, E., Stuitje, A.R., and Levy, A.A. (2005). A new seed-based assay for meiotic recombination in Arabidopsis thaliana. Plant J. *43*, 458–466.

Miki, T., Park, J.A., Nagao, K., Murayama, N., and Horiuchi, T. (1992). Control of segregation of chromosomal DNA by sex factor F in Escherichia coli. Mutants of DNA gyrase subunit A suppress letD (ccdB) product growth inhibition. J. Mol. Biol. *225*, 39–52.

Murashige, T., and Skoog, F. (1962). A Revised Medium for Rapid Growth and Bio Assays with Tobacco Tissue Cultures. Physiol. Plant. *15*, 473–497.

Nelder, J.A., and Wedderburn, R.W.M. (1972). Generalized Linear Models. J. R. Stat. Soc. Ser. A *135*, 370–384.

Ngo, Q.A., Vogler, H., Lituiev, D.S., Nestorova, A., and Grossniklaus, U. (2014). A Calcium Dialog Mediated by the FERONIA Signal Transduction Pathway Controls Plant Sperm Delivery. Dev. Cell *29*, 491–500.

Oh, S.A., Johnson, A., Smertenko, A., Rahman, D., Park, S.K., Hussey, P.J., and Twell, D. (2005). A divergent cellular role for the FUSED kinase family in the plant-specific cytokinetic phragmoplast. Curr. Biol. *15*, 2107–2111.

Oh, S.A., Park, K.S., Twell, D., and Park, S.K. (2010). The SIDECAR POLLEN gene encodes a microspore-specific LOB/AS2 domain protein required for the correct timing and orientation of asymmetric cell division. Plant J. *64*, 839–850.

Okada, T., Endo, M., Singh, M.B., and Bhalla, P.L. (2005). Analysis of the histone H3 gene family in Arabidopsis and identification of the male-gamete-specific variant AtMGH3. Plant J. *44*, 557–568.

Ossowski, S., Schwab, R., and Weigel, D. (2008). Gene silencing in plants using artificial microRNAs and other small RNAs. Plant J. *53*, 674–690.

Pacini, E. (1996). Types and meaning of pollen carbohydrate reserves. Sex. Plant Reprod. *9*, 362–366.

Palatnik, J.F., Allen, E., Wu, X., Schommer, C., Schwab, R., Carrington, J.C., and Weigel, D. (2003). Control of leaf morphogenesis by microRNAs. Nature *425*, 257–263.

Park, J., Lappe, M., and Teichmann, S.A. (2001). Mapping protein family interactions: intramolecular and intermolecular protein family interaction repertoires in the PDB and yeast. J. Mol. Biol. *307*, 929–938.

Park, S.K., Howden, R., and Twell, D. (1998). The Arabidopsis thaliana gametophytic mutation gemini pollen1 disrupts microspore polarity, division asymmetry and pollen cell fate. Development *125*, 3789–3799.

Parker, G. (2003). Isolation of COV1, a gene involved in the regulation of vascular patterning in the stem of Arabidopsis. Development *130*, 2139–2148.

Pina, C., Pinto, F., Feijó, J. a, and Becker, J.D. (2005). Gene family analysis of the Arabidopsis pollen transcriptome reveals biological implications for cell growth, division control, and gene expression regulation. Plant Physiol. *138*, 744–756.

Preuss, D., Rhee, S.Y., and Davis, R.W. (1994). Tetrad analysis possible in Arabidopsis with mutation of the QUARTET (QRT) genes. Science *264*, 1458–1460.

Raj, A., Rifkin, S.A., Andersen, E., and van Oudenaarden, A. (2010). Variability in gene expression underlies incomplete penetrance. Nature *463*, 913–918.

Regan, S.M., and Moffatt, B.A. (1990). Cytochemical Analysis of Pollen Development in Wild-Type Arabidopsis and a Male-Sterile Mutant. Plant Cell *2*, 877–889.

Rhee, S.Y., Osborne, E., Poindexter, P.D., and Somerville, C.R. (2003). Microspore separation in the quartet 3 mutants of Arabidopsis is impaired by a defect in a developmentally regulated polygalacturonase required for pollen mother cell wall degradation. Plant Physiol. *133*, 1170–1180.

Sablok, G., Pérez-Quintero, A.L., Hassan, M., Tatarinova, T. V, and López, C. (2011). Artificial microRNAs (amiRNAs) engineering - On how microRNA-based silencing methods have affected current plant silencing research. Biochem. Biophys. Res. Commun. *406*, 315–319.

Sambrook, J., and Russel, D.W. (2012). Molecular Cloning: A Laboratory Manual (Fourth Edition).

Sanderfoot, A.A., Pilgrim, M., Adam, L., and Raikhel, N. V (2001). Disruption of individual members of Arabidopsis syntaxin gene families indicates each has essential functions. Plant Cell *13*, 659–666.

Sarhadi, E., Bazargani, M.M., Sajise, A.G., Abdolahi, S., Vispo, N.A., Arceta, M., Nejad, G.M., Singh, R.K., and Salekdeh, G.H. (2012). Proteomic analysis of rice anthers under salt stress. Plant Physiol. Biochem. *58*, 280–287.

Schiefthaler, U., Balasubramanian, S., Sieber, P., Chevalier, D., Wisman, E., and Schneitz, K. (1999). Molecular analysis of NOZZLE, a gene involved in pattern formation and early sporogenesis during sex organ development in Arabidopsis thaliana. Proc. Natl. Acad. Sci. *96*, 11664–11669.

Schiøtt, M., Romanowsky, S.M., Baekgaard, L., Jakobsen, M.K., Palmgren, M.G., and Harper, J.F. (2004). A plant plasma membrane Ca2+ pump is required for normal pollen tube growth and fertilization. Proc. Natl. Acad. Sci. U. S. A. *101*, 9502–9507.

Schmid, M., Davison, T.S., Henz, S.R., Pape, U.J., Demar, M., Vingron, M., Schölkopf, B., Weigel, D., and Lohmann, J.U. (2005). A gene expression map of Arabidopsis thaliana development. Nat. Genet. *37*, 501–506.

Schneitz, K., Hulskamp, M., and Pruitt, R.E. (1995). Wild-type ovule development in Arabidopsis thaliana: a light microscope study of cleared whole-mount tissue. Plant J. *7*, 731–749.

Schubert, D. (2004). Silencing in Arabidopsis T-DNA Transformants: The Predominant Role of a Gene-Specific RNA Sensing Mechanism versus Position Effects. PLANT CELL ONLINE *16*, 2561–2572.

Schwab, R., Ossowski, S., Riester, M., Warthmann, N., and Weigel, D. (2006). Highly Specific Gene Silencing by Artificial MicroRNAs in Arabidopsis. *18*, 1121–1133.

Schwacke, R. (1999). LeProT1, a Transporter for Proline, Glycine Betaine, and gamma-Amino Butyric Acid in Tomato Pollen. PLANT CELL ONLINE *11*, 377–392.

Singer, T., and Burke, E. (2003). High-throughput TAIL-PCR as a tool to identify DNA flanking insertions. Methods Mol. Biol. *236*, 241–272.

Slotkin, R.K., Vaughn, M., Borges, F., Tanurdzić, M., Becker, J.D., Feijó, J.A., and Martienssen, R.A. (2009). Epigenetic reprogramming and small RNA silencing of transposable elements in pollen. Cell *136*, 461–472.

Southern, E.M. (1975). Detection of specific sequences among DNA fragments separated by gel electrophoresis. J. Mol. Biol. *98*, 503–517.

Spielman, M., Preuss, D., Li, F.L., Browne, W.E., Scott, R.J., and Dickinson, H.G. (1997). TETRASPORE is required for male meiotic cytokinesis in Arabidopsis thaliana. Development *124*, 2645–2657.

Sun, Y., Qian, H., Xu, X. -d., Han, Y., Yen, L. -f., and Sun, D. -y. (2000). Integrin-Like Proteins in the Pollen Tube: Detection, Localization and Function. Plant Cell Physiol. *41*, 1136–1142.

Taylor, P.E., Glover, J.A., Lavithis, M., Craig, S., Singh, M.B., Knox, R.B., Dennis, E.S., and Chaudhury, A.M. (1998). Genetic control of male fertility in Arabidopsis thaliana : structural analyses of postmeiotic developmental mutants. Planta *205*, 492–505.

Twell, D., Yamaguchi, J., Wing, R.A., Ushiba, J., and McCormick, S. (1991). Promoter analysis of genes that are coordinately expressed during pollen development reveals pollen-specific enhancer sequences and shared regulatory elements. Genes Dev. *5*, 496–507.

Twell, D., Park, S.K., and Lalanne, E. (1998). Asymmetric division and cell-fate determination in developing pollen. Trends Plant Sci. *3*, 305–310.

Tyler, L., Thomas, S.G., Hu, J., Dill, A., Alonso, J.M., Ecker, J.R., and Sun, T.-P. (2004). Della proteins and gibberellin-regulated seed germination and floral development in Arabidopsis. Plant Physiol. *135*, 1008–1019.

Verelst, W., Saedler, H., and Münster, T. (2007). MIKC* MADS-protein complexes bind motifs enriched in the proximal region of late pollen-specific Arabidopsis promoters. Plant Physiol. *143*, 447–460.

Voinnet, O., Rivas, S., Mestre, P., and Baulcombe, D. (2003). An enhanced transient expression system in plants based on suppression of gene silencing by the p19 protein of tomato bushy stunt virus. Plant J. *33*, 949–956.

Wang, Y., Liu, C.L., Storey, J.D., Tibshirani, R.J., Herschlag, D., and Brown, P.O. (2002). Precision and functional specificity in mRNA decay. Proc. Natl. Acad. Sci. U. S. A. *99*, 5860–5865.

Wang, Y., Zhang, W.-Z., Song, L.-F., Zou, J.-J., Su, Z., and Wu, W.-H. (2008a). Transcriptome analyses show changes in gene expression to accompany pollen germination and tube growth in Arabidopsis. Plant Physiol. *148*, 1201–1211.

Wang, Y., Zhang, W.-Z., Song, L.-F., Zou, J.-J., Su, Z., and Wu, W.-H. (2008b). Transcriptome analyses show changes in gene expression to accompany pollen germination and tube growth in Arabidopsis. Plant Physiol. *148*, 1201–1211.

Wang, Y., Zhang, W.-Z., Song, L.-F., Zou, J.-J., Su, Z., and Wu, W.-H. (2008c). Transcriptome analyses show changes in gene expression to accompany pollen germination and tube growth in Arabidopsis. Plant Physiol. *148*, 1201–1211.

Wang, Z.-P., Xing, H.-L., Dong, L., Zhang, H.-Y., Han, C.-Y., Wang, X.-C., and Chen, Q.-J. (2015). Egg cell-specific promoter-controlled CRISPR/Cas9 efficiently generates homozygous mutants for multiple target genes in Arabidopsis in a single generation. Genome Biol. *16*, 144.

Webb, M., and Gunning, B.S. (1994). Embryo sac development in Arabidopsis thaliana II. The cytoskeleton during megagametogenesis. Sex. Plant Reprod. *7*.

Wei, L.Q., Xu, W.Y., Deng, Z.Y., Su, Z., Xue, Y., and Wang, T. (2010). Genome-scale analysis and comparison of gene expression profiles in developing and germinated pollen in Oryza sativa. BMC Genomics *11*, 338.

Weiss, K.M., and Buchanan, A. V. (2009). The Mermaid's Tale — Kenneth M. Weiss, Anne V. Buc hanan | Harvard University Press.

Whittington, A.T., Vugrek, O., Wei, K.J., Hasenbein, N.G., Sugimoto, K., Rashbrooke, M.C., and Wasteneys, G.O. (2001). MOR1 is essential for organizing cortical microtubules in plants. Nature *411*, 610–613.

Wilson, Z.A., Morroll, S.M., Dawson, J., Swarup, R., and Tighe, P.J. (2001a). The Arabidopsis MALE STERILITY1 (MS1) gene is a transcriptional regulator of male gametogenesis , with homology to the PHD- ® nger family of transcription factors. *28*.

Wilson, Z.A., Morroll, S.M., Dawson, J., Swarup, R., and Tighe, P.J. (2001b). The Arabidopsis MALE STERILITY1 (MS1) gene is a transcriptional regulator of male

gametogenesis, with homology to the PHD-finger family of transcription factors. Plant J. *28*, 27–39.

Wilson, Z.A., Song, J., Taylor, B., and Yang, C. (2011). The final split: the regulation of anther dehiscence. J. Exp. Bot. *62*, 1633–1649.

Winter, D., Vinegar, B., Nahal, H., Ammar, R., Wilson, G. V, and Provart, N.J. (2007). An "Electronic Fluorescent Pictograph" browser for exploring and analyzing large-scale biological data sets. PLoS One *2*, e718.

Xing, S., and Zachgo, S. (2007). Pollen lethality: a phenomenon in Arabidopsis RNA interference plants. Plant Physiol. *145*, 330–333.

Yang, C.-Y., Spielman, M., Coles, J.P., Li, Y., Ghelani, S., Bourdon, V., Brown, R.C., Lemmon, B.E., Scott, R.J., and Dickinson, H.G. (2003). TETRASPORE encodes a kinesin required for male meiotic cytokinesis in Arabidopsis. Plant J. *34*, 229–240.

Yates, F. (1934). Contingency Tables Involving Small Numbers and the $\chi 2$ Test.

Yu, S., and Pilot, G. (2014). Testing the efficiency of plant artificial microRNAs by transient expression in Nicotiana benthamiana reveals additional action at the translational level. Front. Plant Sci. *5*, 622.

Zhao, D.-Z., Wang, G.-F., Speal, B., and Ma, H. (2002). The excess microsporocytes1 gene encodes a putative leucine-rich repeat receptor protein kinase that controls somatic and reproductive cell fates in the Arabidopsis anther. Genes Dev. *16*, 2021–2031.

Zimmermann, P., Hirsch-Hoffmann, M., Hennig, L., and Gruissem, W. (2004). GENEVESTIGATOR. Arabidopsis microarray database and analysis toolbox. Plant Physiol. *136*, 2621–2632.

IV. Appendix

List of constructs

Number	Name	Host	Vector backbone	Resistance bacteria	Resistance plants	Promoter	Central part
25	pHA-pUBQ10-amiNA5x	GV3101	pMOA33	rif, gent, spec	kan	UBQ10	amiRNA5x
26	pHA-pLAT52-amiNA5x	GV3101	pMOA33	rif, gent, spec	kan	LAT52	amiRNA5x
27	pQAN-pUBQ10-amiRNA2x	GV3101	pMOA33	rif, gent, spec	basta	UBQ10	amiRNA2x
28	pQAN-pLAT52-amiRNA2x	GV3101	pMOA33	rif, gent, spec	basta	LAT52	amiRNA2x
31	pMDC163-pLAT52-GFP-fABD2	GV3101	pMDC163	rif, gent, kan	hyg	pLAT52	GFP-fABD2 (At fimbrin)
43	pHA1-pLAT52-R-GECO	GV3101	pMOA33	rif, gent, spec	kan	pLAT52	red GECO Ca^{2+} sensor
48	pHA1-pUBQ10_R-GECO	GV3101	pMOA33	rif, gent, spec	kan	UBQ10	red GECO Ca^{2+} sensor
49	pQAN1-pUBQ10-R-GECO	GV3101	pMOA36	rif, gent, spec	bas	UBQ10	red GECO Ca^{2+} sensor
50	pQAN1-pLAT52-R-GECO	GV3101	pMOA36	rif, gent, spec	bas	LAT52	red GECO Ca^{2+} sensor
55	pMDC83-D3	GV3101	pCambia	rif, gent, kan	hyg	35s	D3_gDNA
56	pMDC83-D7	GV3101	pCambia	rif, gent, kan	hyg	35s	D7_gDNA
78	pD7::D7-pMDC83	GV3101	pCambia	rif, gent, kan	hyg	pD7 2000	D7 gDNA
79	pD11::D11-pMDC83	GV3101	pCambia	rif, gent, kan	hyg	pD11 1000	D11 gDNA
81	pEDO-pOLE1::OLE1-HygR-amiRNA5x	GV3101	pCambia	rif, gent, spec	hyg	double GW cassette Geldner lab; OLE1, amiRNA5x; HygR introduced by AN;	

List of *Arabidopsis thaliana* mutant lines

Culture number	Name	Selection	Remarks	Ecotype
50	amiRNA5x 25-1	kan	line carrying pHA-pUBQ10-amiNA5x T-DNA	Col-0
51	amiRNA5x 25-5	kan	line carrying pHA-pUBQ10-amiNA5x T-DNA	Col-0
52	amiRNA5x 25-7	kan	line carrying pHA-pUBQ10-amiNA5x T-DNA	Col-0
53	amiRNA2x 27-4	bas	line carrying pQAN-pUBQ10-amiRNA2x T-DNA	Col-0
54	amiRNA5x 25-2	kan	line carrying pHA-pUBQ10-amiNA5x T-DNA	Col-0
63	D11-GFP fusion in pMDC83	hyg	pD11::D11 ORF in pMDC83 T-DNA	Col-0
64	D7-GFP fusion in pMDC83	hyg	pD7::D7 ORF in pMDC83 T-DNA	Col-0
34	duff11	kan (scilenced)	pBIN-pROK2 T-DNA	Col-0
11	cov1	-	point mutation EMS mutagenesis	Ler
25	atmyb44	kan (scilenced)	pBIN-pROK2 T-DNA	Col-0
28	dcl1-7	-	point mutation EMS mutagenesis	Col-0
27	hen1-1	-	point mutation EMS mutagenesis	Ler

List of oligonucleotides

Experiment	Number	Name	Sequence 5`-3`
amiRNA engineering	an_0001	I_miR5x_Fw	gaTAACGAATTGGGTTGTGACTTtctctcttttgtattcc
	an_0002	II_miR5x_Rv	gaAAGTCACAACCCAATTCGTTAtcaaagagaatcaatga
	an_0003	III_miR5x_Fw	gaAAATCACAACCCATTTCGTTTtcacaggtcgtgatatg
	an_0004	IV_miR5x_Rv	gaAAACGAAATGGGTTGTGATTTctacatatatattcct
	an_0005	I_miR2x_Fw	gaTAAACATTCTACAGGTCGCTGtctctcttttgtattcc
	an_0006	II_miR2x_Rv	gaCAGCGACCTGTAGAATGTTTAtcaaagagaatcaatga
	an_0007	III_miR2x_Fw	gaCAACGACCTGTAGTATGTTTTtcacaggtcgtgatatg
	an_0008	IV_miR2x_Rv	gaAAAACATACTACAGGTCGTTGtctacatatatattcct
	an_0009	I_miR1_Fw	gaTAACTAGTTGCAACAATGCACtctctcttttgtattcc
	an_0010	II_miR1_Rv	gaGTGCATTGTTGCAACTAGTTAtcaaagagaatcaatga
	an_0011	III_miR1_Fw	gaGTACATTGTTGCATCTAGTTTtcacaggtcgtgatatg
	an_0012	IV_miR1_Rv	gaAAACTAGATGCAACAATGTACtctacatatatattcct
	an_0013	I_miR9_Fw	gaTTTTAGATCTGTGTTTAGCGGtctctcttttgtattcc
	an_0014	II_miR9_Rv	gaCCGCTAAACACAGATCTAAAAtcaaagagaatcaatga
	an_0015	III_miR9_Fw	gaCCACTAAACACAGTTCTAAATtcacaggtcgtgatatg
	an_0016	IV_miR9_Rv	gaATTTAGAACTGTGTTTAGTGGtctacatatatattcct
	an_0017	A_Fw	CTGCAAGGCGATTAAGTTGGGTAAC
	an_0018	B_Rv	GCGGATAACAATTTCACACAGGAAACAG
amiRNA constructs cloning	an_0022	adapter attB1_Fw	GGGGACAAGTTTGTACAAAAAAGCAGGCT
	an_0023	adapter attB2_Rv	GGGGACCACTTTGTACAAGAAAGCTGGGT
	an_0024	amiRNA_attB1_Fw	AAAAAGCAGGCTTCCTGCAAGGCGATTAAGTTGGGT
	an_0025	amiRNA_attB2_Rv	AGAAAGCTGGGTGGCGGATAACAATTTCACACAGG
	an_0026	UBQP-HindIII-fw	AGCAAAGCTTCCGACGAGTCAGTAATAAACG
	an_0027	UBQP-KpnI-rv	AAGGTACCCCGCACTCGAGCTGTTAATCAG
	an_0028	UBQ-XbaI-fw	AATCTAGACCGACGAGTCAGTAATAAACGG
	an_0029	UBQ-AscI-rv	AAGGCGCGCCCCGCACTCGAGCTGTTAATC
	an_0030	LAT52-HindIII-fw	AGCAAAGCTTgaatgatcgattctg
	an_0031	LAT52-KpnI-rv	AAGGTACCggtaattggaaatttttttttgg
	an_0032	LAT52-XbaI-fw	AATCTAGAgaatgatcgattctgggtcatttg
	an_0033	LAT52-AscI-rv	AAGGCGCGCCggtaattggaaatttttttttgg
	an_0034	H3.3-HindIII-fw	AGCAAAGCTTtacttctccgaccaaaaac
	an_0035	H3.3-KpnI-rv	AAGGTACCttcttcgagagaacgatg
	an_0036	H3.3-XbaI-fw	AATCTAGAtacttctccgaccaaaaactttc
	an_0037	H3.3-AscI-rv	AAGGCGCGCCttcttcgagagaacgatg
PCR-RFLP / CAPS assay and standard genotyping of GENEVESTIGATOR mutants	an_0058	AciI-dcl-fw	GCCATCTTTGGAATGACTGCTCCG
	an_0059	HaeIII-dcl-fw	GCCATCTTTGGAATGACTGCTTGG
	an_0060	dcl1-7_Pr_rev	CGTTTACAAACAAAAAGTGTC
	an_0061	AciI-hen-fw	GGTGAAGTAGAACCCGGATTTGCTCCG
	an_0062	HhaI-hen-fw	GGTGAAGTAGAACCCGGATTTGCTGCG
	an_0063	hen_Pr_rev	CTTCCACTCCCAGATGACTTTA
	an_0064	AvaII-nga1-fw	GGTTACTTCGTTAGGTCAGTGGAC
	an_0065	BclI-nga1-fw	GGTTACTTCGTTAGGTCAGTTGAT
	an_0066	nga1_Pr_rv	CAAGTTCCTGATTAGCTCTCCC

	an_0067	EcoRI-cov-fw	CAAATCTCAATTGCTTTTTGTAGTGTTATCCGAATT
	an_0068	AciI-cov-fw	CAAATCTCAATTGCTTTTTGTAGTGTTATCCTACCG
	an_0069	cov_Pr_rv	CCAAGTTGTGCATATATTGGAGA
	an_0101	AciI-hen-fw_new	AAGTAGAACCCGGATTTGCTCCG
	an_0102	HhaI-hen-fw_new	AAGTAGAACCCGGATTTGCTGCG
	an_0103	hen_Pr_rev_new	TTCTTCCACTCCCAGATGACTTTATAAGG
	an_0104	EcoRI-cov-fw_new	ATCTCAATTGCTTTTTGTAGTGTTATCCGAATT
	an_0105	AciI-cov-fw_new	ATCTCAATTGCTTTTTGTAGTGTTATCCTACCG
	an_0106	cov_Pr_rv_new	AATTCTTACCAAATACGTTGATTCCAAGTTG
	an_0107	hen1-1_chen_AlwNI_fw	cagttcaatcaatgggcatc
	an_0108	hen1-1_chen_AlwNI_rv	gatgaagcttcccgtctaaaaatcagtatct
	an_0111	SGT15359/At3g61970_nga2 F	GGTCAATCTCATCCACCACC
	an_0112	SGT15359/At3g61970_nga2 R	CGATGTCTCCAGCATCAAGC
	an_0113	SaiI/At1g01030_nga3 F	GCAAGCAGCAGCTCCGGTCCC
	an_0114	SaiI/At1g01030_nga3 R	CCCGGTGAATCGGGACGGAG
	an_0115	SGT7056/At4g01500_nga4 F	GGGTCATCAATCTTCTCAAG
	an_0116	SGT7056/At4g01500_nga4 R	CAGGGATGTAGCCACGGTAG
	an_0117	Ds5_for nga2mut_fw	ACGGTCGGGAAACTAGCTCTAC
	an_0120	nga1_MseI_fw	CGTCATCATCACAGTGGTGGTGG
	an_0121	nga1_MseI_rv	CAGCCACCGCAGCCGCAGGATTGTTCCTTT
Semi-quantitative RT-PCR assay	an_0091	d3_fw_new_revT	AAAGCTATCTACCTCAAACGC
	an_0092	d3_rv_new_revT	AACTTGAAGAAGCAGCCG
	an_0093	d8_fw_new_revT	AAGAAGTGTCCACAAAAGGAG
	an_0094	d8_rv_new_revT	AAGCCTTGCCTTTGTTCTG
	an_0095	d11_fw_new_revT	TAGCCTAGAGAGCAAGTGTCC
	an_0096	d11_rv_new_revT	AAGTTATCTCCTTGGAACCG
	an_0097	d6_fw_new_revT	AGAAGAAGTATGCAGCAAAGG
	an_0098	d6_rv_new_revT	TGCCACTCACCATTTTACC
	an_0099	d4_fw_new_revT	AATACAAGGTCTTCTTCGAGC
	an_0100	d4_rv_new_revT	TTGTTCCCACTTAGTAATTGTTG
	an_0125	d1_fw_revT	ATGAAGTACTTGTGTCCGGTC
	an_0126	d1_rv_revT	TGAGACATCACTTGTTCCCAC
	an_0127	d5_fw_revT	ACTCAAGGGTACAATGATTGC
	an_0128	d5_rv_revT	TGTGTCTCGCTCTGAATAGC
	an_0129	d9_fw_revT	TGGAATCTTGAAATGGCTTC
	an_0130	d9_rv_revT	TAATTATTTGTTTCGGCTCG
	an_0131	d10_fw_revT	TCATAATAAACCTCGAAAAAAAG
	an_0132	d10_rv_revT	ACTTACTATTCTACTATGGATGGTTTC
	an_0135	d2_fw_revT	AGTGGAACTAGCACCGAAAC
	an_0136	d2_rv_revT	TTTGATAGTTGGTAGATTGATAGC
	an_0137	d12_fw_revT	AAACAAGGTCTCGGATATGC
	an_0138	d12_rv_revT	AGTGCTTCTTGTGAGGGTTG
	an_0139	Q elF4a for	TCATAGATCTGGTCCTTGAAACC
	an_0140	Q elF4a rev	GGCAGTCTCTTCGTGCTGAC
	an_0141	Q UBC for	ATGCTTGGAGTCCTGCTTGG
	an_0142	Q UBC rev	TGCCATTGAATTGAACCCTCTC

	an_0143	d7_fw_revT_new_0143	ACTTCATAAACTCGGCATCC
	an_0144	d7_rv_revT_new_0144	TATCAATTTTGTTTCCGCTC
Southern blot probe synthesis	an_0145	basProbe_fw_145	GAGACAAGCACGGTCAACTTC
	an_0146	basProbe_rv_146	ACTTCAGCAGGTGGGTGTAGA
	an_0147	kanProbe_fw_147	ACTGTTCGCCAGGCTCAAG
	an_0148	kanProbe_rv_148	TCAAGAAGGCGATAGAAGGC
	an_0173	Kan probe_FW2_an_173	ACGACGGGCGTTCCTTGC
	an_0190	T3A_probe_FW_190	agctttcgtccgtatcatcg
	an_0191	T3A_probe_RV_191	tcgacacaaaaagcctatactgtac
	MJ primer database	Pr_MJ1_probe_F_kan	GCTTGGGTGGAGAGGCTATT
		Pr_MJ1_probe_R_kan	GTCAAGAAGGCGATAGAAGGCG
Cloning of *DUFF* genes	an_0167	attB1_D3_Cfus_fw_167	AAAAAGCAGGCTTAATGGCGAAAAATTTACTAGC
	an_0168	attB2_D3_Cfus_rv_168	AGAAAGCTGGGTTGTTTTTCATGGCCATCTTTG
	an_0169	attB1_D7_Cfus_fw_169	AAAAAGCAGGCTTAATGGCAAAACTTTCATTAGC
	an_0170	attB2_D7_Cfus_rv_170	AGAAAGCTGGGTTACTGGAGCCATTAGAGGTTT
	an_0171	attB1_D11_Cfus_fw_171	AAAAAGCAGGCTTAATGGGAAAAATTTCATTAGC
	an_0172	attB2_D11_Cfus_rv_172	AGAAAGCTGGGTTGAGCTCGCTGCCGTCGTCTA
	an_0196	D7prom_Hind_fw_196	ATCCAAGCTTATACAATAGTAATCACAAAATTAATAG
	an_0197	D7prom_BamHI_rv_197	TGTTGGATCCTTTTTTTGTTCTTTTTGTTTAATATTTTTT
	an_0198	D11prom_Hind_fw_198	ATCTAAGCTTTTTGTTTGTGTGGAATATTAAATTTG
	an_0199	D11prom__Spe_rv_199	TTACTAGTTTCTTTTTTTTTTTTTTATTCTTAAAAG
Quantitative RT-PCR assay	an_0206	D1_qPCR_fw_206	CGACGCTATGGCTGTCTTGC
	an_0207	D1_qPCR_rv_207	TTTGTTGTTCAGTTACGGCTTTGC
	an_0208	D2_qPCR_fw_208	GGGTGTCAAAGGAGGATCATCG
	an_0209	D2_qPCR_rv_209	TTGTTCACTTGTCATCATTGTTGC
	an_0210	D3_qPCR_fw_210	GAGGCAATGATGTTCGTGAGTTC
	an_0211	D3_qPCR_rv_211	TGTTGATGTCTTGTAGTTCCTTGAG
	an_0212	D4_qPCR_fw_212	TTGAGAAACTTAGGGCATT
	an_0213	D4_qPCR_rv_213	AAGAAGATATGACTTGGAAGA
	an_0216	D6_qPCR_fw_216	GCAGCCACTGGTAAACTCTCC
	an_0217	D6_qPCR_rv_217	GACACACTTCAGCATTTCATCTTTG
	an_0218	D7_qPCR_fw_218	AGAGCGGTTCATCGGTAATGTC
	an_0219	D7_qPCR_rv_219	CAATCGTTTGTGCCCACTTCG
	an_0220	D8_qPCR_fw_220	GCAAGAGTTCAACTATTGTTA
	an_0221	D8_qPCR_rv_221	CTGATACTAGGTCAAGAAGG
	an_0222	D9_qPCR_fw_222	GCAATGTCAGCCCTCATCTCC
	an_0223	D9_qPCR_rv_223	GTTACTTCTCCCACCCGCAATC
	an_0224	D10_qPCR_fw_224	TATGCTGCTGGGAAACTATCTGATG
	an_0225	D10_qPCR_rv_225	CTGCTTCACCTTTGCTGATTTGG
	an_0226	D11_qPCR_fw_226	GGATTCGTGGAGGATGCTTGATG
	an_0227	D11_qPCR_rv_227	CTCCTTGGAACCGCTCTTCTTG
	an_0228	D12_qPCR_fw_228	ACACATTGGAGTTGAAGGAGACC
	an_0229	D12_qPCR_rv_229	GCCGAGACCGTAGACATCATC
	an_0235	D5_qPCR_fw_235	TAGTGATGGTCTTTGTGTC
	an_0236	D5_qPCR_rv_236	TGTCCTTGTCGTAATCTAC
	UG-LS-97	Actin11 fw	AAC TTT CAA CAC TCC TGC CAT G

	UG-LS-98	Actin11 rv	CTG CAA GGT CCA AAC GCA GA
	an_0141	Q UBC for	ATGCTTGGAGTCCTGCTTGG
	an_0142	Q UBC rev	TGCCATTGAATTGAACCCTCTC
Mapping of amiRNA lines T-DNA insertions	an_0263	25-2_fw_WT_RP_263	AGAAGGTGTGATACCATCATTAGT
	an_0264	25-2_rv_WT_RP_264	CACTAATGATGGTATCACACCTTCT
	an_0265	25-2_fw_WT_LP_265	CTCAAGACCTCGACTACTGGAGACTA
	an_0266	25-2_rv_WT_LP_266	TAGTCTCCAGTAGTCGAGGTCTTGAG
	an_0267	25-5_fw_WT_RP_267	acccacccattcacttttaac
	an_0268	25-5_rv_WT_RP_268	gttaaaaagtgaatgggtgggt
	an_0269	25-5_fw_WT_LP_269	ttaggcgaaatttagaggttgtc
	an_0270	25-5_rv_WT_LP_270	gacaacctctaaatttcgcctaa
	an_0271	27-4_fw_WT_RP_271	atgtgaagttttgccactttgag
	an_0272	27-4_rv_WT_RP_272	ctcaaagtggcaaaacttcacat
	an_0273	27-4_fw_WT_LP_273	ttgcagtcactggttcattcc
	an_0274	27-4_rv_WT_LP_274	ggaatgaaccagtgactgcaa
	an_0275	Tail4.LB_rv_275	CATGTAGATTTCCCGGACATGAA
	an_0276	25-5_sec ins_fw_276	ATGCTCTTCTACAGCGAAGCC
	an_0277	25-5_sec ins_rv_277	acctttaaataatactcccatctaac
	an_0292	292_tail3_LB	catcatactcattgctgatcc
	MJ primer database	LB_pMOA_TAIL1	tatagcgcgcaaactaggataaat
		LB_pMOA_TAIL2	tatcgcgcgcggtgtcatcta
		AD1	random short primers with low Tm
		AD2	random short primers with low Tm

List of technical equipment and reagents

ChemiDoc™ XRS+ System, BioRad

7500 Fast Real-Time PCR System, Applied Biosystems®

NanoDrop, Thermoscientific

2100 Bioanalyser, Agilent Technologis

Light microscope DM6000 B, Leica Microsystems

Light microscope Leica DMR, Leica Microsystems

Stereo microscope Leica M205 C, Leica Microsystems

Confocal microscope Leica TCS SP5, Leica Microsystems

Gateway® Cloning Technology, Invitrogen

Fast SYBR® Green Master Mix, Life Technologies

The DIG System Labeling and Detection of Nucleic Acids, Roche

Restriction endonucleases and DNA modifying enzymes, New England Biolabs

Deoxycytidine 5'-[a-32P] triphosphate, Hartmann Analytic

NEBlot Kit for radioactive probe labelling (New England Biolabs)

NucleoSpin® RNA Plant Kit, Macherey-Nagel

NucleoSpin® Gel and PCR Clean-up Kit, Macherey-Nagel

V. Publications

Boisson-Dernier, A., Lituiev, D.S., *Nestorova, A.*, Franck, C.M., Thirugnanarajah, S., and Grossniklaus, U. (2013). ANXUR receptor-like kinases coordinate cell wall integrity with growth at the pollen tube tip via NADPH oxidases. PLoS Biol. *11*, e1001719.

Ngo, Q.A., Vogler, H., Lituiev, D.S., *Nestorova, A.*, and Grossniklaus, U. (2014). A Calcium Dialog Mediated by the FERONIA Signal Transduction Pathway Controls Plant Sperm Delivery. Dev. Cell *29*, 491–500.

Felekis, D., Vogler, H., Mecja, G., Muntwyler, S., *Nestorova, A.*, Huang, T., Sakar, M.S., Grossniklaus, U., and Nelson, B.J. (2015). Real-time automated characterization of 3D morphology and mechanics of developing plant cells. Int. J. Rob. Res. *34*, 1136–1146.

Hedhly, A., *Nestorova, A.*, Grossniklaus, U. (manuscript in preparation). Cartography of heat stress during stamen development in Arabidopsis thaliana.

VI. Acknowledgements

This research project was conducted at the University of Zurich, in the laboratory of Prof. Ueli Grossniklaus. I am exceptionally grateful to my thesis advisor Prof. Grossniklaus, for giving me the chance to work in a great scientific environment, what the Institute of Plant Biology and particularly his research group represents in every aspect.

Furthermore, I would like to thank Hannes Vogler for his encouraging efforts, discussions, and his contribution to the project and the manuscript of this doctoral thesis.

I am grateful to Christian Sailer, who helped me with data analysis and discussions about my project, as well as for his contribution to the manuscript.

To Monica Schauer I am thankful for initiating this scientific work and providing me with initial information concerning the project.

I would also like to thank my referee at the University of Zurich Prof. Enrico Martinoia and my external referee form the University of Lausanne Prof. Niko Geldner for their scientific input and for reading this thesis.

I want to thank the members of the Sex Club Lena, Sharon, Aurel, Heike, Evelyne, Moritz, Nadine, Quy, Andrea Z., Andrea M. for the fruitful discussions and sharing their experience with me.

I wish to thank my former and current colleagues in the lab Daniela, Milka, Lena, Klara, Nadine, Alex, Sharme, Deborah, Kostas, Aurel, Kostas, Afif, Rosa, Sharon, Nuno, Giom, Dima L., Evelyne, Poly, Gorka, Mayank, Sam, Christian S., Marian, Nina, Celia, Hampe, and Joana for their help, scientific input, kindness, and friendship. To Daniela I am very grateful for her gracious presence in the lab, for the valuable advices and support, as well as for translating the Summary part of this thesis in German.

Special thanks to the people, who shared their great experience and knowledge with me and made me part of their exciting scientific work: Aurel, Afif, Marian, Quy, Sharon, and Hannes.

I am very thankful to the P2 technical assistance team Valeria, Christof, Daniela, Fred, Arturo, Peter, Rosa, and Matthias for their support and organizational work.

I am thankful to all current and former members of Ueli's lab for providing very nice and supportive working atmosphere.

I thank my husband Peter for helping me in every aspect during this work and also for his valuable contribution to this manuscript.